The functionalization of spherically shaped carbon-based nanomaterials

By

Zikhona Nobuntu Tetana

Submitted in fulfilment of the requirements for the degree of

Masters of Science in the Faculty of Science

Department of Chemistry

University of the Witwatersrand

Private Bag X03

WITS

2050

Supervisors: Professor Neil J. Coville

Professor Willem A. L. van Otterlo

March 2009

DECLARATION

I declare that “The functionalization of spherically shaped carbon-based nanomaterials” is my own, unaided work under the supervision of Professor Neil J. Coville and Professor Willem A. L. van Otterlo. It is being submitted for the degree of Masters of Science in the University of Witwatersrand, Johannesburg. It has not been submitted for any degree or examination in any other university, and all sources I have used or quoted have been indicated and acknowledged by means of complete references.

Name: Zikhona Nobuntu Tetana (Ms)

Signature of candidate

……day of ……..2009

DEDICATION

TO MY MOTHER BULELWA ADELAIDE TETANA

ACKNOWLEDGEMENTS

I would like to warmly thank my supervisors, Professor Neil J. Coville and Professor Willem A. L. van Otterlo for their outstanding contributions to the success of this research project.

I am also grateful to Mr. Messai Mamo for his kind advice and discussions. I would also like to thank Dr. K. C. Mondal, Prof. A. Strydom, Dr. S. D. Mhlanga, Prof. M. J. Witcomb, Prof. J. Havel, and Mr. R. Erasmus for their fruitful collaboration.

I also thank Mr. Rudolph Erasmus, Mr. Richard Mampa, Mr. T. A. van der Merwe, and Dr. Manuel A. Fernandes for their assistance with Raman spectroscopy, nuclear magnetic resonance spectroscopy, mass spectrometry and X-ray diffraction analysis, respectively.

I would also like to thank all the members of the CATOMAT group, past and present, for providing an interesting and enjoyable working environment.

I would not have been able to achieve any of my goals without the love and support of my family and friends. I thank my parents for their prayers and for being with me throughout my scholastic career. May the Lord God bless you for all you have done.

The financial support for this work by the DST/NRF Centre of Excellence in Strong Materials is gratefully acknowledged. I extend my gratitude to the Johannesburg Water (Pty) Ltd for financial support.

I finally wish to thank God Almighty for His endless love, support, strength, and courage He gave as I engaged in this research.

ABSTRACT

In this dissertation, the synthesis and characterization of side-chain fullerene-containing polymers has been accomplished and reported (chapter 3). This was achieved by first synthesizing a C_{60}-cyclohexadiene cycloadduct, followed by its polymerization with norbornene via a ring opening metathesis polymerization (ROMP) procedure using the Grubbs' second generation catalyst. For comparison purposes, 1,4,5,6,7,7-hexachloro-5-norbornene-endo-2,3-heptylimide monomer was also copolymerized with C_{60}-cyclohexadiene cycloadduct. The novel materials were characterized using FT-IR, UV-VIS, NMR spectroscopic techniques as well as TGA and DSC analyses. The complex 1,4,5,6,7,7-hexachloro-5-norbornene-endo-2,3-heptylimide was also characterized by single crystal X-ray diffraction. The resulting copolymers revealed that the main fullerene features were retained in the polymers

In the second part of this dissertation, carbon spheres (CSs) with high purity were synthesized by the CVD method using acetylene as a carbon source (chapter 4). The CSs were characterized using Raman spectroscopy, TGA and TEM and data revealed their graphitic and crystalline nature. Successful functionalization of CSs with cyclopentadiene (CS-C_5H_6) and cyclohexadiene (CS-C_6H_8) was achieved by way of a Diels-Alder type cycloadditon. The functionalized CSs showed good solubility in organic solvents such as chloroform, dichloromethane and DMF. Boron-doped carbon spheres were also synthesized and characterized, with special attention placed on the diameters of carbon spheres obtained in the presence of the boron source. Characterization of the CSs synthesized was performed by means of Raman spectroscopy, TEM, and laser ablation mass spectrometry analysis. The average diameter and shell thickness of the carbon spheres are greatly influenced by the boron incorporation into the CSs, resulting in CSs with a larger diameter.

TABLE OF CONTENTS

SECTION **PAGE**

LIST OF FIGURES

FIGURES **PAGE**

LIST OF TABLES

TABLES **PAGE**

LIST OF ABBREVIATIONS

a. u.	Arbitrary units
CCD	Cooled charge coupled detector
CNT(s)	Carbon nanotubes(s)
CS(s)	Carbon sphere(s)
CVD	Chemical vapour deposition
DMF	*N*,*N*-Dimethylformamide
DSC	Differential Scanning Calorimetry
FAB	Fast atom bombardment
FT-IR	Fourier transform infrared
HPLC	High-performance liquid chromatography
HRTEM	High-resolution transmission electron microscope
I_D/I_G ratio	The intensity ratio of D to G band
I_h symmetry	Icosahedral symmetry
IR	Infrared
LUMO	Lowest unoccupied molecular orbital
MS	Mass spectrometry
m/z	Mass-to-charge ratio
NMR	Nuclear magnetic resonance
ROMP	Ring Opening Metathesis Polymerization
TGA	Thermal Gravimetric Analysis
Tg	Glass transition temperature
THF	Tetrahydrofuran
TLC	Thin layer chromatography
TMS	Tetramethylsilane
TOFMS	Time-of-flight mass spectrometer
UV-VIS	Ultra-violet visible

CHAPTER 1
INTRODUCTION

1.1 Background to the study

Nanoscience is the study of how materials behave when their sizes are reduced to the nanoscale, while nanomaterials are the materials that are employed in nanotechnology. Nanotechnology is generally the application of ideas from science and engineering for use in the fabrication of new materials and devices. These products make abundant use of physical properties associated with small scales. Nanotechnology has also been defined as the design, production, characterization, and application of structures, devices, and systems by controlled manipulation of size and shape at the nanometer (nm) scale (atomic, molecular, and macromolecular scale) that produces structures, devices, and systems with at least one novel or superior property [1].

Over the past decade, nanomaterials have been the subject of massive interest [2]. They can be made by a 'top down' approach, producing very small structures from larger pieces of material, for example by etching structures into bulk materials such as silicon as in the fabrication of silicon chips. They can also be made by a 'bottom up' approach, atom by atom or molecule by molecule, harnessing ionic, covalent, non-covalent or metallic bonds. In this approach one can use self-assembly, in which the atoms or molecules arrange themselves into a structure due to their natural properties [1]. Crystals grown for the semiconductor industry and polymers are examples of products formed by self-assembly. An alternative to self-assembly is to use tools to move each molecule or atom individually. Although molecule manipulation is difficult and not suitable for industrial applications, the discovery of the scanning tunneling microscope (STM) and atomic force microscope (AFM) have been essential for the development of nanoscience and nanotechnology research.

Nanomaterials, noteworthy for their very small feature dimensions, have the potential for wide-ranging industrial, biomedical, and electronic applications. Nanomaterials can be

ceramics, metals, polymeric materials, or composite materials [2]. Their important characteristic is a very small feature dimension in the range of 1-100 nm. There are two principal factors that cause the properties of nanomaterials to differ significantly from other materials: greatly increased surface area and quantum size effects [1]. These factors can enhance properties such as reactivity, strength and electrical conduction. Materials reduced to the nanoscale can show extremely different optical, electrical and magnetic properties when compared to what they exhibit on a macroscale, enabling unique applications for the nanomaterials. For instance, a material such as gold, which is chemically inert at usual scales, can serve as a powerful chemical catalyst at the nanoscale [2]. Copper nanoparticles smaller than 50 nm are considered super hard materials that do not show the same malleability and ductility as bulk copper [2]. Nanocomposites based on polymeric materials are also important in explaining nanomaterial behaviour. For instance, the addition of small amounts of 2 % by volume of silicate nanoparticles to a polyamide resin increases the strength of the resin by 100 % [2]. Addition of nanoparticles improves the mechanical properties and thermal stability, in some instances allowing use of polymer-matrix nanocomposites at temperatures at an additional 100 °C above normal service conditions [2]. Polymer-based nanocomposites can also be used in anti-corrosion coatings on metals, thin-film sensors and packaging films. Processing and forming of light materials is one of the main reasons for the rapidly growing applications of carbon nanomaterials. Lightweight materials with high strength and stiffness are likely to find applications in aircraft and spacecraft components.

One of the most important aims of nanotechnology nowadays is the development of new or enhanced materials [1]. Scientists throughout the world have been attracted to the study of the structure, texture and diversity of various carbon materials due to their wide range of applications [3, 4]. Among the materials that can be used as additives are carbon-based nanomaterials. These include fullerenes (C_{60}), carbon spheres (CSs), carbon nanotubes (CNTs), carbon onions, carbon beads and nanofibers. These nanomaterials have promising applications in nanotechnology, biosensing, electronics, polymer composites, hydrogen storage, catalysis, electrodes and drug delivery, due to their exceptional characteristics [5]. Carbon nanomaterials also reveal a rich polymorphism.

Discovery of a new carbon material morphology leads to new potential application fields. In particular, it is expected that the original nanometric morphologies of CNTs could have an important potential impact in applicative areas such as molecular electronics or high-strength composite materials [6]. Reports have shown that once carbon nanomaterials are added to a polymer the strength of a polymer can be enhanced [7].

Doping of heteroatoms into carbon nanostructures adds another dimension to these structures' characteristics. Doping nitrogen or boron into carbon layers affects the electronic structure, catalytic activity and electrical conductivity properties of the doped materials. For example Kim *et al.* [8] showed that an enhanced carbon nanotube growth resulted from nitrogen incorporation into a carbon nanotube wall which reduced the elastic strain energy to form a tubular graphitic layer of a carbon nanotube. The enhanced carbon nanotube growth by incorporation of nitrogen is due to a decrease in the activation energies required for nucleation and growth of the tubular graphitic layer [8]. Blase and the co-workers [9] reported that electron microscopy and electron diffraction patterns revealed that B-doping considerably increased the length of carbon nanotubes and led to a remarkable preferred zigzag chirality.

The preparation of carbon-containing polymeric materials is noteworthy for several reasons. For instance, when a small amount of C_{60}, CNTs or CSs are introduced into a polymer system, many properties of the polymer such as photoconductivity [10], mechanical properties [11], optical limiting properties [12], etc. are enhanced. Another reason to synthesize carbon-containing polymeric materials is to overcome the drawbacks of carbon nanostructures for large-scale applications, due to their insolubility or near insolubility in most common solvents, and their tendency to aggregate very easily [13]. These problems can be overcome by first functionalizing the carbon materials with organic groups to give soluble derivatives that are easy to analyse and characterize [14-23].

1.2 Objectives

The objectives of this project are as follows:

(i) To synthesize a C_{60}-cyclohexadiene monomer.

(ii) To polymerize the resulting monomer with norbornene derivatives via a Ring Opening Metathesis Polymerization (ROMP) in the presence of the Grubbs' second generation catalyst.

(iii) To perform the synthesis and functionalization of carbon spheres with cyclohexadiene or cyclopentadiene.

(iv) To carry out the synthesis of boron-doped carbon spheres using acetylene as the carbon source and BF_3 in MeOH as the boron source.

(v) To characterize the new carbon-containing materials using techniques such as thermal analysis, nuclear magnetic resonance spectroscopy, infrared spectroscopy, ultra-violet visible spectroscopy, mass spectrometry, Raman spectroscopy and transmission electron microscopy.

1.3 Outline of the dissertation

Below is an outline of this dissertation:

Chapter 2 (Literature review): This chapter gives a review of the literature related to carbon nanomaterials such as carbon nanotubes, fullerenes, carbon spheres, etc. The properties and applications of these carbon nanomaterials are discussed.

Chapter 3 (The synthesis of C_{60}-containing polymers): This chapter describes the research work done on fullerene (C_{60}). The introduction, experimental, results and discussion, and conclusion to the synthesis of C_{60}-containing polymers are presented in this chapter.

Chapter 4 (Synthesis, functionalization and doping of carbon spheres): In this chapter, the research done on carbon spheres is presented. The introduction, experimental, results

and discussion, and conclusion to the synthesis, doping and functionalization of carbon spheres are presented in this chapter.

Chapter 5 (Conclusions and recommendations): In this chapter, conclusions are drawn based on the results obtained with respect to the initial objectives. It also represents recommendations for future studies.

1.4 References

1. www.nanowerk.com, 12 April **2008**.
2. Nanomaterials: www.csa.com, 12 August **2008**.
3. G. L. Che, B. B. Lakshmi, E. R. Fischer, C. R. Martin, *Nature*, **1998**, 393, 346.
4. M. B. Shiftlett, H. C. Foley, *Science*, **1999**, 285, 1902.
5. E. L. Wolf, *Nanophysics and Nanotechnology: An introduction to Modern Concepts in Nanoscience*, John Wiley and Sons: New York, **2004**.
6. M. S. Dresselhaus, G. Dresselhaus, Ph. Avouris, *Carbon nanotubes: synthesis, structure, properties and applications*. In: *Topics in applied physics*, *Vol. 80*, Berlin: Springer, **2000**.
7. See for example: T. Song, S. H. Goh, S. Y. Lee, *Polymer*, **2003**, 44, 2563.
8. T.-Y. Kim, K.-R. Lee, K. Y. Eun, K.-H. Oh, *Chem. Phys. Lett.*, **2003**, 372, 603.
9. X. Blase, J.-C. Charlier, A. De Vilta, R. Car, *Phys. Rev. Lett.*, **1999**, 83, 5078.
10. K. Yoshino, X. H. Yin, K. Muro, S. Kiyomatsu, S. Morita, A. A. Zakhidov, *Jpn. J. Appl. Phys.*, **1993**, 32, L357.
11. A. B. Dalton, S. Collins, E. Munoz, J. M. Razal, V. H. Ebron, J. P. Ferraris, J. N. Coleman, B. G. Kim, R. H. Baughman, *Nature*, **2003**, 423, 703.
12. J. Shinar, Z. V. Vardeny, Z. H. Kafafi, editors. *Optical and electronic properties of fullerenes and fullerene-based materials*. New York: Marcel Dekker, **2000**.
13. R. S. Ruoff, D. S. Tse, R. Malhotra, D. C. Lorents, *J. Phys. Chem.*, **1993**, 97, 3379.
14. F. Wüdl, *Acc. Chem. Res.*, **1992,** 25, 157.
15. R. Taylor, D. R. M. Walton, *Nature*, **1993**, 363, 685.

16. A. Hirsch, *Angew. Chem., Int. Ed. Engl.*, **1993**, 32, 138.
17. A. Hirsch, *The Chemistry of Fullerenes*, Thieme, Stuttgart, **1994**.
18. F. Diederich, L. Isaacs, D. Philip. *Chem. Soc. Rev.*, **1994**, 23, 243.
19. A. Hirsch, *Synthesis*, **1995**, 895.
20. R. Taylor, *The Chemistry of the Fullerenes*, World Scientific, Singapore, **1995**.
21. A. B. Smith (ed), *Fullerene Chemistry, Tetrahedron Symposia-in-Print Number 60*, **1996**, 52, 4925.
22. F. Diederich, C. Thilgel, *Science*, **1996**, 271, 317.
23. M. Prato, *J. Mater. Chem.*, **1997**, 7, 1097.

CHAPTER 2
LITERATURE REVIEW

2.1 Carbon nanomaterials

Carbon is found freely in nature in three allotropic forms: amorphous, graphite and diamond. Carbon can share electrons with up to four different atoms. Carbon has an affinity for bonding with other elements as well as with itself. Carbon-carbon bonds are strong and stable. This allows carbon to form many different compounds of varying size and shape. The shapes of molecules may be understood by looking at the hybridization adopted by each of the atoms in a molecule. When carbon is bonded to four other atoms with no lone electron pairs, the hybridization is sp^3 and the arrangement is tetrahedral. When carbon is bonded to three other atoms (two single bonds, one double bond) the carbon is sp^2 hybridized and the structure results in a flat trigonal arrangement with 120° angles between bonds. A carbon atom bound to two other atoms (two double bonds or one single plus one triple bond) is sp hybridized and forms a linear arrangement with an angle of 180° between bonds. The physical properties of carbon vary widely with the allotropic form. For example, graphite is opaque, black, very soft and slippery, while diamond is highly transparent, the hardest material known and has a high melting point. Also, diamond has a very low electric conductivity while graphite is a very good conductor of electricity. All forms of carbon are solids under normal conditions and highly stable, requiring a high temperature to react [1].

Amorphous forms of carbon such as soot, charcoal and activated carbon are materials consisting of very small particles of graphite. The amorphous form has a variety of carbon atoms arranged in a non-crystalline, irregular, glassy state, which is basically graphite with the carbon atoms not held in a crystalline macrostructure. Graphite comprises of a two-dimensional network of sp^2-hybridised carbon atoms and a sheet of linked hexagonal rings. Each carbon atom is bonded trigonally to three others. There are strong covalent bonds between carbon atoms in each layer and only weak Van der Waals forces exist between layers. On the other hand, diamond is comprised of a three-

dimensional network of sp^3-hybridised carbon atoms. Each carbon atom is bonded tetrahedrally to four others, making a three-dimensional network of puckered six-membered ring of atoms. Other allotropes have also been discovered, such as fullerenes. Many different carbon shapes have been made such as buckyballs, carbon nanotubes (CNTs), carbon nanobuds, nanofibres, aggregated diamond nanorods, lonsdaleite, glassy carbon, carbon nanofoam, and linear acetylenic carbon [1]. Some allotropes of carbon are shown in **Figure 2.1** [1]. The buckyballs are large molecules made of carbon bonded trigonally forming spheroids. CNTs are structurally similar to buckyballs, except that each carbon atom is bonded trigonally in a curved sheet that forms a hollow cylinder. All these carbon nanomaterials are potentially useful and can be employed in nanotechnology.

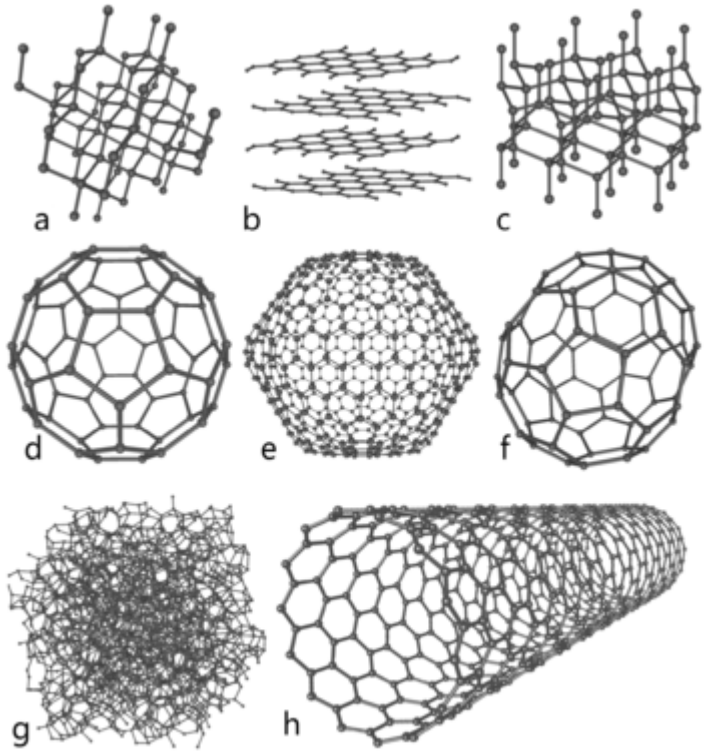

Figure 2.1: Some forms of carbon: (a) diamond; (b) graphite; (c) lonsdaleite; (d)-(f) fullerenes (C_{60}, C_{540}, C_{70}); (g) amorphous carbon (h) carbon nanotubes (figure taken from reference [1]).

Various forms of carbon such as carbon nanofibres [2, 3], carbon onions [4-6], carbon trees [7], carbon spheres [8-13], ordered mesoporous carbons [14], carbon nanowalls [15] and carbon capsules [16], have been synthesized and studied by scientists around the world. Carbon nanotubes and other carbon structures are potential candidates for use in conductive and high-strength composites [17], drug delivery [18], nanotweezers [19], gas storage media [20], semiconductor devices [21], and field emission displays [22]. A variety of methods have been established for both the synthesis of different carbon structures and to study their morphology [23].

In this dissertation the focus has been on spherical carbon materials namely, fullerenes and solid carbon spheres. These compounds will be discussed separately.

2.2 Fullerenes

2.2.1 Historical Introduction

In 1970, Eiji Osawa of Toyohashi University of Technology predicted the existence of C_{60}. He observed that the structure of a corannule molecule was a subset of a soccer-ball shape, and he made the hypothesis that a full ball shape could also exist and that it would be 'superaromatic' [24]. In 1985 these predictions were shown to be correct. Since the initial discovery of the existence of polyhedral carbon clusters, the fullerenes, in 1985 by Kroto *et al.* [25] and the subsequent development of preparative methods for their fabrication at the beginning of the 1990s [26], the chemical properties and numerous chemical methodologies to functionalize these uncommon molecules has been investigated. Kroto, Smalley and Curl were awarded the 1996 Nobel Prize in chemistry for their roles in the discovery of this class of compounds. The word "fullerene" is now used to refer to the whole class of hollow closed cage molecules consisting of only carbon atoms.

Fullerenes have received much attention by scientists in many fields. Motivation for this attention has been provided by a range of players: chemists for the molecular nature of

the solid phase and the synthesis of a huge family of novel compounds that can be prepared from fullerenes, materials scientists for generating sources of monodisperse nanostructures that can be assembled in films and crystal forms and whose properties can be controlled by doping and intercalation, and device engineers because of fullerenes' potential use in optical limiting and switching devices and in photoconductor applications for niche photoresistor purposes [27]. Some potential applications for fullerenes include: superconductors, lubricants, catalysts due to their high reactivity, drug delivery systems, pharmaceuticals and targeted cancer therapies, hydrogen storage, optical devices, chemical sensors, photovoltaics, polymer additives, polymer electronics such as Organic Field Effect Transistors (OFETS), and antioxidants and cosmetics, to 'mop up' free radicals [28]. Since the commercial availability of C_{60}, research on this new form of carbon has expanded at a rapid rate.

2.2.2 The structural features of fullerenes

Carbon shows a variety of stable forms ranging from three dimensional semiconducting diamond, to two dimensional semimetallic graphite, to one dimensional conducting and semiconducting carbon nanotubes and to zero dimensional fullerenes. All these compounds show many interesting properties. Fullerenes and carbon nanotubes have sp^2-hybridised carbon atoms. Structural features of fullerenes are similar to graphite. However, fullerenes are molecules of discrete size, and they are spherical because they have pentagonal rings that prevent the formation of sheets and hence encourage the formation of 3-D structures.

Fullerene, also known as Buckminsterfullerene, C_{60}, is composed entirely of carbon. C_{60} was named after Richard Buckminster Fuller because of the similarity of the shape of C_{60} to the geodesic dome he designed [24]. C_{60} is the smallest stable, and also the most abundant fullerene, with icosahedral (I_h) symmetry. With the success in synthesizing macroscopic quantities of fullerenes, a number of other fullerenes such as C_{70} (the second most abundant fullerene, with D_{5h} symmetry), C_{74}, C_{76}, C_{78}, C_{80} and C_{84} (low abundant fullerenes) have been isolated and characterized [29]. A common feature noted for all the

higher fullerenes, including C_{60} and C_{70}, is that they all have isolated pentagons. The higher fullerenes all have very low symmetry [30]. The lower symmetry of these higher fullerenes results in the formation of a large number of potential structural isomers which are difficult to separate. As a result, the work done on fullerene chemistry has focused on C_{60} and C_{70} [31]. Because of their exceptional properties, structure and versatility, fullerenes have proven to be ideal materials for nanotechnology studies.

2.2.3 The synthesis of fullerenes

The first production of fullerenes was developed by Smalley and co-workers in the early 1980s [32] and consisted of laser vaporization of a graphite rod, followed by entrainment of the ablated species in a molecular beam. The photoionized species were then mass analyzed by time-of-flight mass spectrometry (TOFMS). In 1990, an inexpensive and efficient method to synthesize large quantities of fullerenes was discovered by Krätchmer and Huffman [26 (a)-(b)]. The method they used to synthesize fullerenes employed the passage of a large current between two graphite electrodes in a helium atmosphere. The resulting carbon plasma arc between the electrodes cooled into a sooty residue from which various fullerenes could be isolated as soluble, well-defined solids. The major species were identified as C_{60} and C_{70} through mass spectrometry and by comparison of the infrared spectrum with hypothetical predictions for C_{60}, which had previously been proposed to account for cluster beam observations [25, 33]. The IR spectrum observed by Krätchmer and Huffman showed four sharp strong absorptions (1429, 1183, 577 and 528 cm^{-1}), which at elevated He pressures originated from I_h-C_{60}. Taylor and co-workers [29, 34] confirmed the structure of C_{60} and C_{70} by using mass spectrometry which showed strong peaks at *m/z* 720 and 840, corresponding to C_{60} and C_{70}. They also ran the ^{13}C NMR spectra of the purified material, which for C_{60} and C_{70} gave a single line and five lines respectively.

In fullerene production mixtures of C_{60}, C_{70} and higher fullerenes are always formed. Fullerene purification is the most important key to fullerene science and determines the prices and the success of practical applications of fullerenes. The first purification

method for C_{60} was by high performance liquid chromatography (HPLC) from which small amounts could be generated at large expense. A practical method for purification of soot enriched in C_{60} and C_{70} starts with extraction in toluene followed by filtration with a paper filter. Toluene is evaporated and the residue (the toluene-soluble soot fraction) redissolved in toluene and subjected to column chromatography. C_{60} elutes first with a purple colour and C_{70} next showing a reddish-brown colour [35].

2.2.4 The properties of C_{60}

2.2.4.1 The structure of C_{60}

The structure of the C_{60} molecule is that of a truncated icosahedron, which resembles a round soccer ball. The fullerene is made of twenty hexagonal and twelve pentagonal rings [24]. The sixty carbon atoms in C_{60} are located at the vertices of a truncated icosahedron where all carbon sites are equivalent, and this is consistent with the observation of a single line in the ^{13}C NMR spectrum [29]. A schematic diagram of a C_{60} molecule is shown in **Figure 2.2**.

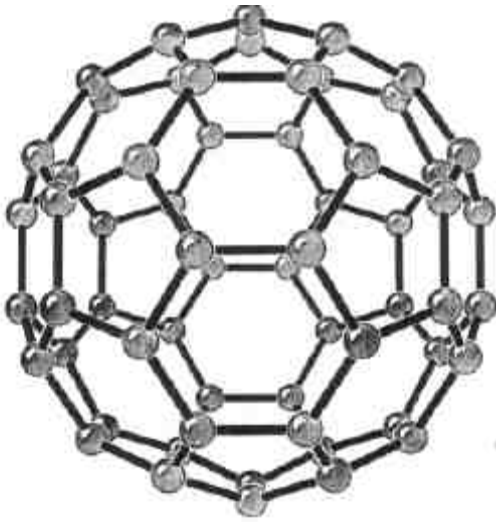

Figure 2.2: Schematic diagram of a C_{60} molecule (figure taken from reference [36]).

C_{60} has 30 reactive π bonds within the hexagonal rings, and none of the pentagons make contact with each other. The C_{60} molecule has two bond lengths, the (6,6) ring bonds

(between two hexagons) are shorter than the (6,5) ring bonds (between a hexagon and a pentagon) [24, 27, 37, 38]. This is because to have a π bond in a pentagonal ring would lead to higher local curvature on the fullerene ball and would also increase ring strain [24, 27, 37]. The two bonds on the pentagonal edges are electron-poor single bonds and one bond joining two hexagons is an electron-rich double bond [27]. The X-ray diffraction bond length values are 135.5 pm for the (6,6) bond and 146.7 pm for the (5,6) bond [35].

2.2.4.2 The solubility of C_{60}

The solubility of fullerenes decreases with increasing size [24]. In polar and H-bonding solvents C_{60} is basically insoluble. It is sparingly soluble in alkanes and the solubility decreases with the number of atoms. Toluene and carbon disulphide are common solvents used for the fullerenes [37, 39]. Fullerene-containing materials are generally more soluble than the parent molecule [24]. The organic derivatization of C_{60} has produced an increasingly high number of compounds which, while retaining most of the original properties of fullerene, are easier to handle [39].

2.2.4.3 The reactivity of C_{60}

Fullerenes are not very reactive due to the stability of the graphite-like bonds. To increase its reactivity, researchers have been able to attach active groups to the surfaces of fullerenes [40]. As mentioned before, C_{60}, with I_h symmetry, has only one type of carbon atom and two types of C-C bonds: those at (6,6) ring junctions and those at (6,5) ring junctions. The characteristic reactions of fullerenes are redox reactions, radical additions, nucleophilic additions, carbene additions, cycloadditions and polymerizations [35]. The strong electron withdrawal by the fullerene cage makes fullerenes very unreactive towards most electrophiles. Substitution reactions are not possible with fullerene since it contains no H atoms that could be substituted. However, substitution reactions do occur on derivatives of C_{60} containing additional groups. Addition reactions to C_{60} usually occur at the π bonds in the hexagonal rings. Theoretical work has demonstrated that the bonds at the (6,6) ring junctions in C_{60} will be more reactive than those at the (6,5) ring junctions [41, 42]. The nucleophilic addition at (6,6) ring junctions decreases angle strain by changing sp^2-hybridized carbons into sp^3-hybridized ones. This change in

hybridization decreases the bond angles from ~120° in sp^2 orbitals to ~109.5° in sp^3 orbitals. This allows for the bonds to bend less when closing the sphere and therefore the molecule becomes more stable. Generally, nucleophilic additions give covalent monoadducts as the major products; higher additions occur more slowly as the electrophilicity of C_{60} derivatives becomes increasingly reduced with increasing reduction in the conjugated fullerene chromophore [43]. However, the addition of a nucleophile in a stoichiometric amount to a (6,6) bond of fullerene has been shown to lead to a complex mixture containing one product of monoaddition together with several multiple addition products. Prato [39] reported that the monoadduct can usually be purified by chromatography. A mixture of diadducts can contain up to eight different positional isomers, with the number of possible isomers increasing with the number of additions. Isomers inside each family of adducts tend to possess the same chromatographic properties, and this makes the separation a very complex operation. Hence, addition conditions are usually optimized for the maximum yield of the monoaddition product, with little attention given to more highly functionalized fullerenes [39]. It is not surprising that nucleophilic addition reactions can take place readily because of the high electrophilic reactivity of fullerenes. Multiaddition products are no less useful than monoadducts if they can be synthesized selectively and in high yield. Richly functionalized fullerenes show interesting properties such as biochemical activity (e. g. DNA cleavage, etc.) [44-48] and photochemical functionality (e. g. photovoltaics, etc.) [49, 50].

Addition reactions have the largest synthetic potential in C_{60} chemistry. Fullerene, with its electron affinity (2.8 eV) [33], is a reactive 2π component in cycloaddition reactions such as the Diels-Alder addition, and reacts as an electron deficient dienophile with a number of electron rich dienes, including aromatic and non-aromatic systems [33, 42, 51]. Cycloadditions to fullerenes are popular for their ability to control the reaction so that only one addend attaches to the cage, making chemical analysis of the products quite easy [24]. Other cycloaddition reactions such as [1+2], [2+2], [3+2], [6+2], [8+2] and [4+2] (Diels-Alder) cycloadditions have been shown to be useful tools for the modifications of fullerenes [52]. Here the C_{60} with a relatively low lying LUMO always

reacts as a dienophile. Cycloaddition of C_{60} to quadricyclane [53], C_{60} to cyclopentadiene [52] and C_{60} to cyclooctatetraene [54] have successfully given stable cycloaddition products.

2.2.5 Reactions of C_{60}

Researchers have been able to increase the reactivity of fullerenes by attaching active groups to their surfaces, for the purpose of obtaining specific chemical or physical properties of the fullerenes. Redox reactions lead to salts. On the other hand, addition reactions can lead to covalent exohedral fullerenes, endohedral fullerenes, heterofullerenes, quasi-fullerenes and open cage fullerenes [37].

Other atoms can be trapped inside fullerenes to form inclusion compounds known as endohedral fullerenes. When the atom trapped inside is a metal, they are known as metallofullerenes [55]. Endohedral fullerenes offer a wide range of new possibilities in nanomaterials science since they show electronic structures generally different from those of the empty parent cage. In addition, they are usually stable under ambient conditions [56]. In biomedical sciences they have been able to encapsulate metals with magnetic or radioactive properties for the generation of magnetic resonance imaging agents and radiotracers [57]. Heterofullerenes are fullerenes in which one or more carbon atoms of the cage are substituted by hetero-atoms, for example, a boron atom [58]. Quasi-fullerenes are fullerenes containing ring systems other than pentagonal and hexagonal rings [24, 37]. Open cage fullerenes are fullerenes in which one or more bonds are removed chemically exposing an opening [59]. In open cage fullerenes it is possible to insert into it small molecules such as hydrogen, helium or lithium. The first such open cage fullerene was reported by Prato and co-workers in 1995 [60].

Exohedral fullerenes, in which molecules are formed by a chemical reaction between fullerenes and other chemical groups, are the most versatile of all species of fullerenes [61]. Exohedral fullerenes include organometallic fullerene complexes, halogenated fullerenes, fullerene-based polymers and ordinary organic molecules attached to

fullerene. In organometallic chemistry a fullerene acts as a ligand to a metal. Fullerene samples suitable for X-ray diffraction studies have been difficult to obtain, in general, due to the poor crystal quality of the products. However, organometallic derivatives in which a metal complex is bonded to the outer surface of the fullerenes have produced crystalline samples of good quality. The first example of an organometallic derivative of C_{60} was reported in 1991 by Fagan and co-workers [62].

2.2.6 Fullerene polymeric derivatives

Fullerene and its derivatives have a number of interesting electronic [63], magnetic [64], and chemical properties [65]. It has been shown that the unique properties of the parent C_{60} are retained in its derivatives [39, 66]. Thus, C_{60}-containing polymeric derivatives are expected to possess similar physical, electronic, optical, and catalytic properties to the parent C_{60} [66]. A number of studies on polymer containing fullerene have been carried out for the purpose of embedding fullerenes in composite materials [67]. Fullerenes have been incorporated into polymers by various methods. These include the use of 1,3-dipole cycloaddition to azido-substituted polystyrene [68], addition to amino-containing polymers [69] or by attaching the fullerene covalently and reversibly to a cyclopentadiene-functionalized polymer resin [69].

The incorporation of C_{60} into polymers is an important area of research. The combination of a fullerene with its unique geometrical and electronic properties with the well known properties of polymers allows for the features of a new class of composite materials with unique properties [56, 70]. Some literature reports have shown that these materials demonstrate outstanding structural, electrochemical and photophysical properties which are currently under intensive study [56]. For instance, electroactive and photoactive polymers or polymers with nonlinear optical properties can be prepared by this approach. The resulting materials can be used for surface coating, photoconducting devices, or to generate novel molecular networks [39, 71]. It has also been shown that introducing C_{60} into polymers affects the mechanical behaviour, tensile strength and fracture toughness of the polymers [72].

Depending on the relative spatial arrangement of the fullerene unit in the polymer chain, various kinds of polymeric fullerenes can be prepared: side-chain polymers, main-chain polymers, fullerene-end-capped polymers, immobilized fullerenes on solid surfaces, crosslinked polymers, fullerodendrimers, star-shaped fullerene polymers, etc [56, 73, 74] (**Scheme 2.1**).

Because of their structure, three-dimensional fullerenes and polymers are useful scaffolds for the production of high molecular weight structures. Consequently, combination of polymers and fullerenes has led to the synthesis of a wide range of new materials showing appealing features. These are based on the possibility of improved properties by modification of the chemical nature of the components or chemical bonding between them [74].

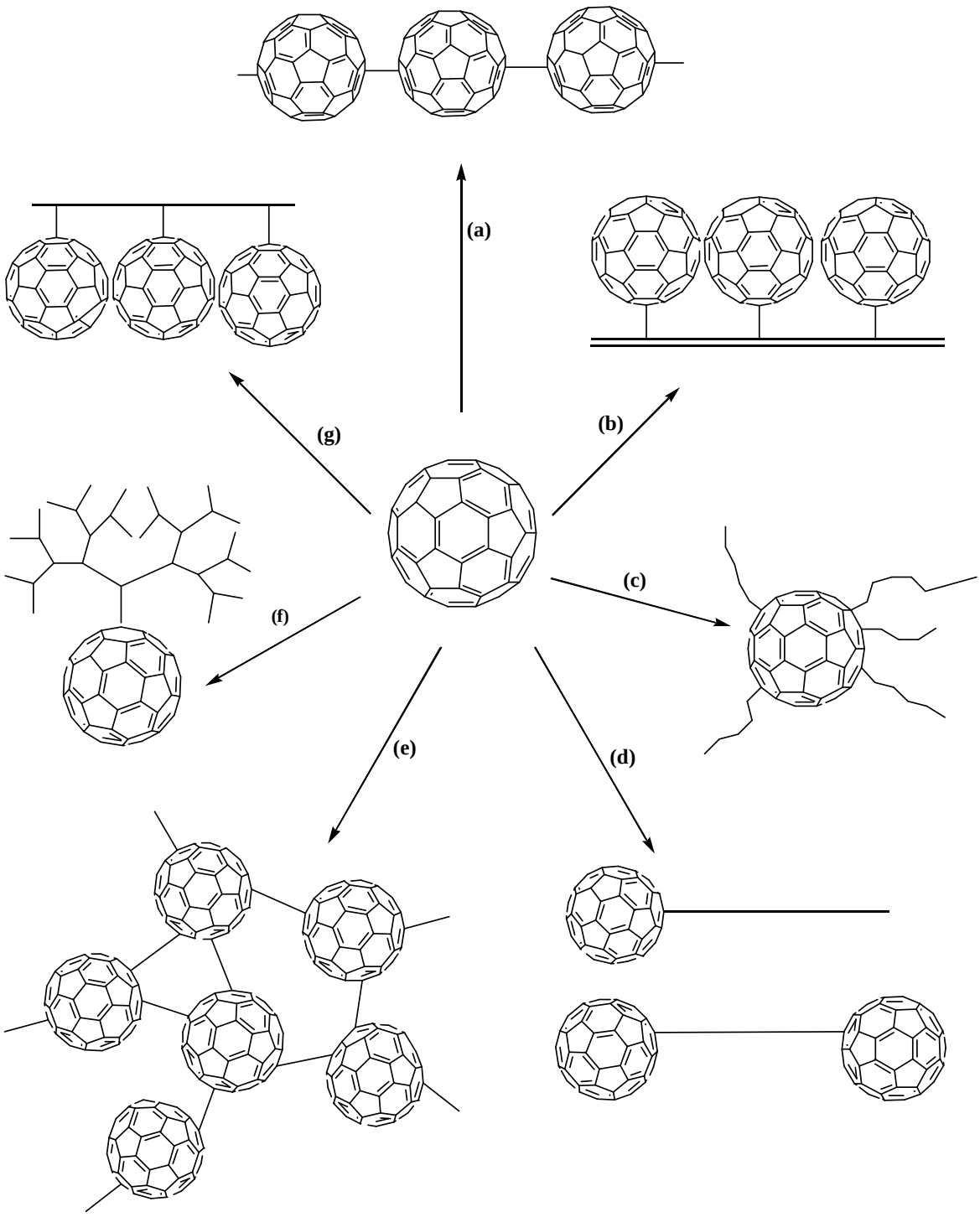

Scheme 2.1: Different kinds of polymeric fullerenes: (a) main-chain fullerene polymer; (b) immobilization of fullerenes on solid surfaces; (c) star-shaped fullerene polymers; (d) fullerene-end-capped polymers; (e) cross-linked polymers; (f) side-chain fullerene polymers; (g) fullerodendrimers [73].

(a) Main-chain fullerene polymers

These are fullerenes that are found in the backbone of the polymer (**Scheme 2.1a**). They are sometimes referred to as 'pearl necklace' or in-chain polymers. The polymer may consist of directly or indirectly linked fullerenes, linked by a small 'spacer' between its fullerenes [75]. The first example of main-chain C_{60} polymers was prepared by Benincori *et al*. via electrochemical polymerization [76]. Subsequently, many papers have been published on the preparation of such polymers [77]. **Scheme 2.2** shows the synthesis of the main-chain polymer, poly(4,49-carbonylbisphenylene-trans-2-fullerenoibisacetamide). This polymer was prepared via the polycondensation of trans-2-fullerenobisacetic acid and 4,49-diaminobenzophenone in the presence of large excess of triphenyl phosphate and pyridine [77(b)].

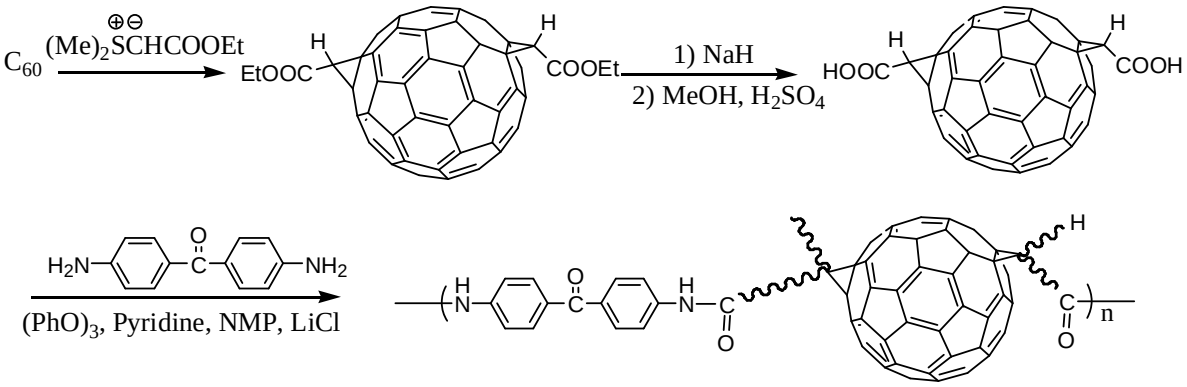

NMP = *N*-methyl-2-pyrrolidone

Scheme 2.2: The synthesis of C_{60} main-chain polymer [77(b)].

Very few examples of copolymers containing C_{60} in the main chain of the polymer are known. This is because of the low regioselectivity found in the double addition on the C_{60}, resulting in the formation of the regioisomeric mixture and also the cross-linked products, by multiple additions on the C_{60} units. There are two different synthetic approaches to prepare main-chain polymers: (1) direct reaction between C_{60} and a proper symmetrical difunctionalized monomer and (2) polycondensation between a C_{60} bisadduct (or a mixture) and a difunctionalized monomer [74]. The first polymer of the

latter kind was reported in 1992 by Loy and Assink, though thermogravimetric analysis revealed that the C_{60}-xylylene copolymer was generally cross-linked [78].

(b) Immobilization of fullerenes on solid surfaces

Immobilization of fullerenes on solid surfaces constitutes another important kind of polymeric fullerene. Fullerene-containing thin films on solid surfaces are of interest because of the possibility of transferring the unique properties of fullerene to bulk materials by surface coating [73]. This can be attained by immobilization of amine groups on indium tin oxide surfaces followed by the reaction of the amine groups with C_{60} [79]. Another method is to covalently attach a pyridyl-terminated, self-assembled monolayer of C_{60} to a silicon oxide surface [80]. Prato *et al.* [81] reported the use of silicon alkoxide-functionalized fullerenes in the preparation of high-performance liquid chromatography (HPLC) stationary phases, which when tested with simple aromatic compounds revealed high efficiency both in organic and water-rich media. The silicon alkoxide group actually assures chemical grafting to silica (**Scheme 2.3**) [81].

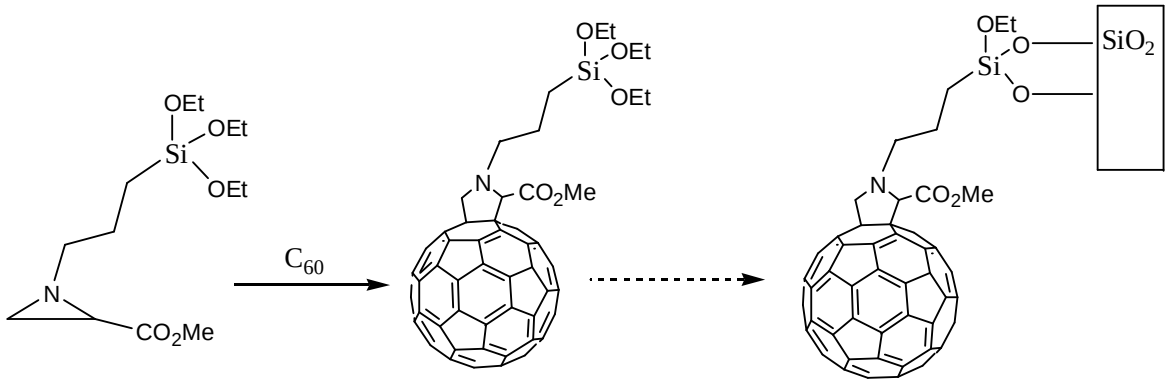

Scheme 2.3: Grafting of C_{60} onto a silica surface [81].

(c) Star-shaped fullerene polymers

Star-shaped fullerene polymers, also known as ‘flagellenes’, are polymers in which the fullerene is the star centre. They consist of two to ten long and flexible polymer chains covalently attached to a fullerene unit with topologies similar to that of sea stars or resembling the shape of flagellate-unicellular protozoa [74]. ‘Living’ anionic

polymerization allows better control of the molecular weights as well as their distributions and has been the method mostly used for the preparation of polystyrene-C_{60} star polymers. The polymers with the formula $C_{60}(PS)_x$ (PS = polystyrene, x = 1-10), were found to be highly soluble and melt processable, making them amenable to spin-coating, melt extrusion and solvent casting [74, 75]. C_{60}-containing star-shaped copolymers have also been made by the reaction between C_{60}-fullerenols and diisocyanated urethane polyether prepolymer, followed by quenching with 1-dodecanol (**Scheme 2.4**) [82].

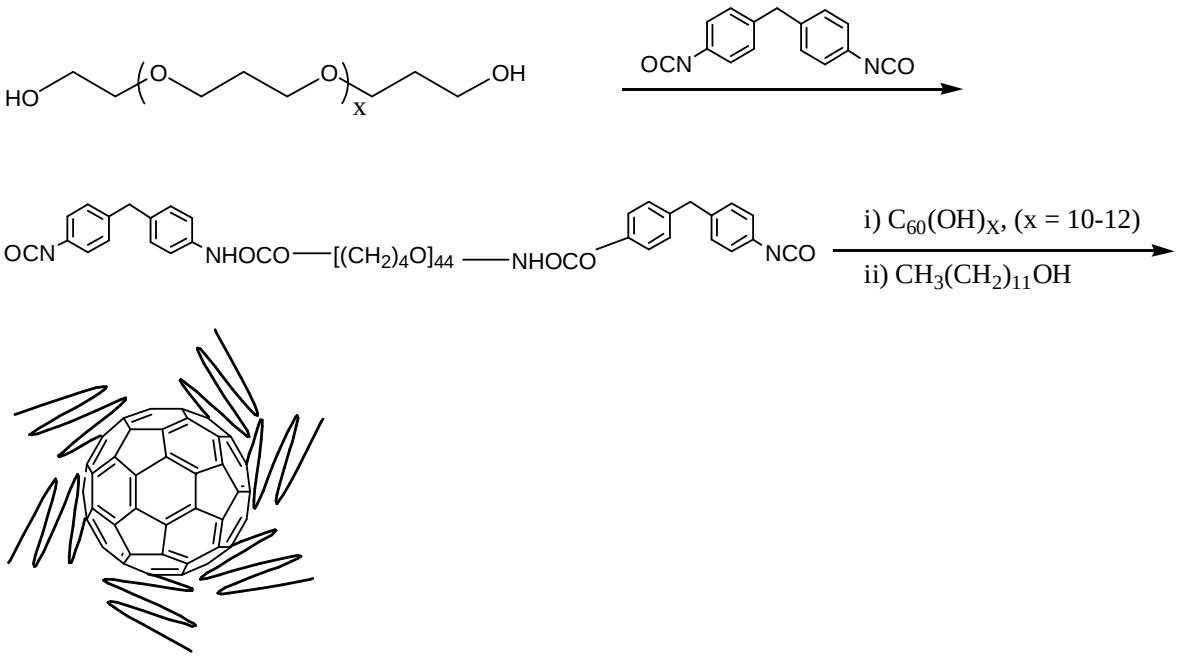

Scheme 2.4: The synthesis of a C_{60}-containing star polymer [82].

(d) Fullerene end-capped polymers

Fullerene end-capped polymers, also known as 'telechelic', are polymers terminated by a fullerene unit. In fullerene end-capped polymers the C_{60} units are located at the terminal positions of the polymer chain. By introducing one or two C_{60} moieties at the end of the chain it has been possible to modify the hydrophobicity of the parent polymer, thus radically changing its behaviour in blends of H-donor or H-acceptor polymers [74]. Goh *et al.* reported the preparation of mono- and bi-C_{60}-end-capped poly(ethylene

glycol)s (PEG) [83]. **Scheme 2.5** shows the synthesis of bi-C_{60}-end-capped PEG, which showed H-bonding interactions, forming an interpolymer complex with a number of H-donating polymers such as poly(p-vinylphenol) [83], poly(vinyl chloride) [84] and poly(acrylic acid) [85]. In addition, films of bi-C_{60}-end-capped PEG were tested in mechanical measurements. They showed good mechanical properties stemming from a network-like structure owing to the strong aggregation of C_{60} [86].

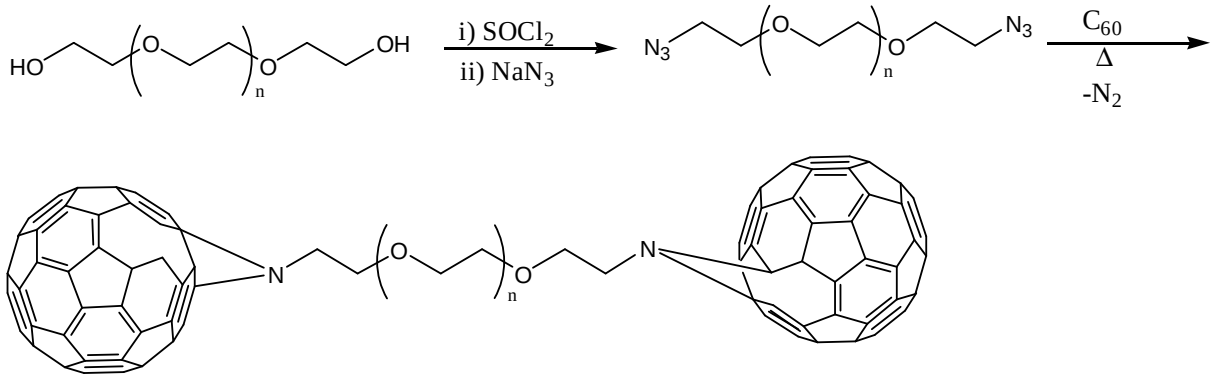

Scheme 2.5: The synthesis of a bi-C_{60}-end-capped poly(ethylene glycol) [83].

(e) Cross-linked polymers

Cross-linked polymers, also known as starburst fullerenes, are random polymers irradiating from a fullerene spheroid. They are made from random and quick reactions that take place with the help of a C_{60} cage, in three dimensions. Additionally, careful control of the addition reactions to multiply reactive C_{60} double bonds is necessary, or else the dimensionality of the final products can increase significantly [74]. Cross-linked polymers can have multifunctionalized fullerenes but are known to be imperfectly characterized polymers. Under elevated pressure, styrene and its derivatives have been widely used as a co-monomer to react with C_{60} via both free-radical polymerization [87, 88] and 'living' anionic polymerization [89], to produce cross-linked C_{60}-containing polymers. Another important class of polymers which has been used in the preparation of C_{60}-containing cross-linked networks is represented by the polyurethanes. **Scheme 2.6** shows a C_{60}-containing cross-linked polymer synthesized from fullerenols, $C_{60}(OH)_{10\text{-}12}$, and a suitable diisocyanate-functionalized prepolymer [90]. Thermal mechanical analysis

of the resulting polymer showed that the use of fullerenols as cross-linkers improved the properties of polyurethane elastomers as well as the tensile strength at break. It was also found that fullerene-containing cross-linked polyurethanes showed optical limiting properties in a film with a modulation in the transmittance that depended linearly on the amount of fullerene present in the material [91].

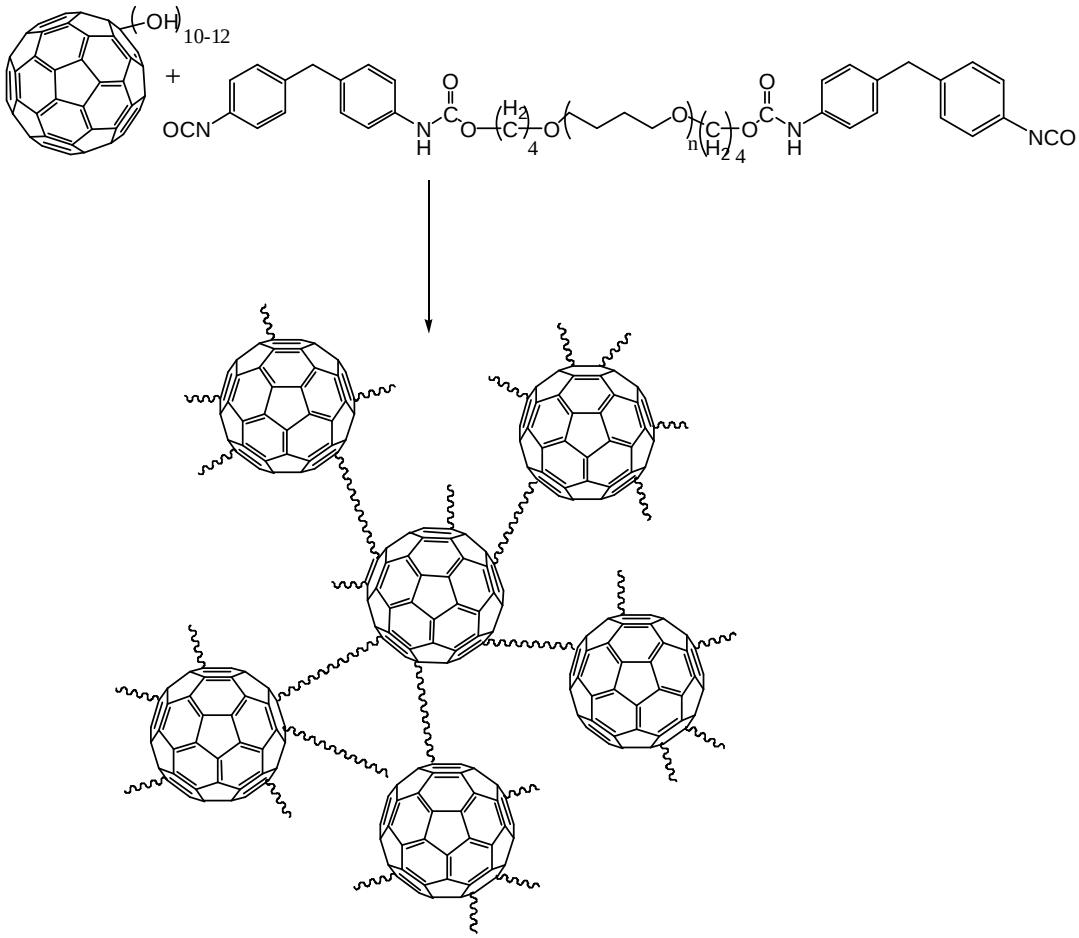

Scheme 2.6: The synthesis of C_{60}-containing cross-linked polymer [90].

(f) Side-chain fullerene polymers

These are polymers bearing pendant fullerenes. They are also known as 'pendant', charm-bracelet' or on-chain polymers. The fullerenes may be attached in a regular manner to a polymeric backbone chain to give a pendant chain effect [75]. The syntheses of C_{60} side-chain polymers and main-chain polymers have been widely developed and generate processable fullerene-based materials. Two different synthetic methods have

been used to prepare side-chain fullerene polymers: (1) direct introduction of either C_{60} or a C_{60} derivative monomer into a previously prepared polymer (non-covalent immobilization), and (2) synthesis of a C_{60} derivative which can be directly polymerized or copolymerized together with other monomer(s) [74]. The second method may be favourable in cases where, (1) the fullerene unit should be more strongly bound, (2) heterogeneous mixtures of C_{60} and the polymer tend to undergo phase separation, or (3) a perfect tuning of the material properties is desirable [92]. The first effort to make side-chain fullerene polymers was by Wudl and co-workers in 1992 (**Scheme 2.7**) [93]. They first prepared a low molecular weight bis-hydroxydiphenylmethanofullerene and then obtained a C_{60}-containing polyester as well as polyurethane via a polycondensation reaction. These two novel materials had a low degree of polymerization due to the large steric hindrance of the C_{60} unit. In addition, the materials were insoluble in most common organic solvents. [73, 74].

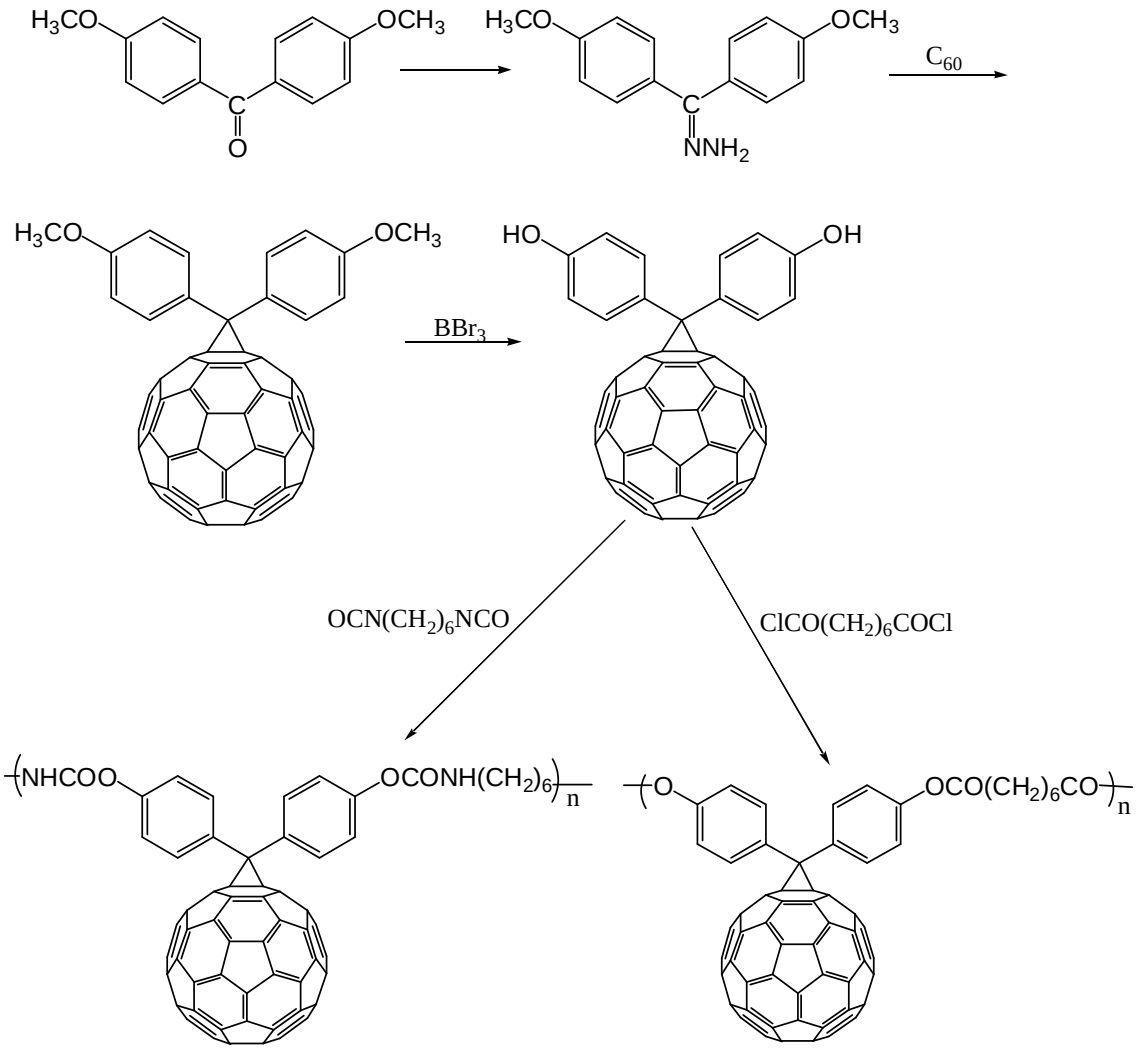

Scheme 2.7: The preparation of polyester and polyurethane C_{60} derivatives [93].

The cycloaddtion reaction is another important method for preparing side-chain fullerene polymers. Kraus and Müllen prepared a C_{60}-containing polymer by introducing fullerene into the side chain of poly(dimethylsiloxane). The product was reported to have excellent film forming capabilities [94]. Another interesting class of C_{60}-side-chain polymers is based on the use of organometallic catalysts. Prato *et al.* used Mo(CH-Bu^t)(NAr)[OCMe$(CF_3)_2]_2$ as a catalyst for a ring opening metathesis polymerization (ROMP) between a norbornene-modified C_{60} and an excess of norbornene [66] (see **Scheme 3.2** and **3.3** in **Chapter 3**). This methodology will be described in detail in the next chapter as it provides the background for much of the work performed in this thesis.

(g) Fullerodendrimers

Fullerodendrimers are constructed from a C_{60} core and repeatedly branched side chains that are characterized by their structure perfection, i.e. highly symmetric and monodispersed macromolecules. Fullerodendrimers can be synthesized using the technique used to prepare the polymers shown in **Scheme 2.3**. Generally, fullerodendrimers are more soluble in organic solvents than polymers [74, 95]. A fullerene-containing liquid crystalline dendrimer was prepared by Dardel *et al.* (**Scheme 2.8**) [96]. They synthesized this dendrimer by the addition reaction of mesomorphic malonate-based dendrimers with C_{60}. In addition, fullerodendrimers, have also been used for the delivery of drugs [96].

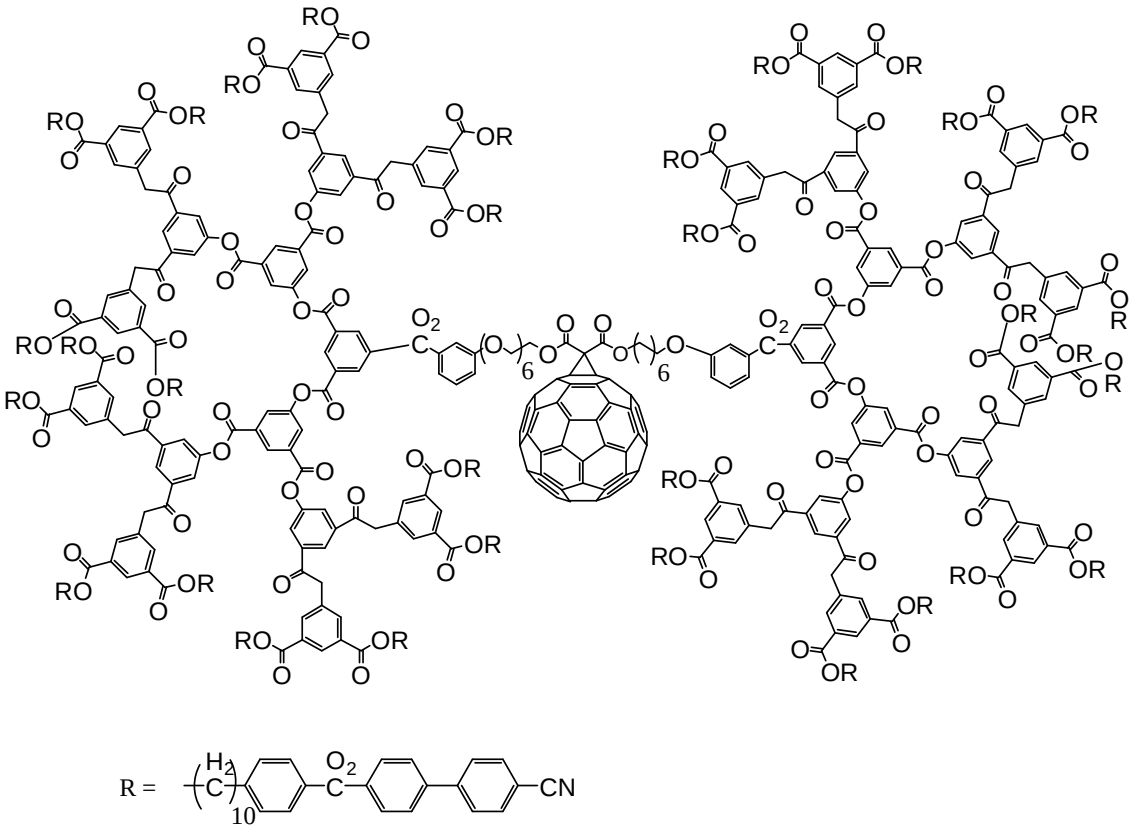

Scheme 2.8: Synthesis of C_{60}-containing dendrimer. [96].

2.2.7 Characterization Techniques used for C_{60}-based materials

(i) Mass spectrometry (MS)

Mass spectrometry presents knowledge of the molecular weight and certain structural features of a compound. In MS, a sample is injected into a mass spectrometer, where it is vaporized and then bombarded with a beam of high-energy particles (for example electrons). The energy of the electron beam can be varied, but a beam of about 70 eV is commonly used. When the electron beam hits the molecule, it displaces an electron out of the compound. This gives a molecular ion ($M^{+\cdot}$). Because the energy of the electron beam is greater than the energy required to break most of the bonds in an organic compound, the electron beam causes many of the molecular ions to break apart to give radicals, cations, and other radical cations [97]. The technique identifies and quantifies molecules based on their mass to charge ratios (*m/z*). A mass spectrum comprises of a plot of the relative abundance of each fragment against its *m/z* value. The peak in the mass spectrum with the largest value of *m/z* is called the molecular ion. The base peak is the one with the greatest abundance and is assigned a relative abundance of 100 %.

(ii) Ultra-violet / visible (UV/Vis) spectroscopy

UV/Vis spectroscopy is a technique used for qualitative and quantitative determination of compounds in solution as well as solids using diffuse reflectance spectroscopy (DRS). The technique gives information about conjugated π electron systems. UV/Vis spectroscopy involves the absorption of electromagnetic radiation; ultraviolet light with wavelength ranging from 180 to 400 nm and visible light ranging from 400 to 780 nm [97]. The absorption of energy as a result of an electronic transition causes an absorption band in the UV/Vis spectrum. The amount of energy absorbed by the compound is directly related to concentration of the compound in the solution.

(iii) Infrared spectroscopy (IR)

Infrared spectroscopy is one of the techniques used to identify functional groups that are present in a molecule [98]. IR spectroscopy involves the twisting, bending,

rotating, and vibrational motions of atoms in a molecule. Upon interaction with infrared radiation, portions of the incident radiation are absorbed at particular wavelengths. The multiplicity of vibrations occurring simultaneously produces a highly complex absorption spectrum, which is uniquely characteristic of the functional groups consisting of the molecule and the overall formation of the atoms as well [99].

(iv) Differential Scanning Calorimetry (DSC)

DSC is a thermoanalytical technique used to measure the temperatures and heat flows associated with transitions in materials as a function of temperature and/or time. By monitoring the difference in heat flow between the sample and reference, DSC is able to measure the amount of heat absorbed or released during such transitions. Both the reference and the sample are kept at very nearly the same temperature throughout the experiment. DSC data give information about physical and chemical changes that involve endothermic and exothermic processes, or changes in heat capacity, and is widely used to characterize the thermophysical properties of polymers. Using this technique it is possible to determine the melting temperature (Tm), crystallization temperature (Tc), glass transition temperatures (Tg or softening) and thermal stability of a sample. Glass transitions may occur when the temperature of an amorphous solid is increased. These transitions appear as a step in the baseline of the recorded DSC signal. This is due to the sample undergoing a change in heat capacity; no formal phase change occurs. As the temperature increases, an amorphous solid will become less viscous. Tc is due to transition from amorphous solid to crystalline solid; this is an exothermic process and results in a peak in the DSC signal. As the temperature increases the sample eventually reaches its melting temperature, which results in an endothermic peak in the DSC curve [100].

(v) Thermogravimetric Analysis (TGA)

TGA is a thermal analysis technique that is used to measure changes in the mass of a sample as a function of temperature and/or time in a controlled atmosphere. TGA is commonly used to determine polymer degradation temperatures, residual solvent levels, absorbed moisture content and the amount of inorganic (non-combustible) filler in

polymer or composite material compositions [101, 102]. From TGA curves, data on the kinetics and thermodynamics of the various chemical reactions, reaction mechanisms, reaction intermediates and final reaction products are obtained [99]. In TGA, a sample is loaded into an aluminium cup that is supported on an analytical balance located outside the furnace chamber. The balance is zeroed and the sample cup is heated according to a predetermined thermal cycle. The sample is continuously weighed while being heated to higher temperatures and the mass loss is recorded as a function of temperature.

(vi) Nuclear Magnetic Resonance (NMR) Spectroscopy

NMR spectroscopy is the absorption of electromagnetic radiation used to determine the structure of an organic compound. In NMR spectroscopy, the distinctive absorption of energy by certain spinning nuclei in a strong magnetic field, when irradiated by a second and weaker field perpendicular to it, permits identification of atomic configurations in molecules. Absorption occurs when these nuclei undergo transitions from one alignment in the applied field to an opposite one. The amount of energy required to cause a particular nucleus to realign depends upon such factors as field strength, electronic configuration around the particular nucleus, anisotropy, type of molecule, and intermolecular interaction. The result is often the description of complete sequences of groups or arrangement of atoms in the molecule [99]. Therefore, NMR spectroscopy is a useful tool for identification and characterization of molecules.

2.3 Carbon spheres

2.3.1 Introduction

The diverse range of structures and morphologies of carbon with wide technical applications is made possible due to the many combinations of sp, sp^2 and sp^3 hybridizations [103]. The discoveries of fullerenes [25] and the elongated fullerenes, the carbon nanotubes, in arc-discharged carbon by Iijima in 1991 [104], have stimulated intense research activities and an interest in further developments in the nanotechnology and nanoscience of carbonaceous structures since the materials have unique size

dependent properties [105, 106]. Most of the disordered carbons observed are believed to be due to the presence of sp^2/sp^3 mixed carbons. The increase in the sp^2 carbon ratio tends to establish the graphitic structure that favours the electronic character, as confirmed by high conductivity and large diamagnetism [107]. CNTs are one of the strongest and lightest materials known, both in terms of tensile strength and elastic modulus. This extraordinary strength results from the covalent sp^2 bonds formed between the individual carbon atoms and that is stronger than the bonds formed from sp^2 carbons found in diamond [108]. The strength and flexibility of CNTs makes them of potential use in controlling other nanoscale structures, which suggests they will have an important role in nanotechnology engineering.

Spherical carbon structures have become increasingly important due to their excellent properties [109, 110] and potential applications in many industrial fields [111-114]. Because of their intrinsic properties such as high strength, high thermal resistance and light weight, spherical carbon structures could be used in high strength composites [115], wear-resistant materials [116], photonic crystals, catalysts supports [117], anodes in secondary lithium ion batteries [118, 119] or as an adsorbent [120, 121]. These spherical materials with different structures ranging from C_{60} and carbon onions to carbon spheres (CSs) have closed or unclosed graphene layers [109]. As mentioned before, graphite has carbons with three-fold coordinated sp^2 hybridization forming strong intra-layers bonding within the hexagonal carbon-rings, and has weakly unsaturated π-bonding with adjacent layers perpendicular to the hexagonal network, in contrast to diamond [122]. C_{60} on the other hand, is believed to be chemically inert because of the weakly unsaturated π-bonding normal to the surface. Carbon spheres have similar properties to graphite or fullerene, which allow them to be used to fabricate diamond films, lubricating materials and special rubber additives [122]. However, there is an increasing need for the production of CSs in large quantities under mild conditions for cost-effective production. Serp and co-workers have classified carbon structures into three categories according to size: (i) the C_n family and the well graphitized onion like structures ranging between 2 and 20 nm; (ii) the CSs with diameters between 50 nm to 1 μm; and (iii) the carbon beads with diameters of one to several microns [112, 115, 122, 123].

The carbon spheres, also called fullerene soot, have been reputed to be found as major products in the fullerene synthesis [124]. Fullerene carbon spheres were identified by Iijima [125] using high-resolution transmission electron microscopy (HRTEM). Ugarte [126] reported that CSs with diameter of a few nanometers were obtained from soots that contain tubular and polyhedral graphitic particles formed under intense high-energy electron-beam irradiation in a high-resolution transmission electron microscopy. Carbon spheres can also be produced as a by-product during the preparation of CNTs or carbon nanofibers, where metal catalysts are employed [122, 127, 128].

Carbon spheres can be of two types; hollow or solid. Solid carbon spheres (~210 nm diameter) have been prepared by Wang and Kang [114, 123, 129] using the thermal decomposition of methane in the presence of a metal oxide catalyst. They claim to have a selective process to produce either carbon spheres at 1100 °C or completely pure CNTs at 950 °C. Govindaraj *et al.* have prepared CSs from the pyrolysis of methane in a hydrogen atmosphere at 1140 °C without a catalyst [130]. Qian *et al.* have also used toluene as a feedstock for the production of CSs without any catalysts. Serp *et al.* have also reported on the production of CSs using a chemical vapour deposition process [112]. Recently, Kroto and co-workers reported on the large-scale synthesis and characterization of CSs prepared by the direct pyrolysis of hydrocarbons with two to eight carbon atoms [103]. They employed a double furnace apparatus, where the hydrocarbon was introduced into the lower temperature vaporization furnace (250 °C), and the feedstock vapour was carried through the system in argon and underwent pyrolysis at temperatures between 900 and 1200 °C.

2.3.2 Production methods for carbon spheres

As there is an emerging need for the production of high purity carbon spheres in large quantities, many kinds of preparation methods have been developed [124, 131]. Carbon spheres have been produced by the methods similar to those used to produce carbon nanotubes [111, 113, 118, 127, 128, 132]. Methods such as chemical vapour deposition (CVD) [112, 122], arc plasma [113], mixed-valence oxide-catalytic carbonization [115],

reduction of carbides with metal catalysts [133], and pyrolysis of carbon sources and catalyst [127] have been reported for the fabrication of carbon spheres. Of these, the CVD method is the most popular and cost-effective, and is hence used for the large scale synthesis of high quality carbon spheres. The CSs obtained by Alili and co-workers from CVD methods were all made with uniform dimensions and in high purity, without any other by-products being detected [134]. Generally, the preparation of CSs using a CVD method involves a carbon-containing gas such as methane, acetylene, etc., as the carbon source. Use of an energy source, such as a plasma or a resistively heated coil, provides the energy for transforming the gaseous carbon molecules. The molecules are then converted into reactive carbon atoms which then diffuse onto the growing carbon surface, forming carbon spheres. It has been reported that controlled growth and continuous mass production of CSs with uniform diameters is achieved by varying the flow-rate and composition of the carrier gas [115].

2.3.3 Growth mechanism for carbon spheres

Li *et al.* reported that the growth of carbon spheres results from the thermal decomposition of a carbon precursor into carbon atoms, followed by the precipitation of the carbon deposits [135]. The carbon spheres are composed of curling graphitic flakes and are believed to exhibit many dangling bonds at the surfaces [111, 114]. To form a graphitic CS the atomic structure of each flake must be one of the known graphite carbon rings, and the graphitic lattice must be modulated to accommodate the curvature of the sphere [114]. There are three different types of graphitic carbon rings that initiate larger growth (**Figure 2.3**) [111, 114]. These are a flat hexagonal layer, a pentagonal carbon ring which causes the hexagonal network to curve inward, forming a surface with positive curvature and a heptagonal carbon ring which forces the hexagonal lattice to be curved outward, forming a negative curvature [111, 114].

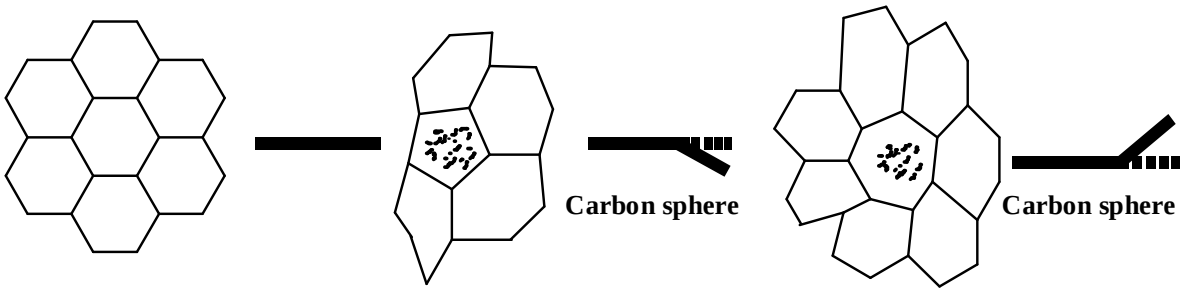

Figure 2.3: (a) Hexagonal, (b) pentagonal, and (c) heptagonal carbon ring structures in graphitic flakes (figure taken from reference [114]).

It is believed that carbon spheres are nucleated from a pentagonal carbon ring, growth of which gives a quasi-icosahedral spiral shell carbon particle [136], (**Figure 2.4**, [114]). The geometrical configurations of the graphitic flakes can be qualitatively constructed using the combination of pentagonal, heptagonal and hexagonal rings and the variation in size of these graphitic flakes can create any curvature required to meet the geometry of the inner layers [114].

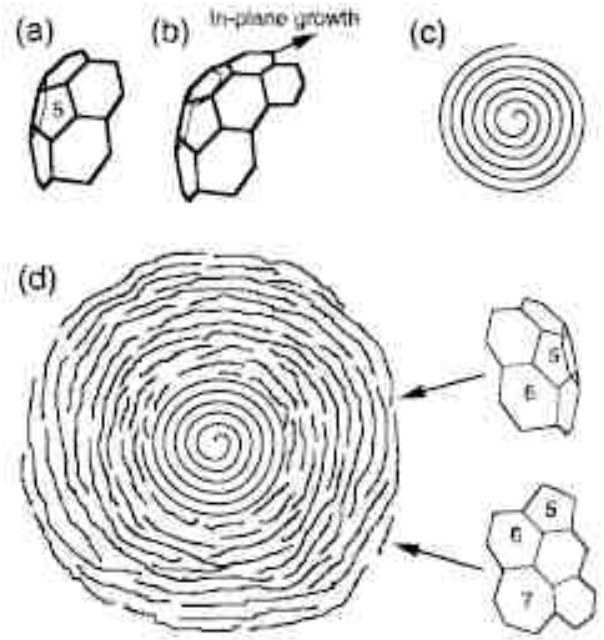

Figure 2.4: (a) Nucleation of a pentagon, (b) growth of a quasi-icosahedral shell, and (c) formation of a spiral shell carbon particle. (d) Growth of a large size carbon sphere (figure taken from reference [114]).

2.3.4 Doping of carbon nanostructures

As mentioned before, doping of heteroatoms into carbon nanostructures adds another dimension to these structures' characteristics. Doping of heteroatoms into graphite-like carbon structures is believed to modify the electronic structure and thereby modify their electrical conductivity properties [137]. For example, N-doped CNTs may lead to the formation of electron-excess *n*-type semiconducting nanotubes [137-139]. This is due to the lone pairs of electrons, conjugating with the delocalized π-system of the standard graphene sheet. Electron deficiency in graphite can also be achieved by incorporating boron, which acts as acceptor, into the lattice [140, 141]. Other effects may arise in boron-doped carbon materials such as: (a) boron not only acts as an acceptor by increasing the number of hole-carriers in the valence band, but it also acts as a scattering centre, therefore reducing carrier mobility; (b) the diamagnetic susceptibility decreases, due to the larger effective mass of charge carriers; (c) because the Fermi level intercepts the valence band, the electronic density of states increases, therefore leading to enhanced paramagnetic susceptibility [142, 143].

Boron-doping also influences significantly the field emission performance of CNTs. Charlier and co-workers demonstrated that B-doped tubes show great potential as building blocks for stable and intense field emission sources, thus opening new avenues in vacuum microelectronics [144]. B-doped CNTs may lead to electron-deficient p-type semiconducting nanotubes [137-139]. Provided that one can control, at the nanometer level, the position and distribution of heteroatom such as B (or N) in CNTs, various types of nanostructured junctions with controlled electronic properties could be possibly prepared [145]. Ma *et al.* reported that B-doping results in the improvement of graphite crystallinity, and therefore a decrease in the total number of accessible active surface sites for oxygen [146].

2.3.5 Functionalization of carbon nanostructures

A number of studies have been done on the functionalization of carbon materials. Cycloaddition reactions are a very useful method for the functionalization of C_{60} [147, 148]. Recently, Cioffi *et al.* reported the functionalization of single wall carbon nanohorns via 1,3-dipolar cycloaddition [149]. They mentioned that the organic functionalization of single wall carbon nanohorns may be advantageous for the use of nanohorns in materials science and may increase their solubility in water for possible biomedical applications. CNTs are unreactive and therefore not suitable for direct use in various applications. It is therefore essential to first functionalize CNTs before they are used for applications. It was demonstrated that the functionalization of CNTs [150, 151] via 1,3-dipolar cycloaddition [152] allows an increase in their solubility in organic solvents as well as their processing ability [153]. Although chemical functionalization disturbs the extended π-conjugation of CNTs and thus reduces the electrical conductivity of isolated nanotubes, it has been shown that covalent functionalization can improve the electrical properties of the composites [154, 155]. In their paper, Kang and Wang [111] demonstrated high chemical activity of spheres. They reported that the carbon atoms at the edge of the curling graphitic flakes must have dangling bonds with unpaired sp^2 orbitals, and these sites are expected to be chemically active.

2.3.6 Characterization techniques used for carbon spheres

(i) Transmission electron microscopy

Transmission electron microscopy (TEM) is a technique that is used to produce images of a sample by illuminating the sample with a beam of electrons. TEM works on the same principle as a light microscope except that electrons are used instead of light to observe the finer details of a specimen. The advantage of TEM is that it gives much higher resolution compared to light microscopy thereby allowing detailed study and comparison of specimens. TEM is useful in determining the morphology (size, shape and the arrangement of particles in a specimen), diameter, length and other characteristics of the carbon-based nanomaterials and other compounds. Sample preparation is important,

as the sample has to be thin. Since the sample is thin a beam of electrons is able to pass through the sample and the transmitted electrons produce an image of the sample.

(ii) Raman spectroscopy

Raman spectroscopy is one of the important methodologies that has been extensively used as a non-destructive technique to characterize the complex microstructure of carbon-based materials. It is very sensitive to structural disorder that breaks the graphitic lattice translational symmetry as it measures features in small crystals [156]. It is also sensitive to the lengths, strengths and arrangements of chemical bonds in a material, but less sensitive to the chemical composition. When monochromatic light is scattered by molecules, a small fraction of the scattered light is observed to have a frequency different from that of the irradiating light; this is known as the *Raman effect* [157]. The Raman effect arises when a beam of intense monochromatic light passes through a sample that contains molecules that can undergo a change in molecular polarizability as they vibrate. The position of the bands is modified according to the carbon forms. For CNTs the characteristic peaks are found in three spectral regions; namely the radial breathing mode (RBM), the tangential mode (G-band), and the disorder-induced mode (D-band) corresponding to the excitation of related vibrational modes [158, 159]. The RBM peaks in the range 120-250 cm^{-1} are characteristics of single-wall CNTs and they correspond to atomic vibrations of the carbon atoms in the radial direction. The G-band, characterized by peaks at around 1580 cm^{-1} indicates graphitic features. The D-band, characterized by a peak around 1345 cm^{-1} shows disordered features in graphitic sheets. The structural quality of a carbon material can be determined by the I_D/I_G ratio, i.e. the ratio between the intensities of the peaks G and D. The lower the I_D/I_G ratio, the more graphitic the structural quality of the material [160].

(iii) Thermogravimetric analysis

The details on the use of TGA are described in **Section 2.2.7**. TGA can be used to study the thermal stability of the CSs and to confirm the functionalization of the carbon spheres.

2.4 References

1. http://en.wikipedia.org/wiki/Carbon, 12 August **2008**.
2. R. L. Van der Waal, T. M. Ticich, V. E. Curtis, *J. Phys. Chem. B*, **2000**, 104, 11606.
3. Y.-M. Shyu, F. Chau-Nan Hong, *Diam. Relat. Mater.*, **2001**, 10, 1241.
4. J. Du, Z. Liu, Z. Li, B. Han, Z. Sun, Y. Huang, *Mater. Chem. Phys.*, **2005**, 93, 178.
5. V. L. Kuznetsov, A. L. Chuvilin, Y. V. Butenko, I. Y. Mal'kov, V. M. Titov, *Chem. Phys. Lett.*, **1994**, 222, 343.
6. T. Cabioc'h, E. Thune, M. Jaouen, *Chem. Phys. Lett.*, **2000**, 320, 202.
7. Y. J. Jung, B. Wei, J. Nugent, P. M. Ajayan, *Carbon*, **2001**, 39, 2195.
8. D. Ugarte, *Nature*, **1992**, 359, 707.
9. W. M. Qiao, Y. Song, S. Y. Lim, S. H. Hong, S. H. Yoon, I. Mochida, T. Imaoka, *Carbon*, **2006**, 44, 158.
10. Z. L. Wang, Z. C. Kang, *J. Phys. Chem.*, **1996**, 100, 5163.
11. Z. C. Kang, Z. L. Wang, *Philos. Mag. B.*, **1996**, 73, 905.
12. J. Y. Miao, D. W. Hwang, K. V. Narasimhulu, P. I. Lin, Y.T. Chen, S. H. Lin, L. P. Hwang, *Carbon*, **2004**, 42, 813.
13. H.-S. Qian, F.-M. Han, B. Zhang, Y.-C. Guo, J. Yue, B.-X. Peng, *Carbon*, **2004**, 42, 761.
14. R. Ryoo, S. H. Joo, M. Kruk, M. Jaroniec, *Adv. Mater.*, **2001**, 13, 677.
15. Y. Wu, P. Qiao, T. Chong, Z. Shez, *Adv. Mater.*, **2002**, 14, 64.
16. S. B. Yoon, K. Sohn, J. Y. Kim, C.-H. Shin, J.-S. Yu, T. Hyeon, *Adv. Mater.*, **2002**, 4, 19.
17. S. Frank, P. Poncharal, Z. L. Wang, W. A. de Heer, *Science*, **1998**, 280, 1744.
18. H. Haiyong, E. E. Remsen, T. Kowalewski, K. L. Wooley, *J. Am. Chem. Soc.*, **1999**, 121, 3805.
19. P. Kim, C. M. Lieber, *Science*, **1999**, 286, 2148.
20. C. Liu, Y. Y. Fan, H. T. Cong, H. M. Cheng, M. S. Dresselhaus, *Science*, **1999**, 286, 1127.

21. J. Kong, C. Zhou, A. Morpurgo, H. T. Soh, C. F. Quate, C. Marcus, H. Dai, *Appl. Phys. A.*, **1999**, 69, 305.
22. M. Shim, A. Javey, N. W. S. Kam, H. J. Dai, *J. Am. Chem. Soc.*, **2001**, 123, 11512.
23. A. M. Benito, Y. Maniette, E. Munoz, M. T. Matrinez, *Carbon*, **1998**, 36, 681.
24. R. Taylor, *Lecture notes in fullerene chemistry: A handbook for Chemists*, Imperial College Press, London, **1999**.
25. H. W. Kroto, J. R. Heath, S. C. O'Brien, R. F. Curl, R. E. Smalley, *Nature*, **1985**, 318, 162.
26. (a) W. Kratschmer, L. Lamb, K. Fostiropoulos, D. R. Huffman, *Nature*, **1990**, 357, 354; (b) W. Kratschmer, L. Lamb, K. Fostiropoulos, D. R. Huffman, *Chem. Phy. Lett.*, **1990**, 170, 167; (c) H. W. Kroto, A. W. Allaf, S. P. Balm, *Chem. Rev.*, **1991**, 91, 1213.
27. M. S. Dresselhaus, G. Dresselhaus, P. C. Eklund, *Science of Fullerenes and Carbon nanotubes*, Elsevier Science, USA, **1996**.
28. www.AZoNano.com, 12 August **2008**.
29. R. Taylor, J. P. Hare, A. K. Abdul-Sada, H. W. Kroto, *J. Chem. Soc., Chem. Commun.*, **1990**, 1423.
30. P. W. Fowler, D. E. Manolopoulos, *An atlas of fullerenes*, Oxford University Press Inc., New York, **1995**.
31. J. L. Segura, N. Martin, *Chem. Rev.*, **1999**, 99, 3119.
32. T. G. Dietz, M. A. Duncan, D. E. Powers, R. E. Smalley, *J. Chem. Phys.*, **1981**, 74, 6511.
33. R. F. Curl, R. E. Smalley, *Science*, **1988**, 242, 1017.
34. R. Taylor, A. G. Avent, P. R Birkett, T. J. S. Dennis, J. P. Hare, P. B. Hitchcock, J. H. Holloway, E. G. Hope, H. W. Kroto, G. J. Langley, M. F. Meidine, J. P. Parsons, D. R. M. Walton, *Pure Appl. Chem.*, **1993**, 65, 135.
35. http://en.wikipedia.org/wiki/Fullerene_chemistry, 15 September **2008**.
36. H. Ajie, M. M. Alvarez, S. J. Anz, R. D. Beck, F. Diederich, K. Fostiropoulos, D. R. Huffman, W. Krätschmer, Y. Rubin, K. E. Schriver, D. Sensharma, R. L. Whetten, *J. Phys. Chem.*, **1990**, 94, 8630.

37. A. Hirsch, M. Brettreich, *Fullerenes: chemistry and reactions*, Weinheim, Germany, **2005**.
38. J. R. Heath, S. C. O'Brien, Q. Zhang, Y. Liu, R. F. Curl, H. W. Kroto, F. K. Tittle R. E. Smalley, *J. Am. Chem. Soc.*, **1985**, 107, 7779.
39. M. Prato, *J. Mater. Chem.*, **1997**, 7, 1097.
40. Fullerene www.wikipedia.com, 31 April **2006**.
41. A. L. Balch, M. M. Olmstead, *Chem. Rev.*, **1998**, 98, 2123.
42. P. J. Fagan, J. C. Calabrese, B. Malone, *Acc. Chem. Res.*, **1992**, 25, 134.
43. F. Diederich, *Pure Appl. Chem.*, **1997**, 69, 395.
44. H. Tokuyama, S. Yamago, E. Nakamura, T. Shiraki, Y. Sugiura, *J. Am. Chem. Soc.*, **1993**, 115, 7918.
45. S. H. Friedman, D. L. DeCamp, R. P. Sijbesma, G. Srdavon, F. Wudl, G. L. Kenyon, *J. Am. Chem. Soc.*, **1993**, 115, 6506.
46. R. P. Sijbesma, G. Srdavon, F. Wudl, J. A. Castoro, C. Wilkins, S. H. Friedman, D. L. DeCamp, G. L. Kenyon, *J. Am. Chem. Soc.*, **1993**, 115, 6510.
47. E. Nakamura, H. Isobe, N. Tomita, M. Sawamura, S. Jinno, H. Okayama, *Angew, Chem, Int. Ed.*, **2000**, 39, 4254.
48. E. Nakamura, H. Isobe, *Acc. Chem. Res.*, **2003**, 36, 807.
49. N. S. Sariciftci, L. Smilowitz, A. Heeger, F. Wudl, *Science*, **1992**, 258, 1474.
50. G. Yu, J. Guo, J. C. Hummelen, F. Wudl, A. Heeger, *Science*, **1995**, 270, 1789.
51. A. Hirsch, *The chemistry of fullerenes*, Thieme, Stuttgart, **1994**.
52. V. M. Rotello, J. B. Howard, T. Yadav, M. M. Conn, E. Viani, L. M. Giovane, A. L. Lafluer, *Tetrahedron Lett.*, **1993**, 34, 1561.
53. N. Zhang, S. R. Schricker, F. Wudl, *Chem. Mater.*, **1995**, 7, 441.
54. H. Ishida, K. Komori, K. Itoh, M. Ohno, *Tetrahedron Lett.*, **2000**, 41, 9839.
55. M. Saunders, H. A. Jimenz-Vazquez, R. J. Cross, S. Mroczkowski, D. E. Gilbin, R. J. Poreda, *J. Am. Chem. Soc.*, **1994**, 116, 2193.
56. N. Martin, *Chem. Commun.*, **2006**, 2093.

57. (a) S. Laus, B. Sitharaman, E. Toth, R. D. Bolskar, L. Helm, S. Asokan, M. S. Wong, L. J. Wilson, and A. E. Merbach, *J. Am. Chem. Soc.*, **2005**, 127, 9368, (b) E. Toth, R. D. Bolskar, A. Borel, G. Gonzalez, L. Helm, A. E. Merbach, B. Sitharaman, and L. J. Wilson, *J. Am. Chem. Soc.*, **2005**, 127, 799.
58. A. Hirsch, B. Nuber, *Acc. Chem. Res.*, **1999**, 32, 795.
59. M. M. Roubelakis, G. C. Vougioukalakis, M. Orfanopoulos, *J. Org. Chem.*, **2007**, 72, 6526.
60. J. C. Hummelen, M. Prato, F. Wudl, *J. Am. Chem. Soc.*, **1995**, 117, 7003.
61. www.foresight.org/conference/MNT11/Abstracts/Osipov/index.html, 15 April **2006**.
62. P. J. Fagan, J. C. Calabrese, B. Malone, *Science*, **1991**. 252, 1160.
63. (a) C. Jehoulet, Y. S. Oben, Y.-T. Kim, F. Zhou, A. J. Bard, *J. Am. Chem. Soc.*, **1992**, 114, 4237; (b) Q. Xie, E. Perez-Cordero, L. Echegoyen, *J. Am. Chem. Soc.*, **1992**, 114, 3978; (c) Y. Wang, R. West, C.-H. Yuan, *J. Am. Chem. Soc.*, **1993**, 115, 3844.
64. P.-M. Allemand, K. C. Khemani, A. Koch, F. Wudl, K. Holkzer, S. Donovan, G. Gruner, J. D. Thompson, *Science*, **1991**, 253, 301.
65. F. Wudl, A. Hirsch, K. C. Khemani, T. Suzuki, P.-M. Allemand, A. Koch, H. Eckert, G. Srdavon, H. M. Webb, *ACS Symp. Ser.*, **1992**, 481 (Fullerenes), 161.
66. N. Zhang, S. R. Schricker, F. Wudl, M. Prato, M. Maggini, G. Scorrano, *Chem. Mater.*, **1995**, 7, 441.
67. K. E. Geckeler, A. Hirsch, *J. Am. Chem. Soc.*, **1993**, 115, 3850.
68. C. J. Hawker, *Macromolecules*, **1994**, 27, 4836.
69. (a) K. I. Guhr, M. D. Greaves, V. M. Rotello, *J. Am. Chem. Soc.*, **1994**, 116, 5997; (b) B. Nie, K. Hasan, M. D. Greaves, V. M. Rotello, *Tetrahedron Lett.*, **1995**, 36, 3617.
70. C. Mathis, B. Schmaltz, M. Brinkmann, *C. R. Chimie*, **2006**, 9, 1075.
71. M. Prato, *Fullerene Materials*, *Topics in Current Chemistry*, **1999**, 199, 173.
72. See for example: T. Song, S. H. Goh, S. Y. Lee, *Polymer*, **2003**, 44, 2563 .
73. C. Wang, Z. Guo, S. Fu, W. Wu, D. Zhu, *Prog. Polym. Sci.*, **2004**, 29, 1079.
74. F. Giacalone, N. Martin, *Chem. Rev.*, **2006**, 106, 5136.

75. R. Taylor, *The Chemistry of the Fullerenes*, World Scientific, Singapore, **1995**.
76. T. Benincori, E. Brenna, F. Sannicolo, L. Trinmarco, G. Zotti, P. Sozzani, *Angew. Chem., Int. Ed.*, **1996**, 35, 648.
77. (a) B. Nie, V. M. Rotello, *Macromolecules*, **1997**, 30, 3949; (b) L. Xiao, H. Shimotani, M. Ozawa, J. Li, N. Dragoe, K. Saigo, K. Kitazawa., *J. Polym. Sci., Part A: Polym. Chem.*, **1999**, 37, 3632; (c) H. Okamura, T. Terauchi, M. Minoda, T. Fukuda, K. Komatsu, *Macromolecules*, **1997**, 30, 5279; (d) A. Gügel, P. Belik, M. Walter, A. Kraus, E. Harth, M. Wagner, J. Spickermann, K. Müllen, *Tetrahedron*, **1996**, 52, 5007.
78. D. A. Loy, R. A. Assink, *J. Am. Chem. Soc.*, **1992**, 11, 3977.
79. K. M. Chen, W. B. Caldwell, C. A. Mirkin, *J. Am. Chem. Soc.*, **1993**, 115, 1193.
80. J. A. Chupa, S. T. Xu, R. F. Fischetti, *J. Am. Chem. Soc.*, **1993**, 115, 4383.
81. A. Bianco, F. Gasparrini, M. Maggini, D. Misiti, A. Polese, M. Prato, G. Scorrano, C. Toniolo, C. Villani, *J. Am. Chem. Soc.*, **1997**, 119, 7550.
82. L. Y. Chiang, L. Y. Wang, S. Tseng, J. Wu, K. Hsieh, *J. Chem. Soc., Chem. Comm.*, **1994**, 2675.
83. X. D. Huang, S. H. Goh, S. Y. Lee, *Macromol. Chem. Phys.*, **2000**, 201, 2660.
84. X. D. Huang, S. H. Goh, *Polymer*, **2002**, 43, 1417.
85. X. D. Huang, S. H. Goh, *Macromolecules*, **2000**, 33, 8894.
86. T. Song, S. H. Goh, S. Y. Lee, *Polymer*, **2003**, 44, 2563.
87. Y. Kojima, T. Matsuoka, H. Takahashi, T. Kuruchi, *J. Appl. Polym. Sci.*, **1997**, 65, 2781.
88. P. I. Navak, K. Yang, P. K. Dhal, S. Alva, J. Kumar, S. K. Tripathy, *Chem. Mater.*, **1998**, 10, 2058.
89. Y. Chen, Y. Zhao, R. Cai, Z. E. Huang, L. Xiao, *J. Polym. Sci., Part B: Polym. Phys.*, **1998**, 36, 2653.
90. L. Y. Chiang, L. Y. Wang, C. S. Kuo, *Macromolecules*, **1995**, 28, 7574.
91. T. Zhang, K. Xi, X. Yu, M. Gu, S. Guo, B. Gu, H. Wang, *Polymer*, **2003**, 44, 2647.
92. A. Gügel, P. Belik, M. Walter, A. Kraus, E. Harth, M. Wagner, J. Spickerman, K. Müllen, *Tetrahedron*, **1996**, 52, 1996.

93. S. Shi, K. C. Khemani, Q. Li, F. Wudl, *J. Am. Chem. Soc.*, **1992**, 114, 10656

94. A. Kraus, K. Müllen, *Macromolecules*, **1999**, 32, 4214.

95. R. Taylor, *Lecture notes in fullerene chemistry*: *A handbook for Chemists*, Imperial College Press, London, **1999**.

96. B. Dardel, D. Guillon, B. Heinrichb, R. Deschenaux, *J. Mater. Chem.*, **2001**, 11, 2814.

97. Paula, Yurkanis, Bruice, *Organic Chemistry*, Prentice Hall, International ed. Englewood Cliffs, New Jersey, **1995**.

98. L. G. Wade, *Organic Chemistry*, 5th ed. Prentice Hall, New Jersey, **2003**.

99. H. H. Willard, L. L. Merritt, J. A. Dean, F. A. Settle, *Instrumental methods of analysis*. Sixth Edition. Wadsworth Publishing Company. Belmont, California, **1981**.

100. www.flemingptc.co.uk/our-services/dsc-tga, 18 November **2007**.

101. M. E. Brown, *Handbook of thermal analysis and calorimetry Vol. 1, Principles and practice*. Elsevier, Amsterdam, **1998**.

102. P. J. Haine, *Thermal methods of analysis. Principles, applications and problems.* Chapman and Hall, London, **1995**.

103. Y. Z. Jin, C. Gao, W. K. Hsu, Y. Zhu, A. Huczko, M. Bystrzejewski, M. Roe, C. Y. Lee, S. Acquah, H. Kroto, D. R. M. Walton, *Carbon*, **2005**, 43, 1944.

104. S. Iijima, *Nature*, **1991**, 354, 56.

105. M. S. Dresselhaus, G. Dresselhaus, P. Avouris, *Carbon nanotubes: Synthesis structure, properties, and applications*, Springer, Heidelberg, **2001**.

106. F. J. Gomez, R. J. Chen, D. Wang, R. M. Waymouth, H. Dai, *Chem. Commun.*, **2003**, 190.

107. K. Takai, M. Oga, T. Enoki, A. Taomoto, *Diamond. Relat. Mater.*, **2004**, 13, 1469.

108. Carbon nanotube www.wikipedia.com, 08 February **2006**.

109. A. J. Laurence, *Carbon*, **2006**, 44, 158.

110. R. Alcantara, F. J. Fernandez Madrigal, P. Lavela, J. L. Tirado. *Carbon*, **2000**, 38, 1031.

111. Z. L. Wang, Z. C. Kang, *J. Phys. Chem.*, **1996**, 100, 5163.

112. Ph. Serp, R. Feurer, Ph. Kalck, Y, Kihn, J. L. Faria, J. L. Figueiredo, *Carbon*, **2001**, 39, 621.
113. J. S. Qiu, Y. F. Li, Y. P. Wang, C. H. Liang, T. H. Wang, D. B. Wang, *Carbon*, **2003**, 41, 767.
114. Z. L. Wang, Z. C. Kang, *J. Phys. Chem.*, **1996**, 100, 17725.
115. H.-S. Qian, F.-M. Han, B. Zhang, Y.-C. Guo, J. Yue, B.-X. Peng, *Carbon*, **2004**, 42, 761.
116. M. Inagaki, *Synthetic Met.*, **2002**, 125, 139.
117. E. Auer, A. Freund, J. Pietsch, T. Tacke, *Appl. Catal.*, **1998**, 173, 259.
118. M. Sharon, K. Mukhopadhyay, K. Yase, S. Iijima, Y. Ando, X. Zhao, *Carbon*, **1998**, 36, 507.
119. S. Flandrois, B. Simon, *Carbon*, **1999**, 37, 165.
120. V. Vignal, A. W. Morawski, H. Konno, M. Inagaki, *J. Mater. Res.*, **1999**, 14, 1102.
121. M. Inagaki, V. Vignal, H. Konno, A. W. Morawski, *J. Mater. Res.*, **1999**, 14, 3152.
122. J. Y. Miao, D. W. Hwang, K. V. Narasimhulu, P. I. Lin, Y.T. Chen, S. H. Lin, L. P. Hwang, *Carbon*, **2004**, 42, 813.
123. Z. C. Kang, Z. L. Wang, *Philos. Mag. B.*, **1996**, 73, 905.
124. W. M. Qiao, Y. Song, S. Y. Lim, S. H. Hong, S. H. Yoon, I. Mochida, T. Imaoka, *Carbon*, **2006**, 44, 158.
125. S. Iijima, *J. Cryst. Growth*, **1980**, 50, 675.
126. D. Ugarte, *Nature*, **1992**, 359, 707.
127. X. Y. Liu, B. C. Huang, N. J. Coville, *Carbon*, **2002**, 40, 2791.
128. Z. Zhong, H. Chen, S. Tang, J. Ding, J. Lin, K. L. Tan, *Chem. Phys. Lett.*, **2000**, 330, 41.
129. Z. L. Wang, Z. C. Kang, *Carbon*, **1997**, 35, 419.
130. A. Govindaraj , R. Sen, B. V. Nagaraju, C. N. R. Rao, *Philos. Mag. Lett.*, **1997**, 76, 363.
131. L. Q. Xu, W. Q. Zhang, Q. Yang, W. C. Yu, Y. T. Qian. *Carbon*, **2005**, 43, 1084.
132. D. Pradhan, M. Sharon, *Mater. Sci. Eng. B.*, **2002**, 96, 24.

133. Z. S. Lou, Q. W. Chen, J. Gao, Y. F. Zhang, *Carbon*, **2004**, 42, 229.
134. M. Aili, W. Xiaomin, L. Tianbao, L. Xuguang, X. Bingshe. *Mater. Sci. Eng. A*, **2007**, 443, 54.
135. Q. Li, H. Yan, J. Zhang, J. Liu, *Carbon*, **2004**, 42, 829.
136. H. W. Kroto, K. McKay, *Nature*, **1988**, 331, 328.
137. S. Saito, *Science*, **1997**, 278, 77.
138. M. Terrones, N. Grobert, H. Terrones, *Carbon*, **2002**, 40, 1665.
139. O. Stephen P. M. Ajayan, C. Colliex, P. Redlich, J. M. Lambert, P. Bernier, P. Lefin, *Science*, **1994**, 266, 1683.
140. Y. Komatsu, *Carbon*, **1969**, 7, 177.
141. G. Henning, *J. Chem. Phys.*, **1965**, 42, 1167.
142. A. Marchand, *Chem. Phys. Lett.*, **1971**, 7, 155.
143. S. Marinkovic, *Chem. Phys. Lett.*, **1984**, 19, 1.
144. J.-C. Charlier, M. Terrones, M. Baxendale, V. Meunier, T. Zacharia, N. L. Rupesinghe, W. K. Hsu, N. Grobert, H. Terrones, G. A. J. Amaratunga, *Nano. Lett.*, **2002**, 2.
145. Q. Yang, W. Xu, A. Tomita, T. Kyotani, *J. Am. Chem. Soc.*, **2005**, 127, 8956.
146. X. Ma, Q. Wang, L.-Q. Chen, W. Cermignani, H. H. Schobert, C. G. Pantano, *Carbon*, **1997**, 35, 1517.
147. F. Wudl, *Acc. Chem. Res.*, **1992**, 25, 157.
148. M. Prato, T. Suzuki, F. Wudl, V. Lucchini, M. Maggini, *J. Am. Chem. Soc.*, **1993**, 115, 7876.
149. C. Cioffi, S. Campidelli, F. G. Brunetti, M. Meneghetti, M. Prato, *Chem. Commun.*, **2006**, 2129.
150. V. Georgakilas, K. Kordatos, M. Prato, D. M. Guldi, M. Holzinger, A. Hirsch, *J. Am. Chem. Soc.*, **2002**, 124, 760.
151. V. Georgakilas, N. Tagmatarchis, D. Pantarotto, A. Bianco, J-P. Briand, M. Prato, *Chem. Commun.*, **2002**, 3050.
152. M. Prato, M. Maggini, *Acc. Chem. Res.*, **1998**, 31, 519.
153. A. Bianco, M. Prato, *Adv. Mater.*, **2003**, 15, 1765.
154. S. Li, Y. Qin, J. Shi, Z.-X. Guo, Y. Li, D. Zhu, *Chem. Mater.*, **2005**, 17, 130.

155. L. Valentin, I. Armentano, D. Puglia, J. M. Kenny, *Carbon*, **2004**, 42, 323.
156. V. Mennella, G. Monaco, L. Colangeli, E. Bussoletti, *Carbon*, **1995**, 33, 115.
157. H. H. Willard, L. L. Merritt, J. A. Dean, F. A. Settle, Instumental Methods of Analysis, sixth edition, **1981**.
158. J. Maultzsch, S. Reich, C. Thomsen, *Phys. Rev. B.*, **2002**, 65, 233.
159. M. S. Dresselhaus, G. Dresselhaus, R. Saito, *Phys. Reports*, **2005**, 409, 47.
160. C. J. Lee, J. Park, J. A. Yu, *Chem. Phys. Lett.*, **2002**, 360, 250.

CHAPTER 3
THE SYNTHESIS OF C_{60}-CONTAINING POLYMERS

3.1 Introduction

Research in fullerene chemistry is driven by the need to functionalize fullerenes and tune their properties. Since fullerene is not very soluble, adding a suitable functional group to a fullerene can enhance its solubility [1]. By the addition of a polymerizable group, a fullerene-containing polymer can be obtained. As previously stated, when a small amount of a carbon nanomaterial such as C_{60} is introduced into a polymer system, photoconductivity, mechanical and optical limiting properties of the polymer can be improved. Furthermore, C_{60}-containing polymers can possess many of the properties associated with the C_{60} [2-4]. Over the past decades polynorbornene has attracted a great deal of attention because of its industrial applications as a noise- and vibration-dampening agent and a specialty elastomer [5]. The increase in the production of substituted polynorbornenes has grown as a result of these properties, as well as the facile functionalization and polymerization associated with the bicyclic monomer [6-8].

Polymers can be made from cyclic olefins such as norbornene and cyclopentene. Ring opening metathesis polymerization (ROMP), a term coined by a chemist Robert Grubbs, is a type of olefin metathesis polymerization that produces industrially useful products. The driving force for the ROMP reaction is the relief of ring strain in cyclic olefins [9, 10]. A wide variety of catalysts used in ROMP reactions have been discovered. These include a wide range of metals, from a $RuCl_3$/alcohol mixture to the Grubbs' catalyst [11, 12]. In a ROMP reaction, the initiator is usually a metal-carbene species (a compound with a carbon atom double bonded to a metal atom, like molybdenum, ruthenium, or tungsten). The metal-carbene reacts with the double bond of a ring structure forming a highly strained metallacyclobutane intermediate. The strained ring then opens giving a complex in which a metal is attached to a carbon chain containing a carbon-carbon double bond. The propagation step is via the reaction of the new carbene with the double

bond on the next monomer [13]. The mechanism of the ROMP reaction is shown below (**Scheme 3.1**) [10].

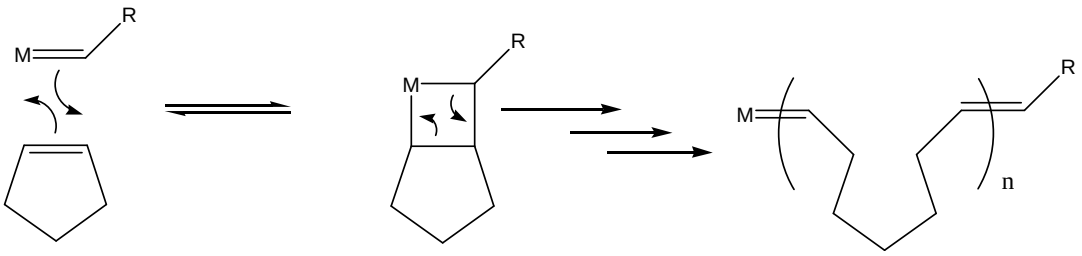

M = Metal

Scheme 3.1: The mechanism of the ROMP reaction.

The choice of a catalyst plays a vital role in a ROMP reaction. For example, if the catalyst is too active, it can metathesize the unstrained olefinic bonds in the growing polymer chain, thereby reducing the molecular weight and increasing the molecular weight distribution (polydispersity) [10]. Another important issue in ROMP catalysis is the substituent effect. The addition of substituents to the ring system can cause the formation of more complex or more functionalized polymer products. In addition, some substituents can react with some of the common catalysts. For example, the first Grubbs' catalyst was poisoned by nitrile or amine groups [14] and many common Mo or W metathetical catalysts are affected by oxygenate or nitrogeneous groups. Ruthenium carbene complexes that are not affected by these functional groups have now been discovered. The most widely used organometallic complex for the ROMP reaction is the Grubbs' second generation catalyst (**Figure 3.1**). Due to its remarkable tolerance to functional groups and its stability towards air and moisture [15], the Grubbs II catalyst allows the polymerization of highly functionalized and sterically hindered monomers to proceed. Finally, functionalized norbornenes have proved to be easily prepared and highly reactive in the ROMP reaction [16]. The carbon materials can undergo reactions such as ROMP with functionalized norbornene derivative monomers [17]. The norbornene-based monomers are popular as they can be readily prepared from Diels-Alder reactions with cyclopentadiene.

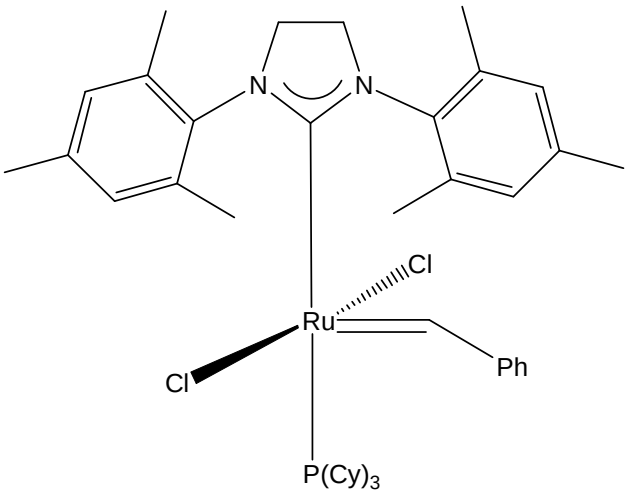

Figure 3.1: The Grubbs' second generation catalyst suitable in ROMP reactions.

The first C_{60}-containing polymer synthesized via a ROMP procedure was reported in 1995 by Zhang and co-workers [17]. They synthesized a high molecular weight polymer from the copolymerization of a C_{60}-quadricyclane adduct and norbornene with a Schrock catalyst (**Scheme 3.2 and 3.3**) [17].

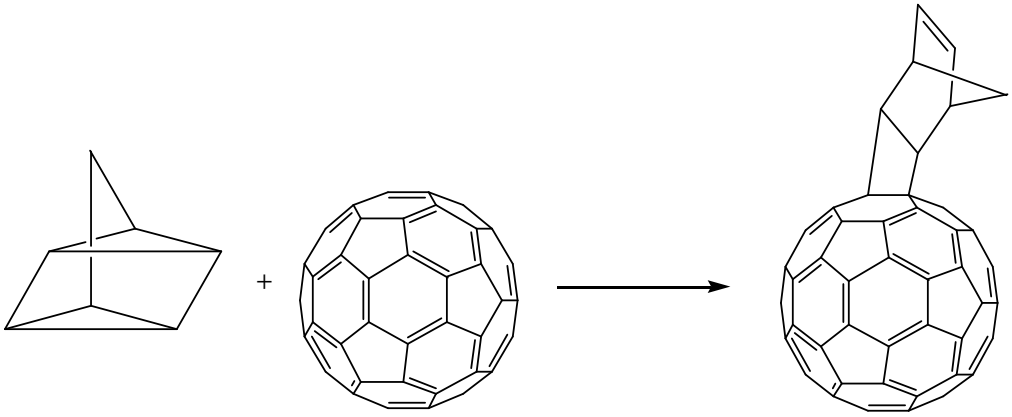

Scheme 3.2: Preparation of C_{60}-quadricyclane cycloadduct [17].

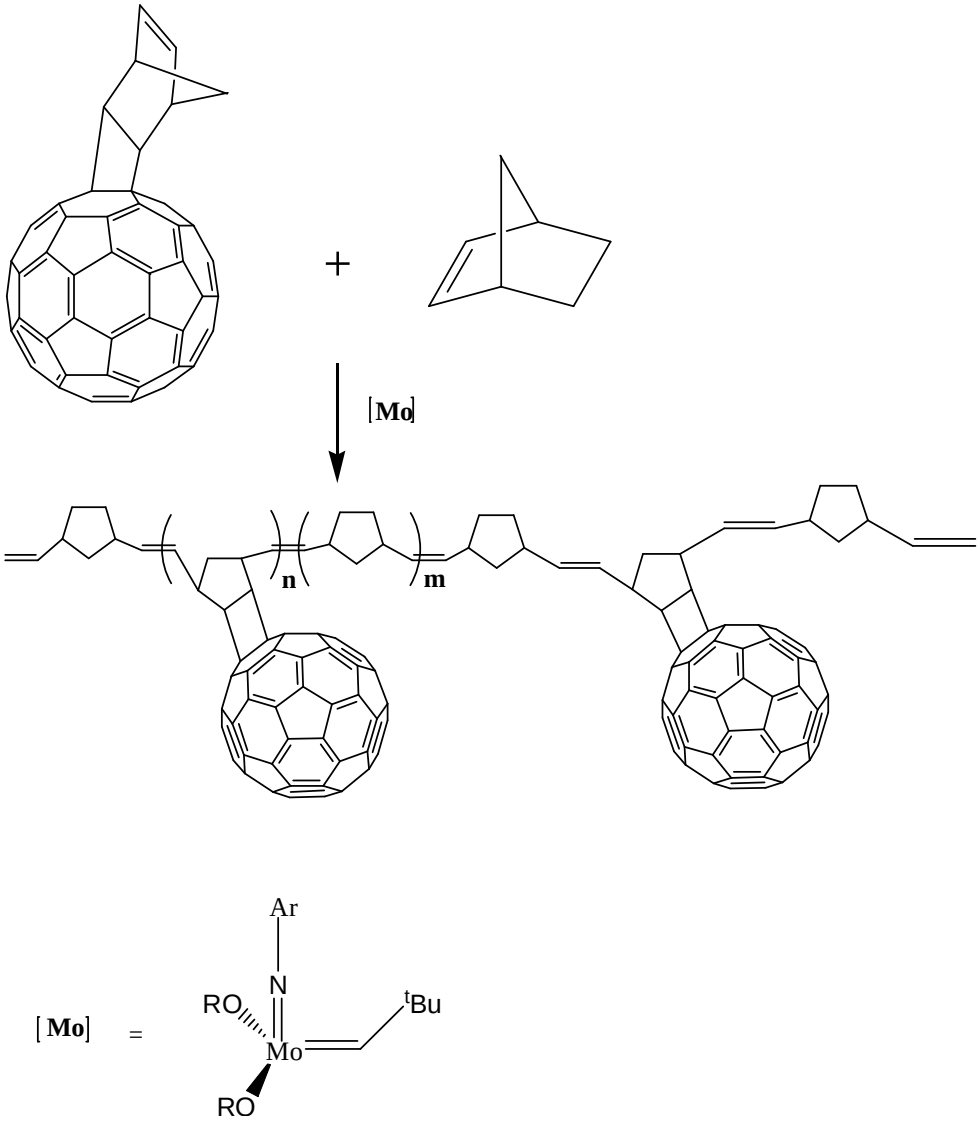

Scheme 3.3: ROMP of C_{60}-quadricyclane cycloadduct-norbornene polymer [17].

In this chapter, the syntheses of C_{60}-containing polymers are reported. The C_{60} molecule **1** was first functionalized with 1,3-cyclohexadiene **2** to obtain a novel C_{60}-cyclohexadiene cycloadduct **3**, see page 53. This co-monomer was then polymerized with norbornene **4** using the Grubbs' second generation catalyst (**Figure 3.1**) via a ROMP approach. As mentioned before, C_{60} derivatives have been incorporated into norbornene polymers. 1,4,5,6,7,7-Hexachloro-5-norbornene-endo-2,3-dicarboxylic anhydride ($C_9H_2Cl_6O_3$) **7** is a chlorinated hydrocarbon used in the synthesis of some flame retardants and polymers [18]. $C_9H_2Cl_6O_3$ is slightly soluble in water and nonpolar organic

solvents such as benzene and easily soluble in slightly polar organic solvents such as methanol. This easily available compound was functionalized with cycloheptylamine to obtain the 1,4,5,6,7,7-hexachloro-5-norbornene-endo-2,3-heptylimide ($C_{16}H_{15}O_2Cl_6N$) **10**. To our knowledge there has been no attempt to utilise $C_{16}H_{15}O_2Cl_6N$ in C_{60}-based polymers. In addition, the fact that this novel compound is so strained and there would be significant relief of ring strain on opening of the fused ring by ROMP, led us to look into its synthesis and its copolymerization with the C_{60}-cyclohexadiene cycloadduct for the purpose of comparison with C_{60}-cyclohexadiene cycloadduct norbornene polymer. The new materials were characterized and their electronic and thermal properties were studied.

3.2 Experimental

3.2.1 Chemicals and materials

Fullerene [C_{60} (99.5 %)], cyclohexadiene, carbon disulfide, chloroform, Grubbs second generation catalyst, potassium bromide, dichloromethane, 1,4,5,6,7,7-hexachloro-5-norbornene-2,3-dicarboxylic anhydride, cycloheptylamine, acetic anhydride, sodium acetate, ethyl vinyl ether and methanol were purchased from the Sigma-Aldrich Chemical Company. Toluene was purchased from Merck and hydrochloric acid was purchased from the Association Chemical Enterprises (Pty) LTD. All chemicals were used as received and all reactions were performed under a nitrogen atmosphere.

3.2.2 Measurements

3.2.2.1 Infrared spectroscopy

IR spectra of the C_{60}-based materials were recorded on a Bruker Vector 22 Fourier Transform Infrared Spectrometer as KBr pellets (2 mg sample and 200 mg KBr). The mixture was pressed using an evacuable die at sufficient pressure to produce a transparent disk. The percentage transmittance over the range of 400-4000 cm^{-1} was recorded.

3.2.2.2 Mass spectrometry

Mass spectra were collected using a VG70-SEQ instrument in a positive ion mode using FAB ionization. Approximately 1 mg of sample was supplied for analysis.

3.2.2.3 Ultra-violet / visible spectroscopy

Ultraviolet and visible spectra of the samples were obtained on a Varian 50 CONC UV/Visible spectrophotometer. Samples of 10 mg of the compound dissolved in dichloromethane were placed in a cuvette. The cuvette was then placed in the instrument and absorbances were recorded. The band positions are expressed in terms of wavelength (nm).

3.2.2.4 Nuclear magnetic resonance spectroscopy

Samples were analysed using a Bruker Avance 300 spectrometer, 300 MHz ^{1}H operating frequency and 75.75 MHz ^{13}C operating frequency. Spectra were recorded in $CDCl_3$:CS_2 (1:1) against a tetramethylsilane (TMS) internal standard. Approximately 10 mg of sample was supplied for analysis. The operating temperature was 300K. Chemical shifts (δ) are expressed in units of ppm. The following abbreviations are used in the assignment of chemical shifts: s (singlet), d (doublet), t (triplet), q (quartet), m (multiplet), mm (multiplet of multiplets).

3.2.2.5 Differential Scanning Calorimetry

A Mettler Toledo DSC 822e was used to analyse the polymers. Polymers (5-10 mg) were analysed in a 40 µl aluminium sample pan with a lid and analysed over a range of temperatures (25-200 °C). A heating rate of 5 °C/min was used with a nitrogen flow of 60 ml/min. Peak positions were recorded in units of degree Celsius (°C).

3.2.2.6 Thermogravimetric Analysis

TGA experiments were performed on a Perkin Elmer, Pyris 1 TGA analyzer under a N_2 atmosphere in the temperature range 25-800 °C at a heating rate of 10 °C/min. Peak positions are recorded in units of degree Celsius.

3.2.2.7 Crystal structure determination

Intensity data were collected on a Bruker SMART 1K CCD area detector diffractometer with graphite monochromated Mo Kα radiation (50 kV, 30 mA). The collection method involved ω-scans of width 0.3°. Data reduction was carried out using the program SAINT+ [19]. The crystal structure was solved by direct methods using SHELXTL [20]. Non-hydrogen atoms were first refined isotropically, followed by anisotropic refinement by full-matrix least-squares calculation based on F^2 using SHELXTL. Hydrogen atoms were first located in the difference map, then positioned geometrically and allowed to ride on their respective parent atoms. Further crystal and refinement data are given in **Appendix B**. Diagrams were generated using SHELXTL [20], PLATON [21] and ORTEP3 [22].

3.2.3 Synthetic procedures

3.2.3.1 The synthesis of C_{60}-cyclohexadiene cycloadduct (3)

The C_{60}-cyclohexadiene cycloadduct **3** was synthesized according to a literature procedure [23] in which one equivalent of both C_{60} **1** (0.500 g, 0.694 mmol) and 1,3-cyclohexadiene **2** (0.056 g, 0.70 mmol) in toluene (30 ml) were stirred at 60 °C to give a purple solution. After stirring for 5 days the reaction mixture changed to a brown colour and the solvent was removed under reduced pressure to give a brown solid. This solid was purified using column chromatography (SiO_2, toluene) to afford the unreacted C_{60} and the expected 1:1 cycloadduct in 28 % yield (72 % yield based on consumed C_{60}). **Scheme 3.4** demonstrates the synthesis of **3.** FAB mass spectrometry showed the expected molecular ion peak at *m/z* 801 for the 1:1 cycloadduct together with the C_{60} peak at *m/z* 721 (**Appendix A1**). The structure was also supported by the IR absorption at 528 cm^{-1}, a characteristic feature of a 6,6-cycloadduct of C_{60}. The use of 5 equivalents of **2** at both 60 °C and 80 °C (48 hours) increased the product yield (74 % and 78 %, respectively), but gave a product that showed both mono and disubstitution. The mass spectra (**Figure 3.2 and Appendix A2**) of these products show a mixture of monoaddition and bisaddition of addends occurring at 6,6 junctions of C_{60}.

^{1}H NMR: 6.10 ppm (2H, s, C=C**H**); 2.53 ppm (2H, m, C-C**H**); 1.25 ppm (4H, d, C-C**H_2**, J_{HH} = 6.8 Hz). **FAB MS:** *m/z* 721, $C_{60;}$ *m/z* 801, monoadduct; *m/z* 881.2, bisadduct.

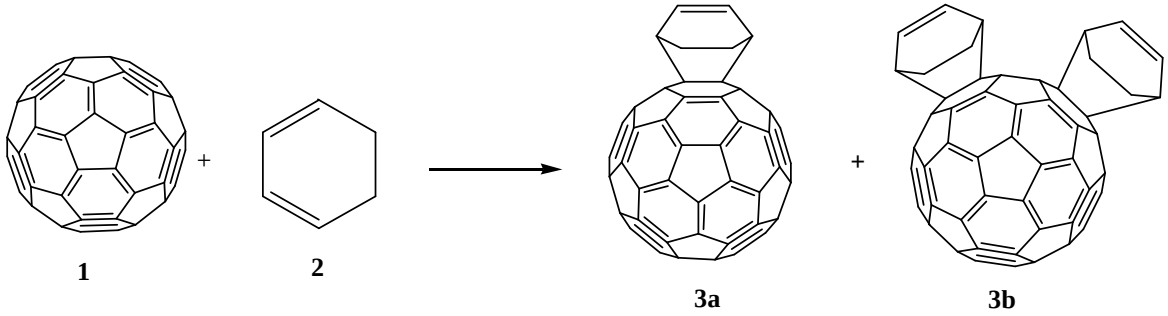

1 **2** **3a** **3b**

Scheme 3.4: The synthesis of C_{60}-cyclohexadiene cycloadduct **3** (**3a** and **3b**).

3.2.3.2 The synthesis of polynorbornene (5)

Norbornene (1.00 g, 10.6 mmol) **4** was stirred in toluene (35 ml) for 15 min under a nitrogen atmosphere at room temperature. Grubbs II catalyst (10.0 mg, 11.8 µmol) was added to the solution and the reaction mixture was left to stir for a further 45 min. The polymerization was terminated by adding a few drops of ethyl vinyl ether (~2-3 drops) and the solution was poured into an excess of MeOH (200 ml) containing a few drops of 1 M HCl to precipitate the crude polymer. MeOH was then removed using a rotary evaporator. The resulting polymer **5 (**shown in **Scheme 3.5)** was dried in a vacuum oven at 35 °C to constant weight and was found to be cream white in colour (0.960 g, yield: 96 % based on norbornene). The *cis*/*trans* ratio for polymer **5** was found to be 59/41 by integrating the *cis* and *trans* olefinic proton resonances at 5.21 and 5.35 ppm, respectively.

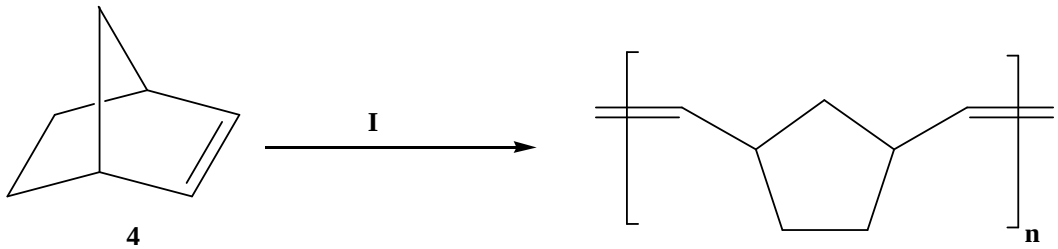

4 **5**

Scheme 3.5: The synthesis of polynorbornene **5** using ROMP. **I** = (a) toluene, Grubbs II catalyst; (b) ethyl vinyl ether, MeOH, 1M HCl.

3.2.3.3 Copolymerization of C_{60}-cyclohexadiene cycloadduct (3) with norbornene (4)

The polymerization reaction was carried out on a molar ratio of 100:1 of norbornene **4** to C_{60}-cyclohexadiene cycloadduct **3**. Norbornene (1.00 g, 10.6 mmol) and C_{60}-cyclohexadiene adduct (0.0849 g, 0.106 mmol) were stirred in a mixture of 1:1 CS_2: $CHCl_3$ (30 ml) for 15 min under a nitrogen atmosphere at room temperature. Grubbs II catalyst (10.0 mg, 11.8 µmol) was added and the reaction mixture was left to stir for a further 1 hour. The reaction mixture was terminated by adding a few drops of ethyl vinyl ether (~2-3 drops) and the solution was poured into an excess of MeOH (200 ml) containing a few drops of 1 M HCl to precipitate the crude polymer. MeOH was then removed using a rotary evaporator. The resulting co-polymer was dried in a vacuum oven at 35 °C to constant weight and was found to give a light brown rubbery material in good yield (0.933 g, 86 %). This reaction was repeated with varying monomer ratios of **4** to **3** to give the products in good yields: 300:1 (0.823 g, 80 % yield), 500:1 (0.834 g 82 % yield), 700:1 (0.789 g, 78 % yield) and 1000:1 (0.816 g, 81 % yield) molar ratios. The obtained polymers (**6A-E** in **Scheme 3.6**) were found to be dark to light brown in colour, with the colour being indicated by the amount of C_{60}-cyclohexadiene cycloadduct used in the reaction.

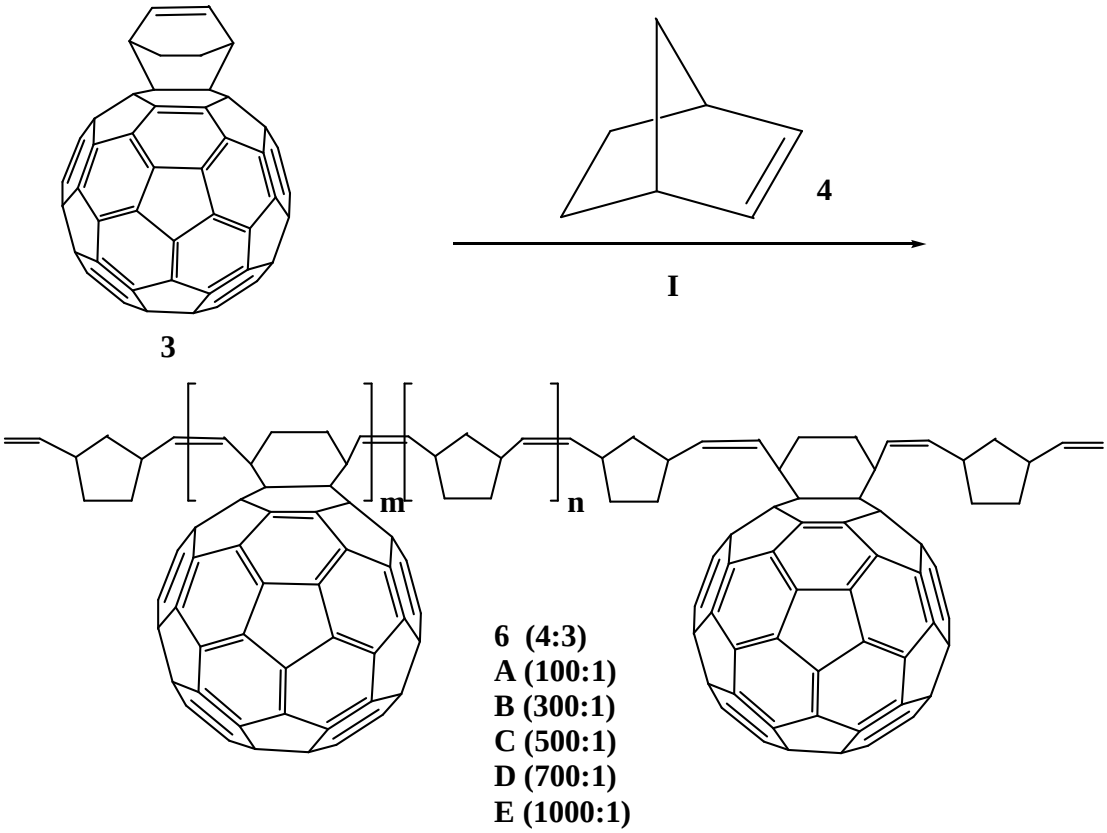

Scheme 3.6: The synthesis of C_{60}-containing norbornene copolymers **6A-E** using ROMP. **I** = (a) toluene, Grubbs II catalyst; (b) ethyl vinyl ether, MeOH, 1M HCl.

3.2.3.4 The synthesis of 1,4,5,6,7,7-hexachloro-5-norbornene-endo-2,3-heptylimide (10)

1,4,5,6,7,7-Hexachloro-5-norbornene-2,3-dicarboxylic anhydride **7** (5.00 g, 13.5 mmol) and cycloheptylamine **8** (1.72 ml, 13.4 mmol) were stirred in toluene (25 ml) at 90 °C for 24 hours under a nitrogen atmosphere. The reaction mixture was then cooled to room temperature. Acetic anhydride (13.00 ml, 13.75 mmol) and sodium acetate (0.917 g, 6.74 mmol) were added to the resulting mixture which was then stirred at 90 °C for a further 24 hours. Upon cooling a white crystalline matrix formed throughout the solution. The solvent was subsequently removed under reduced pressure. The product was then washed with distilled water and left to dry. The product was dissolved in hexane and then filtered into a glass beaker. An undissolved white powder remained on the filter paper and white crystals (**10**) formed (5.55 g, 85 % yield) in the beaker after the hexane had evaporated.

Scheme 3.7 illustrates the synthesis of compound **10**. The crystal structure determination details are given in ***Section 3.2.2.7*** and crystallographic data are given in **Appendix B**.

^{1}H NMR: 3.92 ppm (1H, s, NC-**H**); 3.33 ppm (2H, s, O=C-C-**H**); 2.40-1.85 ppm (12H, mm C_7**H_{12}**).
^{13}C NMR: 171.25 ppm (C=O); 131.19 ppm (C=C); 104.62 ppm (Cl-C-**C**); 79.78 ppm (Cl_2-C); 55.20 ppm (-C-**C**-Cl); 51.72 ppm (C-N); 35.44 ppm (C-C); 31.91 ppm (C-C); 28.39 ppm (C-C).
FAB MS: *m/z* 466, $C_{16}H_{15}O_2Cl_6N^+$; *m/z* 369.9, $C_9H_2O_2Cl_6N^+$; *m/z* 272, $C_5{}^{35}Cl_5{}^{37}Cl^+$.

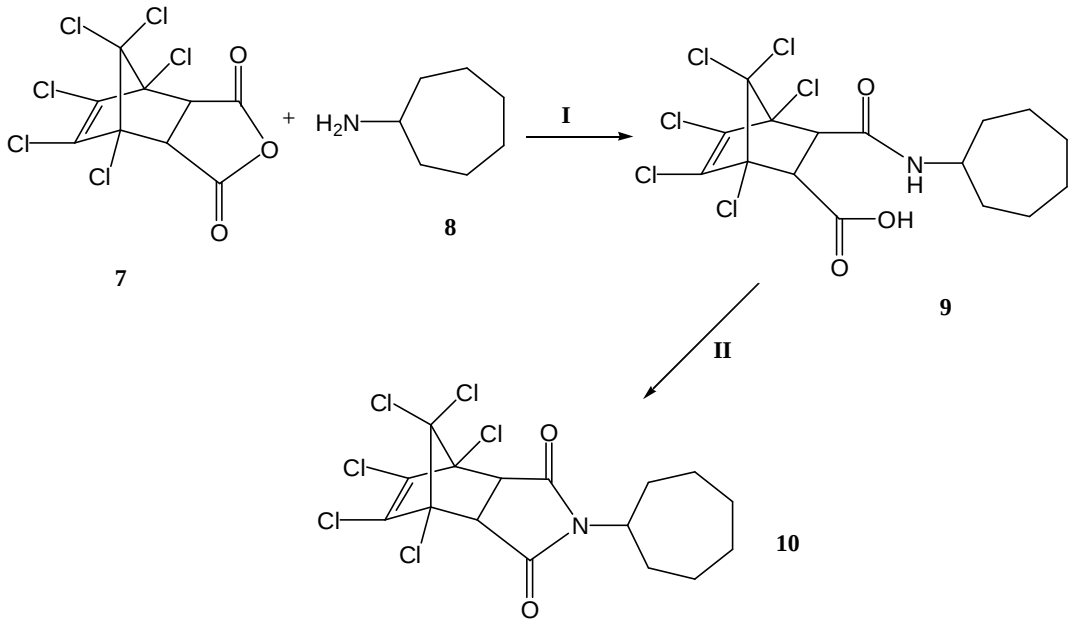

Scheme 3.7: The synthesis of 1,4,5,6,7,7-hexachloro-5-norbornene-endo-2,3-heptylimide **10**. **I** = toluene, 90 °C, N_2 atmosphere for 24 hours; **II** = acetic anhydride $(CH_3CO)_2O$, sodium acetate ($CH_3COONa{\cdot}3H_2O$), 90 °C, 24 hours.

3.2.3.5 Polymerization of 1,4,5,6,7,7-hexachloro-5-norbornene-endo-2,3-heptylimide (10)

1,4,5,6,7,7-Hexachloro-5-norbornene-endo-2,3-heptylimide (1.00 g, 2.15 mmol) **10** was stirred in toluene (35 ml) for 15 min under a nitrogen atmosphere at room temperature. Grubbs II catalyst (10 mg, 11.8 µmol) was added to the solution and the reaction mixture

was left to stir for a further 45 min. The polymerization was terminated by adding a few drops of ethyl vinyl ether (~2-3 drops) and the solution was poured into an excess of MeOH (200 ml) containing a few drops of 1 M HCl to precipitate the crude polymer. MeOH was then removed using a rotary evaporator. The resulting polymer (**11)** was dried in a vacuum oven at 35 °C to constant weight and was found to be a cream white fine powder (0.96 g, 96 % yield).

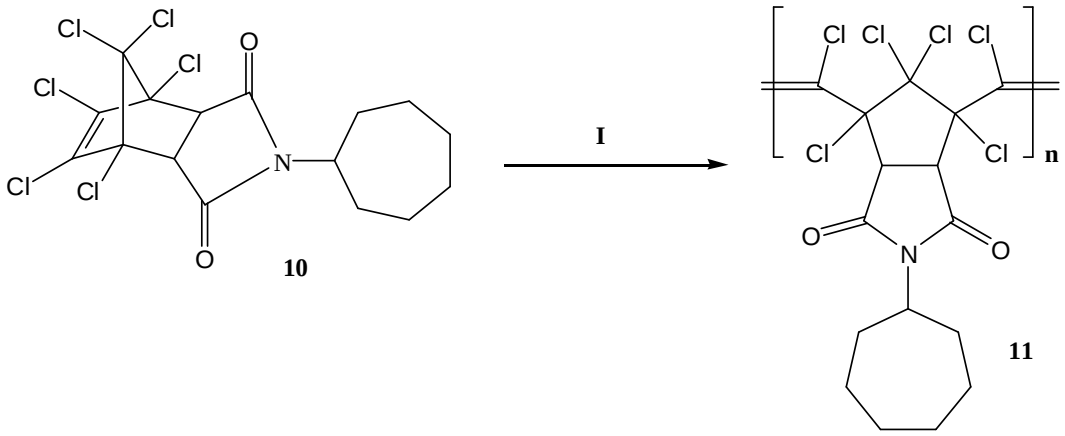

Scheme 3.8: The synthesis of norbornene derivative polymer **11** using ROMP. **I** = (a) toluene, Grubbs II catalyst; (b) ethyl vinyl ether, MeOH, 1M HCl.

3.2.3.6 Copolymerization of C_{60}-cyclohexadiene cycloadduct (3) with 1,4,5,6,7,7-hexachloro-5-norbornene-endo-2,3-heptylimide (10)

The copolymerization reaction was carried out on a molar ratio of 100:1 of 1,4,5,6,7,7-hexachloro-5-norbornene-endo-2,3-heptylimide **10** to C_{60}-cyclohexadiene cycloadduct **3**. The co-monomers **10** (1.00 g, 2.15 mmol) and **3** (0.0172 g, 0.0215 mmol) were stirred in a mixture of 1:1 CS_2: $CHCl_3$ (30 ml) for 15 min under a N_2 atmosphere at room temperature. Grubbs II catalyst (10 mg, 11.8 µmol) was added and the reaction mixture was left to stir for a further 1 hour. The reaction mixture was terminated by adding few drops of ethyl vinyl ether (~2-3 drops) and the solution was poured into an excess of MeOH (200 ml) containing a few drops of 1 M HCl to precipitate the crude polymer. MeOH was removed using a rotary evaporator. The resulting co-polymer was dried in a vacuum oven at 35 °C to constant weight and gave a light brown powder in good yield

(0.956 g, 94 %). This reaction was repeated with varying monomer ratios of **10** to **3** to give the products in good yields: 300:1 (0.905 g, 90 % yield), 500:1 (0.872 g, 87 % yield), 700:1 (0.842 g, 84 % yield) and 1000:1 (0.861 g, 86 % yield) molar ratios. The obtained polymers (**12A-E** in **Scheme 3.9**) were found to be dark to light brown in colour, with the colour being determined by the amount of C_{60}-cyclohexadiene cycloadduct used in the polymerization reaction.

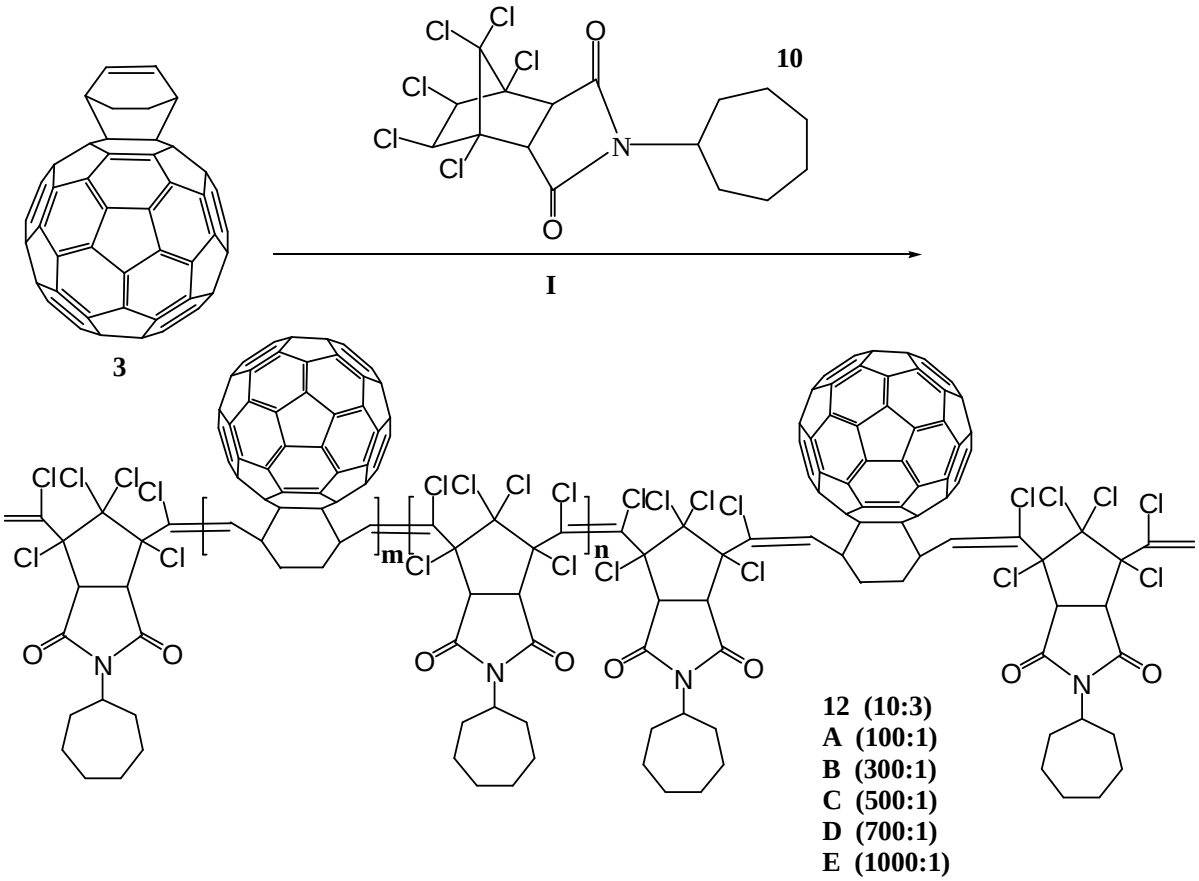

Scheme 3.9: The synthesis of C_{60}-containing norbornene derivative copolymers **12A-E** using ROMP. **I** = (a) toluene, Grubbs II catalyst; (b) ethyl vinyl ether, MeOH, 1M HCl.

3.3 Results and Discussion

3.3.1 The synthesis of C_{60}-cyclohexadiene cycloadduct (3)

The C_{60}-cyclohexadiene cycloadduct **3** was synthesized by a Diels-Alder reaction between C_{60} **1** and cyclohexadiene **2** (**Scheme 3.4**). The use of 5 equivalents of **2** at both 60 °C and 80 °C gave a mixture of monoadduct product **3a** and diadduct product **3b** in good yield. This was confirmed by the mass spectrum (**Figure 3.2**) which showed a mixture of monoaddition **3a** (*m/z* = 801) and bisaddition **3b** (*m/z* = 881.2) products. Addition occurred at the 6,6 junctions of C_{60}. The presence of C_{60} in the materials was confirmed by the observed IR absorption at 528 cm^{-1}, a characteristic feature of a 6,6-cycloadduct of C_{60}. Attempts to separate the mixture of monoadduct and bisadduct products were performed. No separation of complexes was observed by thin layer chromatography (TLC) or column chromatography. This is because a mixture of diadducts can contain up to eight different positional isomers, with the number of possible isomers increasing with the number of additions. Isomers inside each family of adducts tend to possess similar chromatographic properties, and this makes the separations a very complex operation [2]. From the NMR spectra, there was no difference in the ratio of monoadduct versus bisadduct at both 60 °C and 80 °C. Only by FAB MS a monoadduct and bisadduct could be distinguished. Due to the problems of isolation and characterization in relation to the number of possible regioisomers which significantly increase with the number of additions [24], only the product synthesized using 5 equivalents of **2** at 60 °C was used as the co-monomer for polymerization reactions.

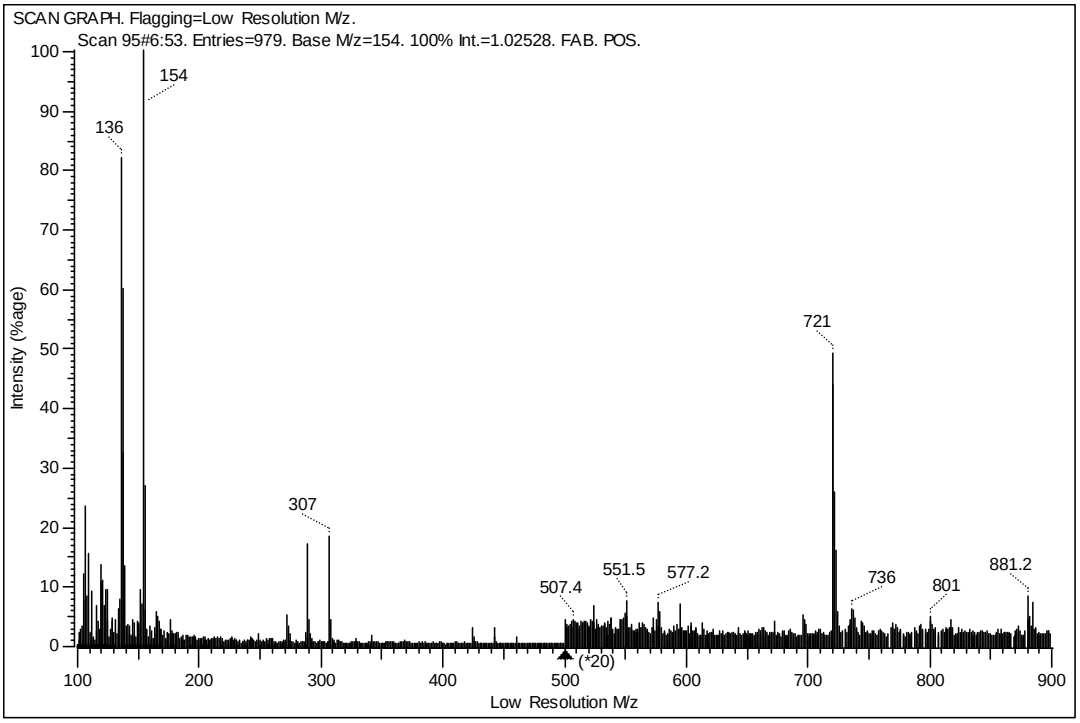

Figure 3.2: The mass spectrum of 1:5 C_{60}-cyclohexadiene cycloadduct **3** at 60 °C, for 48 hours. *m/z* 721, $C_{60;}$ *m/z* 801, monoadduct; *m/z* 881.2, bisadduct.

3.3.2 The synthesis of new copolymers (5) and (6)

The C_{60}-cyclohexadiene cycloadduct **3** and norbornene **4** were premixed in varying molar ratios and copolymerized by way of a ROMP approach with catalytic amounts of Grubbs II catalyst to produce a series of rubbery C_{60}-containing copolymers **6A-E** (**Scheme 3.10**) in good yields (78-86 %). The polymers were found to be readily soluble in CH_2Cl_2, $CHCl_3$, CS_2, THF and toluene. The polymers were also found to be dark to light brown in colour, with the colour being proportional to the amount of C_{60}-cyclohexadiene cycloadduct used. The norbornene polymer **5** was synthesized so as to compare it with the C_{60}-containing norbornene copolymers. The solubility of this polynorbornene was also good in common organic solvents such as CH_2Cl_2, $CHCl_3$ and toluene.

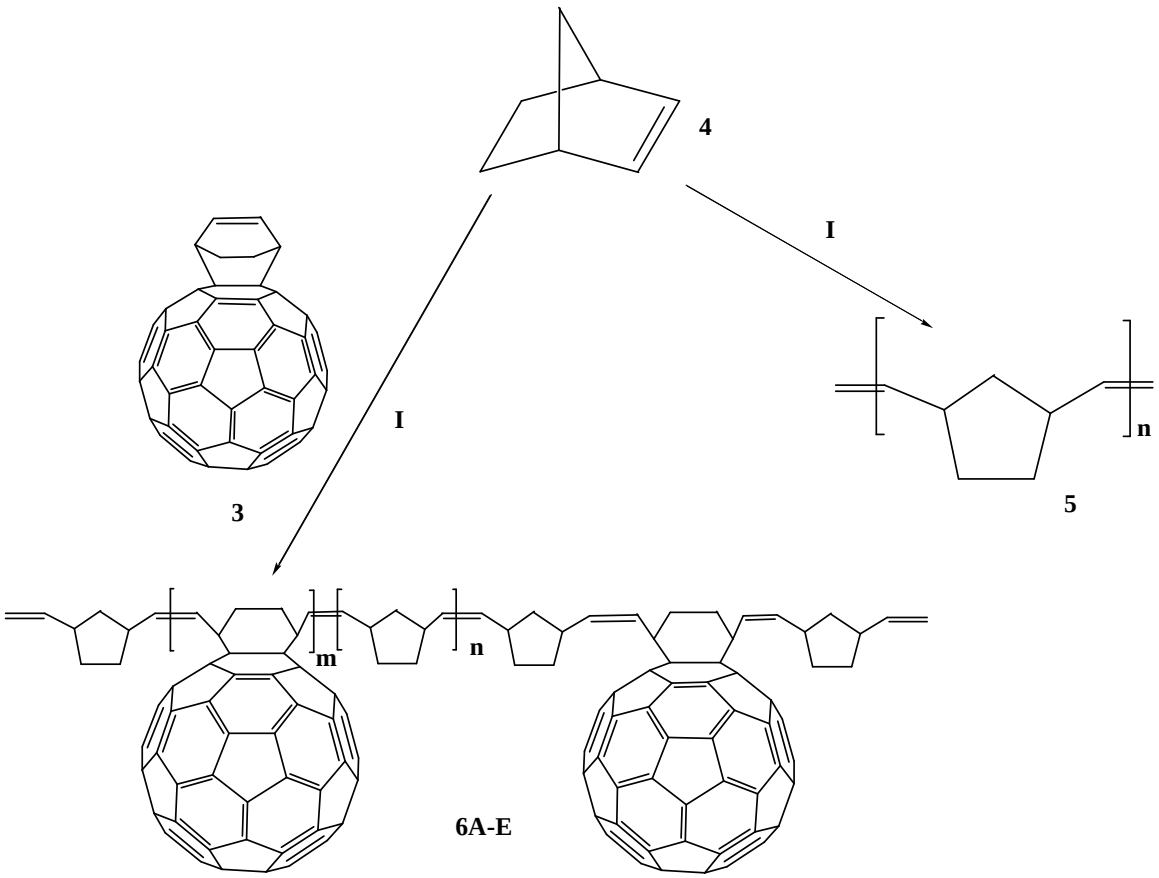

Scheme 3.10: The synthesis of polynorbornene **5** and C_{60}-containing norbornene copolymers **6A-E** using ROMP. **I** = (a) toluene, Grubbs II catalyst; (b) ethyl vinyl ether, MeOH, 1M HCl.

3.3.2.1 Infrared spectroscopy

Figure 3.3 shows the FT-IR spectra of the polynorbornene **5**, C_{60}-containing copolymers **6A-E**, C_{60} molecule **1** and C_{60}-cyclohexadiene cycloadduct **3**. As can be seen, the spectra show the presence of the polynorbornene and the characteristic peak at ~528 cm^{-1} due to the functionalized C_{60} cage in the polymers. The peak due to C_{60} is only observed in polymers with relatively low norbornene content. The peak intensity at ~528 cm^{-1} increased with an increase of the C_{60} content in the polymer [25-27].

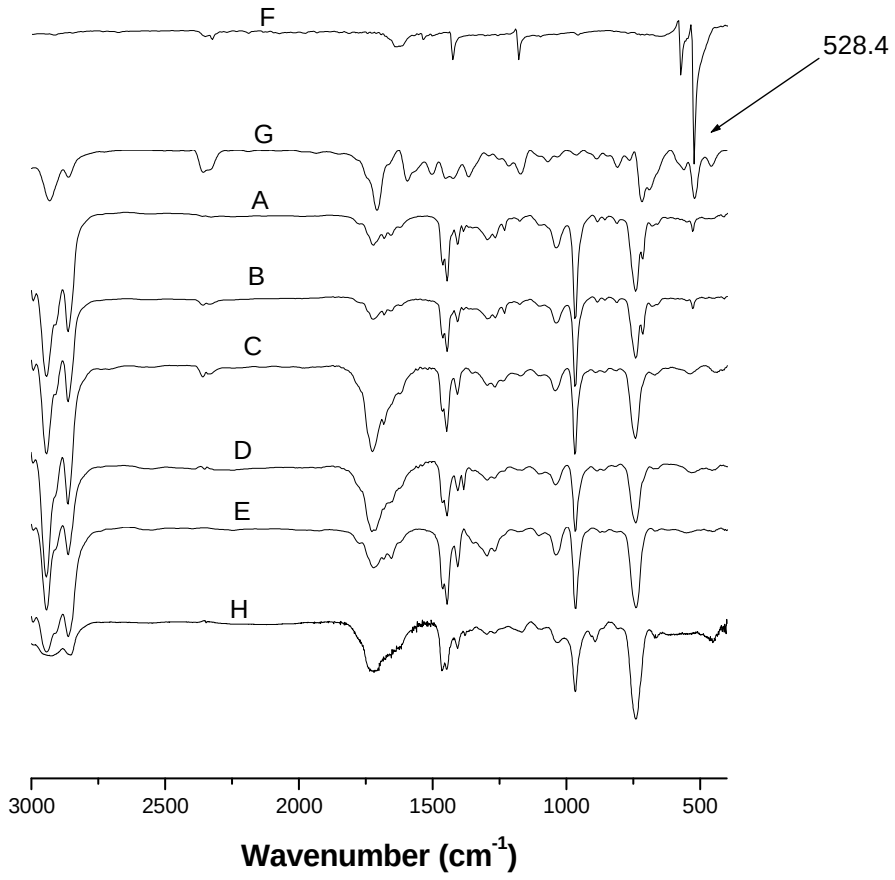

Figure 3.3: FT-IR spectra of the C_{60}-containing norbornene copolymers **6A-E**: mole ratio of **4:3** (A) 100:1, (B) 300:1, (C) 500:1, (D) 700:1, (E) 1000:1, (F) C_{60} **1**, (G) C_{60}-cyclohexadiene cycloadduct **3** and (H) polynorbornene **5**.

3.3.2.2 Differential scanning calorimetry

In the DSC analyses, the glass transition temperatures (Tg) for the C_{60}-containing norbornene polymers **6A-E** and the polynorbornene **5** were determined using a heating rate of 5 °C min^{-1} under a N_2 atmosphere. The DSC thermograms show that the Tg of the copolymers increased modestly with increasing incorporation of C_{60} in the polymer (**Figure 3.4, Table 3.1**). This relationship can be explained in terms of the modification of the plasticizing and reinforcing abilities of the C_{60} in the polymer [28]. Similar observations about the relationship between the Tg and the amount of C_{60} in other C_{60}-

based polymers have been reported in the literature [17, 25, 28-30]. Tang and co-workers proposed that when an amount of C_{60} in polymers is increased many polymer chains may be linked by the C_{60} molecules, therefore increasing the Tg of the polymer [28]. Since a higher Tg is usually observed upon addition of C_{60} to a polymer [17], Prato suggested that fullerenes may be used as additives for increasing the thermal stability of a material [2].

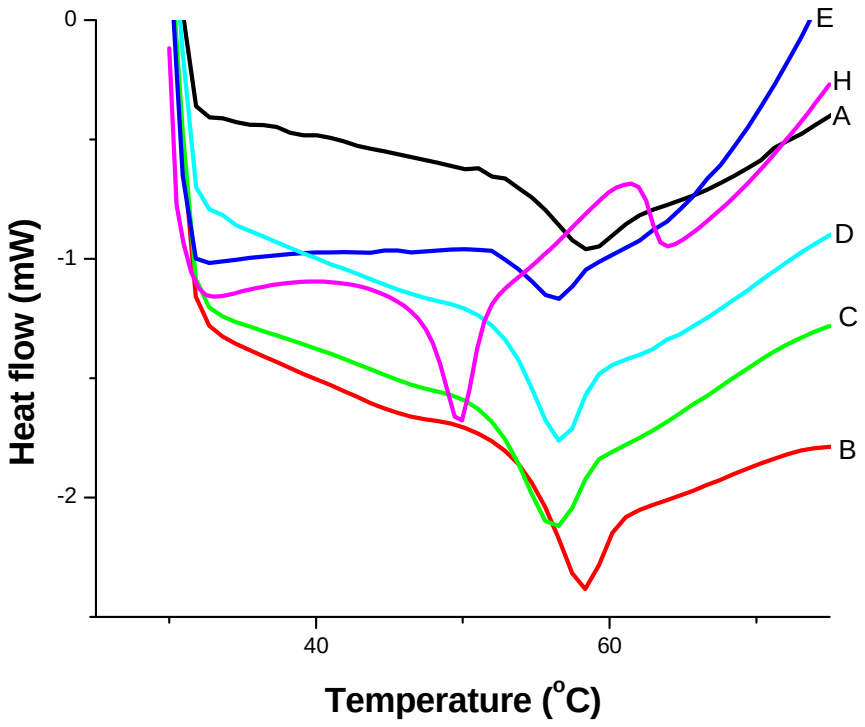

Figure 3.4: DSC thermograms showing Tg peaks of the C_{60}-containing norbornene copolymers **6A-E**: mole ratio of **4:3** (A) 100:1, (B) 300:1, (C) 500:1, (D) 700:1, (E) 1000:1 and (H) polynorbornene **5**.

Table 3.1: Tg of C_{60}-containing norbornene copolymers **6A-E** and polynorbornene **5**

Polymer	Mole ratio 4:3	Tg (°C)
6A	**100:1**	**58.5**
6B	**300:1**	**58.3**
6C	**500:1**	**56.5**
6D	**700:1**	**56.4**
6E	**1000:1**	**56.4**
5(H)	**1:0**	**49.8**

3.3.2.3 Thermogravimetric analysis

Thermal stability tests were performed by thermogravimetric analysis. **Figure 3.5** and **Table 3.2** show a comparison of the mass losses of C_{60}-containing norbornene copolymers **6A-E** and polynorbornene **5** upon heating in a nitrogen atmosphere at a heating rate of 10 °C min^{-1}. In each case, the decomposition temperature was determined by measuring the derivatives of the TGA curves. As the amount of C_{60} in the C_{60}-containing polymers increased the thermal stability of the polymers decreased compared to the polynorbornene **5**. The TGA data showed that the C_{60}-containing polymers were thermally less stable than the polynorbornene **5**. Similar observations by Prato and co-workers on the stability of other C_{60}-based polymers have been reported in the literature [17]. The TGA curves of the C_{60}-containing polymers also showed that they contain about 5-20 % of the material remaining and this may be due to the presence of RuO_x and C_{60}.

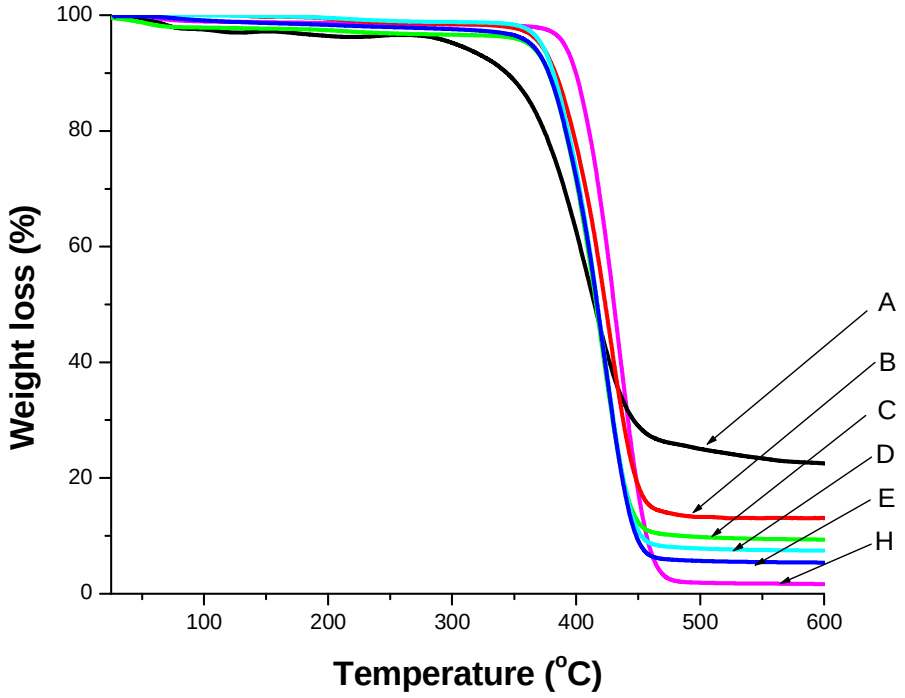

Figure 3.5: TGA curves of the C_{60}-containing norbornene copolymers **6A-E**: mole ratio of **4:3** (A) 100:1, (B) 300:1, (C) 500:1, (D) 700:1, (E) 1000:1 and (H) polynorbornene **5**.

Table 3.2: Thermogravimetric analysis of C_{60}-containing norbornene copolymers **6A-E** and polynorbornene **5**

Polymer	Mole ratio of 4:3	Decomposition temperature(°C)
6A	**100:1**	**415.9**
6B	**300:1**	**423.3**
6C	**500:1**	**424.6**
6D	**700:1**	**424.8**
6E	**1000:1**	**427.5**
5(H)	**1:0**	**434.9**

3.3.2.4 Ultra-violet / visible spectroscopy

UV-vis spectroscopy measurements on the C_{60}-containing norbornene copolymers **6A-E**, C_{60} **1**, C_{60}-cyclohexadiene cycloadduct **3** and polynorbornene **5** in toluene were made and the data obtained are presented in **Figure 3.6** (data summarized in **Table 3.3**. The UV-vis spectra of the C_{60}-containing norbornene copolymers **6A-E** show that the electronic properties of C_{60} are retained in the copolymers, with typical absorptions near 438 nm which are absent in the polynorbornene **5**. The shoulder observed at 438 nm for all the copolymers is characteristic of a 6-6 ring fusion and also previously observed to be characteristic of C_{60} monoadducts [31]. The characteristic peak of the C_{60} derivative at 438 nm in the UV-vis spectra further indicates that C_{60} has probably been covalently attached to the copolymers. Such UV-vis spectra have been observed in many fullerene derivatives and C_{60}-containing polymers. The observed spectral features have been attributed to the scattering of UV light by clusters of C_{60} in solution [32, 33]. Furthermore, as the amount of C_{60} in the copolymers increases, the fullerene peak intensity also increases (**Figure 3.6**).

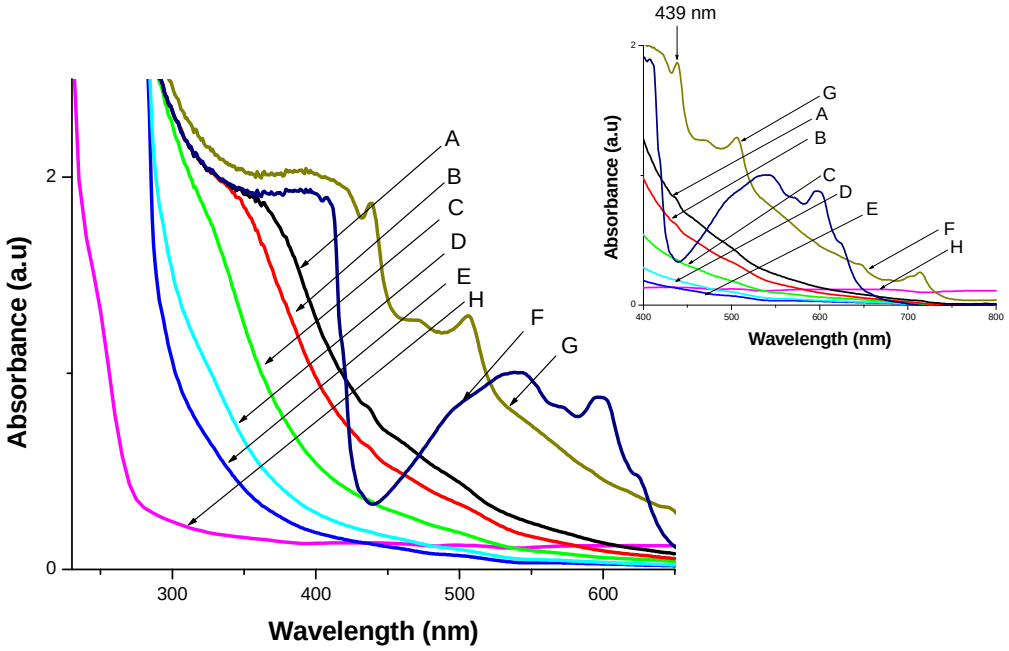

Figure 3.6: UV-visible spectra recorded in toluene of the C_{60}-containing norbornene copolymers **6A-E**: mole ratio of **4:3** (A) 100:1, (B) 300:1, (C) 500:1, (D) 700:1, (E) 1000:1. (F), C_{60} **1** (G) C_{60}-cyclohexadiene cycloadduct **3** and (H) polynorbornene **5**.

Table 3.3: UV-visible λ_{max} of the C_{60}-containing polymers **6A-E** and polynorbornene **5**

Polymer	Mole ratio of 10:3	λ_{max} (nm)
6A	**100:1**	**437.3**
6B	**300:1**	**436.5**
6C	**500:1**	**436.5**
6D	**700:1**	**436.5**
6E	**1000:1**	**436.5**
3(F)	**C_{60}-cyclohexadiene cycloadduct**	**438.5, 506.3**
G	**C_{60}**	**408.2, broad peak 460-650**
5(H)	**1:0**	**No λ_{max}**

3.3.3 The synthesis of 1,4,5,6,7,7-hexachloro-5-norbornene-endo-2,3-heptylimide (10)

The norbornene derivative **7** was functionalized according to a procedure used by Vargas *et al.* [34]. The intermediate product was then cyclized to the endo-imide using acetic anhydride as dehydrating agent (**Scheme 3.7**). The final product was dissolved in hexane and gave **10** as white crystals in high yield. The solubility of this norbornene derivative was good in organic solvents such as toluene and dichloromethane. The structure of the product was confirmed by ^{1}H NMR and ^{13}C NMR spectroscopy, FAB mass spectrometry (**Figure 3.7**) and X-ray crystallography (**Figure 3.8**).

FAB mass spectrometry of the product was performed using low-resolution FAB MS and resulted in *m/z* 466 for $C_{16}H_{15}O_2Cl_6N^+$, *m/z* 369.9 for $C_9H_2O_2Cl_6N^+$ and *m/z* 272 for $C_5{}^{35}Cl_5{}^{37}Cl^+$. High-resolution FAB MS was also used for exact mass measurements of ions and gave *m/z* 466.0175 for the molecular ion $C_{16}H_{15}O_2Cl_6N^+$. Crystal data, structure refinement, torsion angles, bond lengths and angles are shown in **Appendix B**. The bond lengths C-C (average 1.53 Å), C-N (average 1.44 Å) and C-Cl (average 1.74 Å) show a single bond character and C-O (average 1.20 Å) and C-C (1.33 Å) reveal a double bond character, indicating bond distances consistent with the typical C-C, C-N, C-Cl, C=O and C=C bonds.

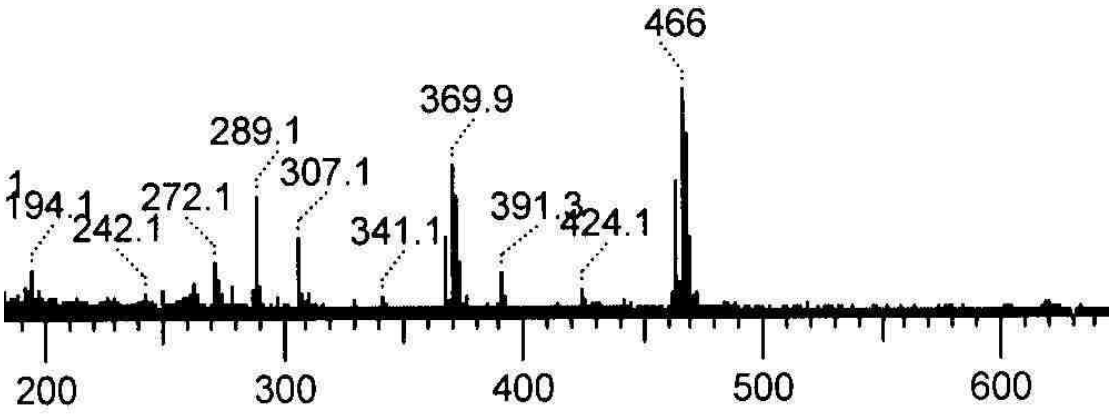

Low Resolution M/z

Figure 3.7: The mass spectrum of 1,4,5,6,7,7-hexachloro-5-norbornene-endo-2,3-heptylimide **10**.

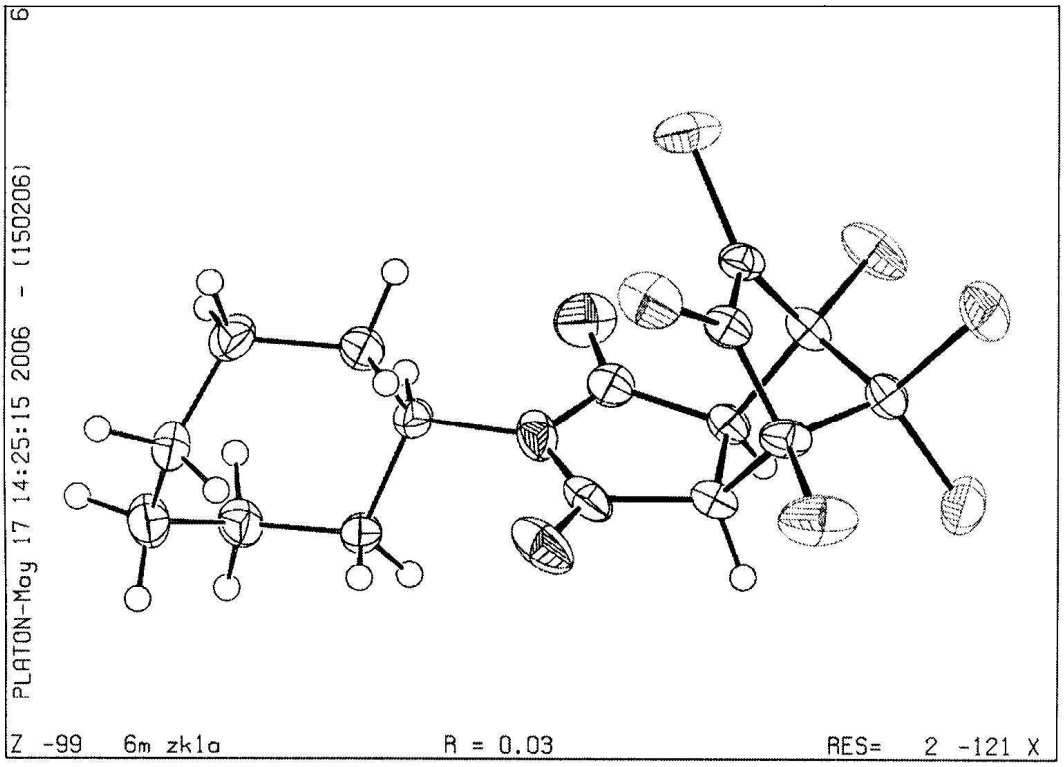

Figure 3.8: The crystal structure of 1,4,5,6,7,7-hexachloro-5-norbornene-endo-2,3-heptylimide **10**. Thermal ellipsoids are drawn at the 50 % probability level.

3.3.4 The synthesis of new copolymers (11) and (12)

The monomer **10** was copolymerized with the C_{60}-cyclohexadiene cycloadduct **3** via a ROMP approach with catalytic amounts of Grubbs II catalyst to produce a sequence of novel C_{60}-containing copolymers **12A-E** (**Scheme 3.11**, showing only the polymers based on the monoadduct **3a**) in good yields (84-94 %). The copolymers were found to be slightly soluble in CH_2Cl_2, CS_2, $CHCl_3$, THF and toluene. This solubility behaviour shows the advantage of having a polymer bonded to C_{60} for improved processability. The polymers were also found to be dark to light brown in colour, with the colour being proportional to the amount of C_{60}-cyclohexadiene cycloadduct **3** used.

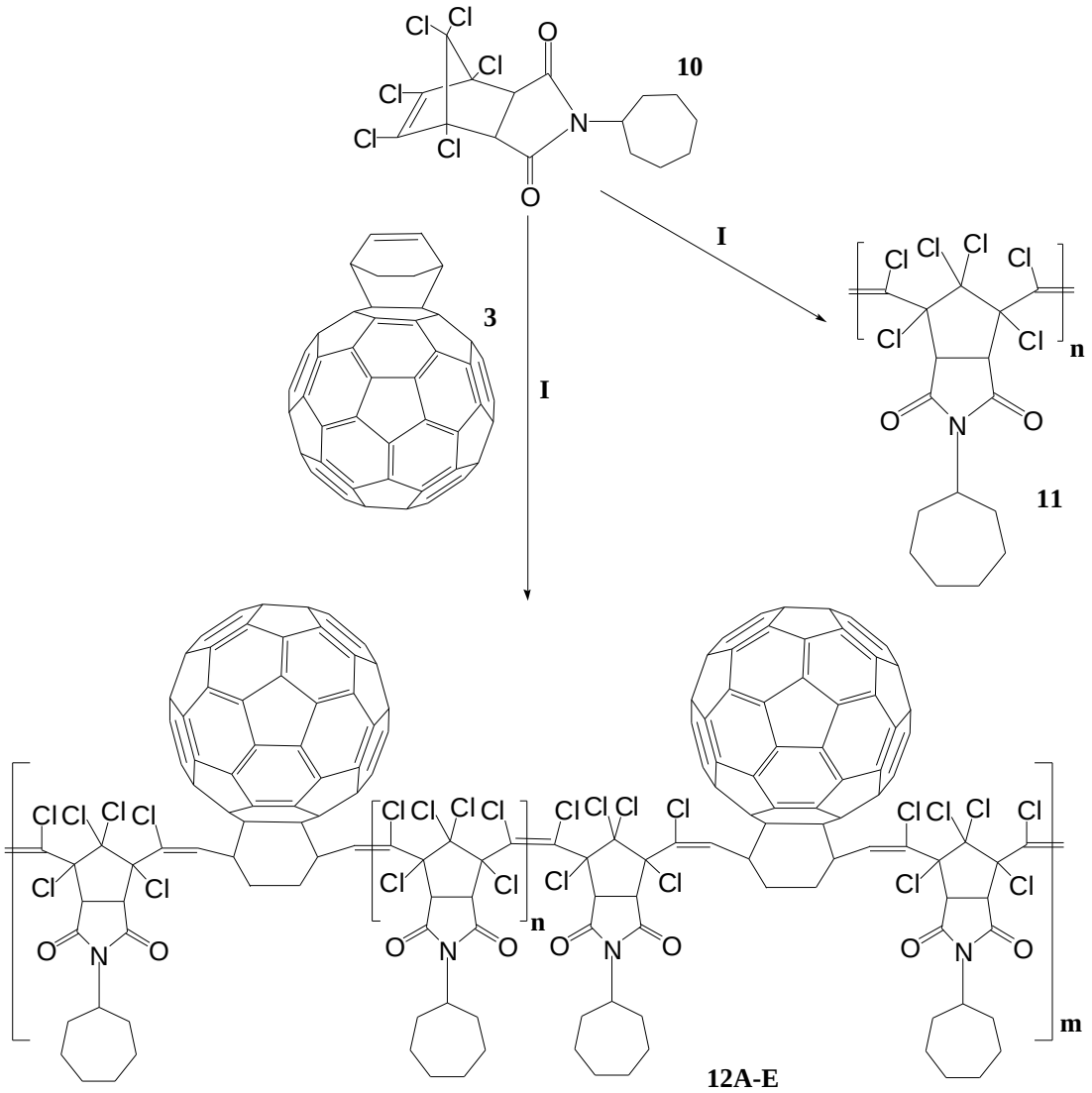

Scheme 3.11: The synthesis of norbornene derivative polymer **11** and C_{60}-containing norbornene derivative copolymers **12A-E** using ROMP. **I** = (a) toluene, Grubbs II catalyst; (b) ethyl vinyl ether, MeOH, 1M HCl.

3.3.4.1 Infrared Spectroscopy

Figure 3.9 shows the FT-IR spectra of the norbornene derivative polymer **11**, C_{60}-containing polymers **12A-E**, C_{60} molecule **1** and C_{60}-cyclohexadiene cycloadduct **3**. The presence of C_{60} and the norbornene derivative polymer were confirmed by the FT-IR data. The presence of C_{60} was confirmed by the observed peak ~528 cm^{-1} due to the functionalized C_{60} cage in the polymer. The weak peak due to C_{60} is only observed in

polymers with relatively low norbornene derivative content. The peak intensity at ~528 cm^{-1} weakly increased with an increase of the C_{60} content in the polymer [25-27].

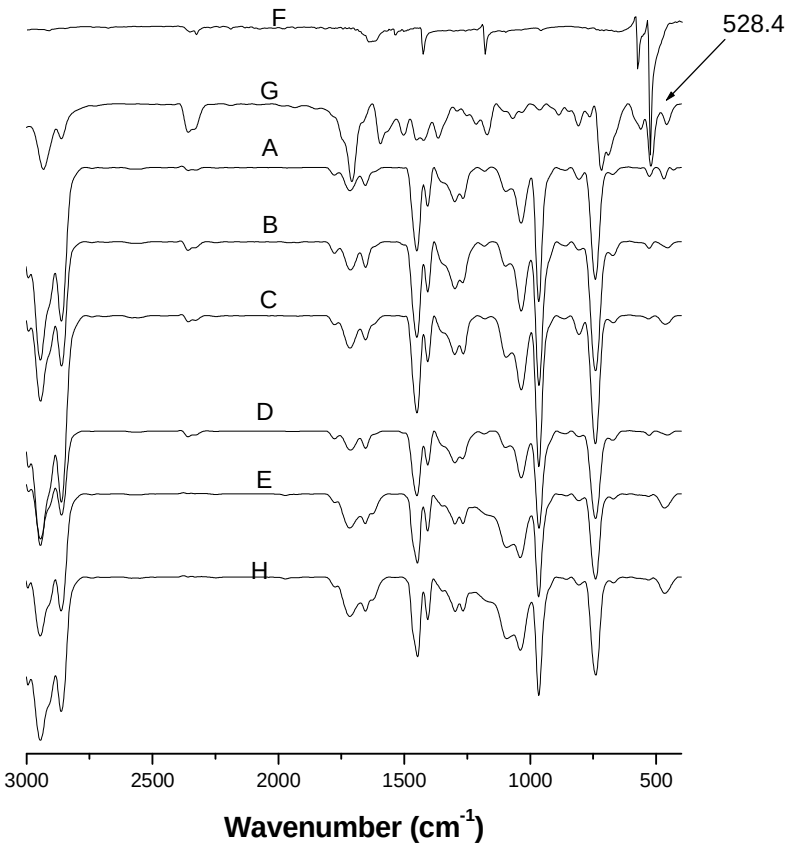

Figure 3.9: FT-IR spectra of the C_{60}-containing norbornene derivative copolymers **12A-E**: mole ratio of **10:3** (A) 100:1, (B) 300:1, (C) 500:1, (D) 700:1, (E) 1000:1, (F) C_{60} **1**, (G) C_{60}-cyclohexadiene cycloadduct **3** and (H) norbornene derivative polymer **11**.

3.3.4.2 Differential scanning calorimetry

In DSC analyses the glass transition temperatures (Tg) for the C_{60}-containing polymers **12A-E** and the norbornene derivative polymer **11** were determined using a heating rate of 5 °C min^{-1} under a N_2 atmosphere. The DSC thermograms showed that the Tg of the copolymers slightly increased with increasing incorporation of C_{60} in the polymer (**Figure 3.10, Table 3.4**). Similar observations about the relationship between the Tg and

the amount of C_{60} in other C_{60}-based polymers have been reported in the literature [17, 25, 28-30]. This relationship can be explained in terms of the modification of the plasticizing and reinforcing abilities of the C_{60} in the polymer [28]. In their paper, Tang and co-workers suggested that when an amount of C_{60} in polymers is increased many polymer chains may be linked by the C_{60} molecules, therefore increasing the Tg of the polymer [28]. Since a higher Tg is usually observed upon addition of C_{60} to a polymer [17], Prato proposed that fullerenes may be used as additives for increasing the thermal stability of a material [2].

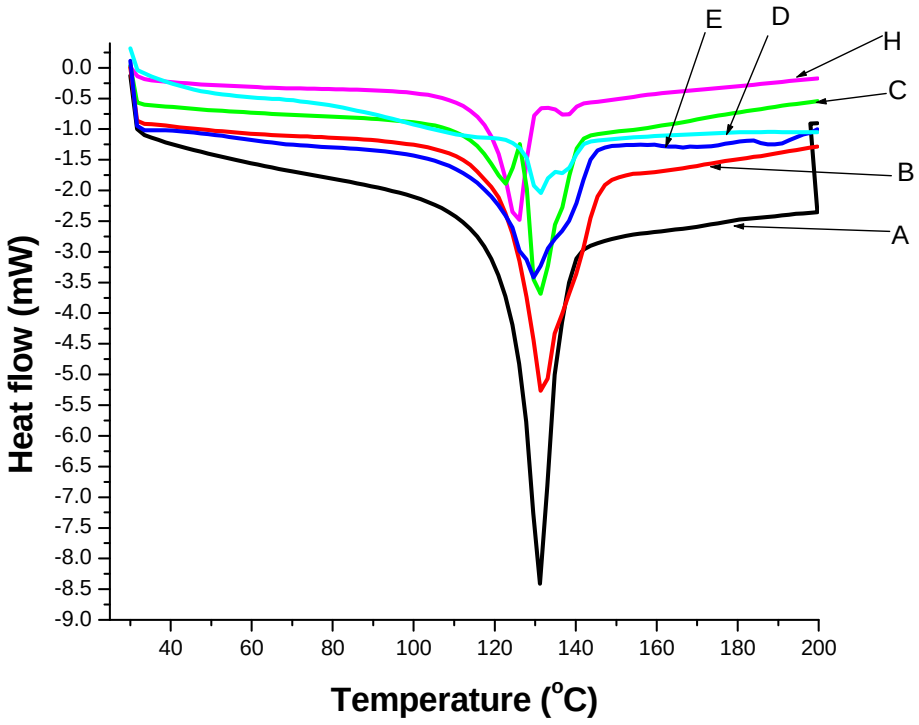

Figure 3.10: DSC thermograms showing Tg peaks of the C_{60}-containing norbornene derivative copolymers **12A-E**: mole ratio of **10:3** (A) 100:1, (B) 300:1, (C) 500:1, (D) 700:1, (E) 1000:1, (H) norbornene derivative polymer **11**.

Table 3.4: Tg of C_{60}-containing norbornene derivative polymers **12A-E** and **11**

Polymer	Mole ratio of 10:3	Tg (°C)
12A	100:1	131.7
12B	300:1	131.4
12C	500:1	131.1
12D	700:1	130.6
12E	1000:1	129.5
11 (H)	1:0	126.3

3.3.4.3 Thermogravimetric analysis

The thermal stability of the polymers was studied by TGA under a N_2 atmosphere at a heating rate of 10 °C min^{-1}. The decomposition temperature was determined by the peak maximum as determined from the derivatives of the curves. As can be seen from **Figure 3.11 and Table 3.5**, as the amount of C_{60} in the C_{60}-containing polymers increased the thermal stability of the polymers increased compared with the norbornene derivative polymer **11**. The TGA showed that the C_{60}-containing polymers were thermally more stable than the norbornene derivative polymer **11**. As seen from **Figure 3.11**, the TGA curves do not approach zero. About 9-20 % of the material is left and this may be due to the presence of RuO_x and fullerene.

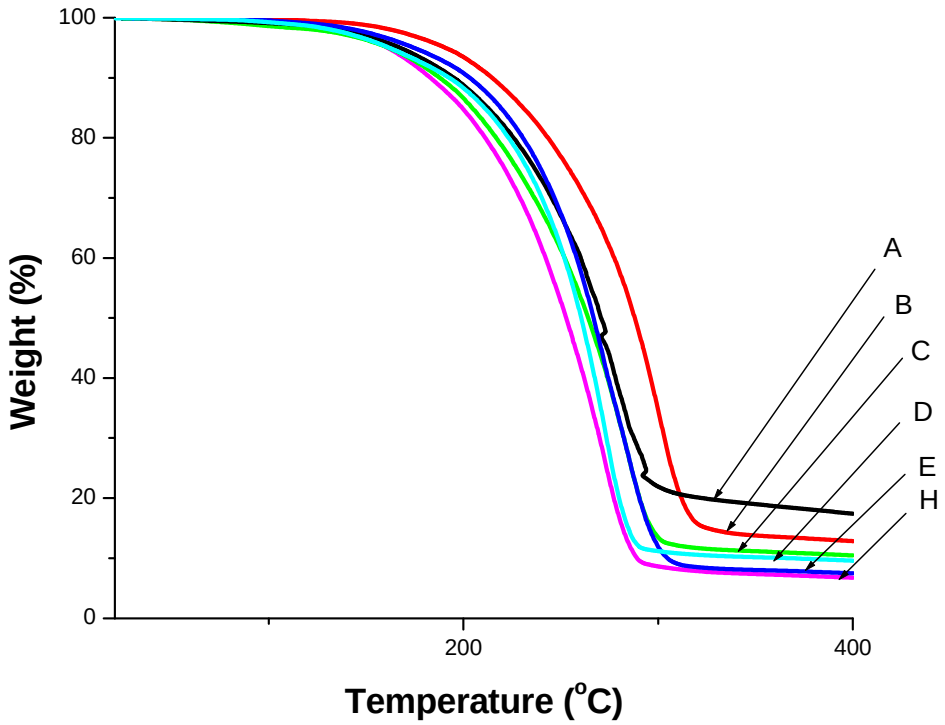

Figure 3.11: TGA curves of the C_{60}-containing norbornene derivative copolymers **12A-E**: mole ratio of **10:3** (A) 100:1, (B) 300:1, (C) 500:1, (D) 700:1, (E) 1000:1, (H) norbornene derivative polymer **11**.

Table 3.5: Thermogravimetric analysis of C_{60}-containing polymers **12A-E** and norbornene derivative polymer **11**

Polymer	**Mole ratio of 10:3**	**Decomposition temperature (°C)**
12A	100:1	301.5
12B	300:1	286.4
12C	500:1	284.8
12D	700:1	283.2
12E	1000:1	278.2
11 (H)	1:0	273.8

3.3.4.4 Ultra-violet / visible spectroscopy

UV-vis spectra of the C_{60}-containing norbornene derivative copolymers **12A-E**, C_{60}, C_{60}-cyclohexadiene and the norbornene derivative polymer **11** were recorded in toluene and are presented in **Figure 3.12** (data summarized in **Table 3.6**). The UV-vis spectra of the C_{60}-containing norbornene derivative copolymers **12A-E** and the C_{60}-cyclohexadiene cycloadduct **3** show some significant differences in comparison with C_{60} but do not show any differences between the samples.

Very characteristic for the spectra of the Diels-Alder cycloadducts of C_{60} are bands with λ_{max} near 438 and 506 nm in the C_{60}-cyclohexadiene cycloadduct **3** and the C_{60}-containing norbornene derivative copolymers **12A-E**. These are absent in the norbornene derivative polymer **11** [35, 36]. The shoulder observed at 438 nm for all the copolymers is highly characteristic of a 6-6 ring fusion of C_{60} monoadducts. The above observations together with the peak broadening beyond 510 nm in the UV-vis spectra further indicate that C_{60} has been covalently attached to the copolymers [32, 33]. Such UV-vis spectra have been observed in many fullerene derivatives and C_{60}-containing polymers. The observed spectral features have been attributed to the scattering of UV light by clusters of C_{60} [32, 33]. The broadening of the absorption bands corresponding to C_{60} in the copolymers can also be attributed to a range of weight distributed derivatives found in these materials [37]. In addition, as the amount of C_{60} in the copolymers increases, the fullerene peak intensity also increases (**Figure 3.12**).

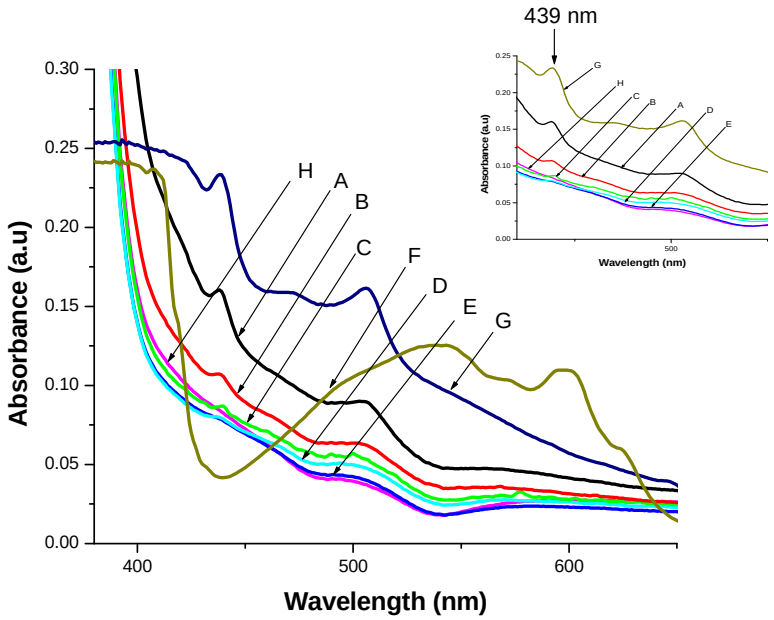

Figure 3.12: UV-visible spectra recorded in toluene of the C_{60}-containing norbornene derivative copolymers **12A-E**: mole ratio of **10:3** (A) 100:1, (B) 300:1, (C) 500:1, (D) 700:1, (E) 1000:1, (F), C_{60} **1**, (G) C_{60}-cyclohexadiene cycloadduct **3** and (H) norbornene derivative polymer **11**.

Table 3.6: UV-visible λ_{max} of the C_{60}-containing polymers **12A-E** and norbornene derivative polymer **11**

Polymer	**Mole ratio of 10:3**	**λ_{max} (nm)**
12A	100:1	438.5, 506.3
12B	300:1	438.5, 506.3
12C	500:1	438.9, 506.3
12D	700:1	438.5, 506.4
12E	1000:1	438.5, 506.4
3(F)	C_{60}-cyclohexadiene cycloadduct	438.5, 506.3
G	C_{60}	408.2, broad peak 460-650
9(H)	1:0	No λ_{max}

3.4 Comparison between the C_{60}-containing norbornene copolymers (6A-E) and the C_{60}-containing norbornene derivative copolymers (12A-E)

Norbornene and a norbornene derivative containing chlorine were chosen as monomers to copolymerize with the C_{60}-cyclohexadiene cycloadduct to obtain **6A-E** and **12A-E** copolymers, respectively. The solubility behaviour of all the synthesized polymers was reasonably good in different organic solvents and totally unlike C_{60}, demonstrating the dramatic effect of polymer attachment on the solubility of fullerene derivatives.

The characterization by FT-IR showed a strong peak (~528 cm^{-1}) due to the incorporated C_{60}'s in the **6A-E** copolymers, whereas a very weak peak due to the C_{60} was observed in the **12A-E** copolymers. It is noted that it is not possible to prove that there is actual covalent incorporation from the C_{60}-cyclohexadiene cycloadduct **3** into the **12A-E** copolymers. Since the 1,4,5,6,7,7-hexachloro-5-norbornene-endo-2,3-heptylimide (**10**) contains a hindered substituted double bond it may not be possible to obtain an interaction of **3** with the polymer.

The relative amount of C_{60} in the C_{60}-containing norbornene derivative copolymers **12A-E** affected the polymers' thermal properties by increasing the decomposition and the glass transition temperatures, as compared to norbornene derivative polymer **11**. However, the C_{60}-containing norbornene copolymers **6A-E** were thermally less stable than the polynorbornene **5**. Pure C_{60} is thermally stable below 600 °C [38], and **6A-E** copolymers decomposed completely above 400 °C, whereas **12A-E** copolymers decomposed at about 300 °C. Therefore, it can be concluded that the **6A-E** copolymers (**Figure 3.6**) were thermally more stable than the **12A-E** polymers (**Figure 3.10**). The DSC thermograms of **6A-E** and **12A-E** showed that the Tg of the copolymers slightly increased with increasing incorporation of C_{60} into the polymer.

3.5 Conclusion

In this report, a route to incorporation of C_{60} into the main chain norbornene-containing polymers using ring opening metathesis polymerization with a Grubbs second generation catalyst was demonstrated based on the chemistry of C_{60}-cyclohexadiene cycloaddition.

The C_{60}-cyclohexadiene cycloadduct **3** was synthesized. This can be related to the facile reaction between the low LUMO energy of C_{60}, the dienophilic nature of the 6,6 double bond and the electron rich diene (cyclohexadiene). It is known that C_{60} shows very limited solubility in any medium, especially polar solvents. The prepared polymers were more soluble in common organic solvents.

FT-IR and UV-vis techniques showed the incorporation of the C_{60} into all synthesized polymers. The UV-vis spectra of all the C_{60}-containing copolymers showed that the electronic configuration of C_{60}-cyclohexadiene is retained in the polymers, with shoulders on the typical absorptions close to 430 nm and 700 nm. The presence of C_{60} affects the polymer properties.

In this study it has been shown that solubility has been improved and also the original electronic and thermal properties of C_{60} are retained in all the synthesized copolymers.

3.6 References

1. http://en.wikipedia.org/wiki/Fullerene_chemistry, 15 September **2008**.
2. M. Prato, *J. Mater. Chem.*, **1997**, 7, 1097.
3. C. Wang, Z. Guo, S. Fu, W. Wu, D. Zhu, *Prog. Polym. Sci.*, **2004**, 29, 1079.
4. F. Giacalone, N. Martin, *Chem. Rev.*, **2006**, 106, 5136.
5. A. S. Abd-El-Aziz, L. J. May, J. A. Hurd, R. M. Okasha, *J. Polym. Sci. Part A: Polym. Chem.*, **2001**, 39, 2716.
6. Z. Komiya, C. Pugh, R. R. Schrock, *Macromolecules*, **1992**, 25, 3609.
7. T. J. Boyd, Y. Geerts, J-K. Lee, D. E. Fogg, G. G. Lavoie, R. R. Schrock, M. F. Rubner, *Macromolecules*, **1997**, 30, 3553.
8. H. D. Maynard, S. Y. Okanda, R. H. Grubbs, *Macromolecules*, **2000**, 33, 6239.
9. http://en.wikipedia.org/wiki/Ring-opening_metathesis_polymerization, 02 October **2008**.
10. http://www.ilpi.com/organomet/romp.html, 27 August **2008**.
11. A. Mutch, M. Leconte, F. Lefebvre, J. M. Basset, *J. Mol. Catal. A: Chemical*, **1998**, 133, 191.
12. M. Scholl, S. Ding, C. W. Lee, R. H. Grubbs, *Org. Lett.*, **1999**, 1, 953.
13. R. H. Grubbs, W. Tumas, *Science*, **1989**, 243, 907.
14. C. Slugovc, S. Demel, S. Riegler, J. Hobisch, F. Stelzer, *J. Mol. Catal. A: Chemical*, **2004**, 213, 107.
15. P. Schwab, R. H. Grubbs, J. W. Ziller, *J. Am. Chem. Soc.*, **1996**, 118, 100.
16. M. A. Tlenkopatchev, S. Fomine, L. Fomina, R. Gabino, T. Owaga, *Polym. J.*, **1997**, 29, 622.
17. N. Zhang, S. R. Schricker, F. Wudl, M. Prato, M. Maggini, G. Scorrano, *Chem. Mater.*, **1995**, 7, 441.
18. http://en.wikipedia.org/wiki/Chlorendic_acid, 16 February **2009**.
19. Bruker SAINT+. Version 6.02 (includes XPREP and SADABS). Bruker AXS Inc., Madison, WI, USA, **1999**.
20. Bruker SHELXTL. Version 5.1. (includes XS, XL, XP, XSHELL) Bruker AXS Inc., Madison, WI, USA, **1999**.

21. A. L. Spek, *J. Appl. Cryst.*, **2003**, 36, 7.
22. L. J. Farrugia, *J. Appl. Cryst.*, **1997**, 30, 565.
23. V. M. Rotello, J. B. Howard, T. Yadav, M. M. Conn, E. Viani, L. M. Giovane, A. L. Lafleur, *Tetrahedron Lett.*, **1993**, 34, 1561.
24. P. Hudhomme, *C. R. Chimie*, **2006**, 9, 881.
25. X. Zhang, A. B. Sieval, J. C. Hummelen, B. Hessen, *Chem. Commun.*, **2005**, 1616.
26. T. Suzuki, Q. Li, K. C. Khemani, F. Wudl, *J. Am. Chem. Soc.*, **1992**, 114, 7301.
27. Z. Y. Wang, L. Kuang, X. S. Meng, J. P. Gao, *Macromolecules*, **1998**, 31, 5556.
28. B. Z. Tang, S. M. Leung, H. Peng, N.-T. Yu, K. C. Su, *Macromolecules*, **1997**, 30, 2848.
29. L. Y. Chiang, L. Y. Wang, C.-S. Kuo, *Macromolecules*, **1995**, 28, 7574.
30. M. A. Mamo, N. J. Coville, W. A. L. van Otterlo, *Fullerenes, Nanotubes, and Nanostructures*, **2007**, 15, 341.
31. S.-G. Liu, L. Shu, J. Rivera, H. Liu, J.-M. Raimundo, J. Roncali, A. Gorgues, L. Echegoyen, *J. Org. Chem.*, 1999, 64, 4884.
32. P. L. Nayak, S. Alva, K. Yang, P. K. Dhal, J. Kumar, S. K. Tripathy, *Macromolecules*, **1997**, 30, 7351.
33. S. Samal, K. E. Geckeler, *Chem. Commun.*, **2000**, 1101.
34. J. Vergas, E.-S. Colin, M. A. Tlenkopatchev, *Eur. Polym. J.*, **2004**, 40, 1325.
35. A. Hirsch, *The Chemistry of the Fullerenes*, Thieme Medical Publishers: New York, **1994**.
36. Y. Tajima, Y. Tezuka, H. Yajima, T. Ishii, K. Takeuchi, *Polymer*, **1997**, 38, 5255.
37. (a) C. Schroder, *Fullerene. Sci. Technol.*, **2001**, 9, 281; (b) D. V. Konarev, V. N. Semkin, R. N. Lyubovskaya, A. Graja, *Synth. Met.*, **1997**, 88, 225.
38. X.-D. Huang, S. H. Goh, S. Y. Lee, *Macromol. Chem. Phys.*, **2000**, 201, 2660.

CHAPTER 4

SYNTHESIS, FUNCTIONALIZATION AND DOPING OF CARBON SPHERES

4.1 Introduction

As mentioned before, carbon spheres (CSs) have excellent properties, similar to those of fullerenes. Due to these high strength, thermal resistance and other intrinsic properties, CSs have been found promising for applications in the preparation of diamond films, lubricating material, rubber additives, etc. The CSs can be prepared without the use of a catalyst using the popular, cost-effective and large scale synthesis of high quality CSs, called the CVD method. For example, Aili and co-workers obtained CSs with uniform dimensions and in high purity, without any other by-products being detected from a CVD method [1].

In this chapter preliminary functionalization of CSs has been explored. Two approaches were used. The first was to do post chemical functionalization of the CSs. In the second approach, functionalization (doping) was performed in situ.

The organic functionalization of carbon nanostructures permits the solubilization of carbon nanomaterials in organic solvents, such that their solution properties and processing abilities can then be studied. Successful covalent functionalization of single-walled CNTs and multi-walled CNTs has been reported [2-6]. Herein we report the functionalization of CSs with cyclopentadiene or cyclohexadiene. These were chosen because they provide a simple methodology to drive the chemical reactivity of the CSs. Very little functionalization has been reported on CSs to date.

Carbon nanostructured materials (e.g. CNTs) are known to have potential applications in many fields: electronics, sensors, polymer composites, hydrogen storage, catalysis and electrodes, due to their exceptional structures at the molecular and nanoscale levels [7].

The doping of carbon nanostructures adds another dimension to the structures' catalytic activity and conductivity properties [8, 9]. It was reported that doping CNTs with nitrogen may lead to n-type semiconducting materials [10], while boron-doped CNTs may lead to electron-deficient p-type semiconducting nanotubes [11-13]. In this study, boron-doped CSs were also prepared and their properties compared with undoped CSs. No reports have appeared on the boron-doping of CSs to date.

4.2 Experimental

4.2.1 Chemicals and materials

Acetylene, BF_3 in methanol**,** cyclopentadiene, cyclohexadiene, chloroform, methanol, sodium sulphate, were purchased from Sigma-Aldrich Chemical Company and used as received.

4.2.2 Synthetic procedures

4.2.2.1 Synthesis of carbon spheres

In this study the synthesis of CSs was achieved by direct pyrolysis of a hydrocarbon gas, acetylene (C_2H_2), in a tubular quartz reactor (51 cm X 1.9 cm i.d), which was placed horizontally in a furnace (**Figure 4.1**). The furnace was electronically controlled and the experimental conditions (reaction temperature, heating rate and gas flow rate) were controlled. The front end of the quartz tube was connected to a glass manifold that allowed free flow of N_2 and C_2H_2 (as a carbon source) gases at atmospheric pressure through the tube. A quartz glass wool plug was placed in the end of the quartz tube, situated outside the furnace.

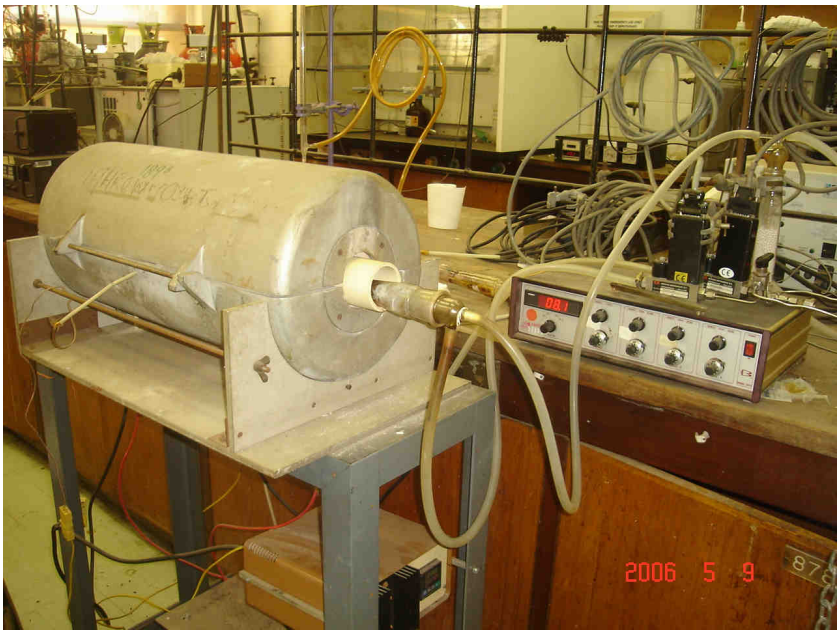

Figure 4.1: The furnace used for the synthesis of carbon spheres.

Prior to synthesis the tube was flushed with N_2 for 20 minutes at a flow rate of 100 ml/min as the reactor was brought to 800 °C. The N_2 gas was replaced with C_2H_2 and passed through the reactor for 2 hours at a constant flow rate of 100 ml/min. This resulted in formation of a sooty deposit on the inner wall of the quartz tube in the hot region of the reactor. The reactor was then cooled to room temperature in a nitrogen atmosphere. The soot was collected, weighed (yield: ca. 2 g) and characterized using high resolution transmission electron microscopy (HRTEM) (Philips CM200 TEM) at 197 kV, TGA (Perkin Elmer, Pyris 1 TGA analyzer) and Raman spectroscopy (Jobin-Yvon T64000 micro-Raman spectrometer). No catalyst was used in the synthesis of the carbon spheres. Unlike products obtained from CNT synthesis, the CSs were very pure and thus required no post-reaction process to remove amorphous material and catalyst.

4.2.2.2 Functionalization of carbon spheres

A second batch of CSs was synthesized under similar conditions as in **Section 4.2.2.1**. Pure carbon spheres were functionalized separately with cyclopentadiene and cyclohexadiene by way of a Diels-Alder type cycloaddition. Carbon spheres (250 mg)

were added to each diene (3 ml) with constant stirring at room temperature for 3 days under an Ar atmosphere. After 2 hours the colour of the reaction mixtures changed to dark brown. Chloroform was added to the reaction mixtures and after stirring for a few minutes, the mixtures were filtered. After separation of the insoluble material, the solvent was removed under reduced pressure. The resulting residues were extracted with dichloromethane, washed several times with deionised water, dried over Na_2SO_4 and the solvent was removed. The resulting materials were dried in an oven affording CS-cyclopentadiene or CS-cyclohexadiene (15 mg (0.6 % yield) and 10 mg (0.4 % yield) in the respective reactions. The functionalized CSs were characterized using TEM (JEOL 100s Electron Microscope), TGA (Perkin Elmer, Pyris 1 TGA analyzer) and Raman spectroscopy (Jobin-Yvon T64000 micro-Raman spectrometer).

4.2.2.3 Synthesis of boron-doped carbon spheres[1]

The furnace shown in **Figure 4.1** was also used for the synthesis of boron-doped carbon spheres. Experimental conditions such as reaction temperature, reaction time, heating rate and gas flow rate were the same as used in the synthesis of the pure carbon spheres. In this study C_2H_2 was used as a carbon source and BF_3 in methanol as a boron source. No catalyst was used. A blank run was recorded with C_2H_2 and MeOH. The C_2H_2 was bubbled through a closed flask containing MeOH. The CSs produced were the same size and gave the same yield as those produced from C_2H_2 in the absence of MeOH. The reaction was repeated by bubbling C_2H_2 through 1.3 M BF_3 in MeOH to achieve B-doped CSs. The resulting CSs were characterized using high resolution transmission electron microscopy (HRTEM) (Philips CM200 TEM) at 197 kV, equipped with a LaB_6 emitter, an Oxford ISIS EDX super ultra-thin windowed detector and a Gatan Model 678 Imaging Filter (GIF). Raman spectroscopy was performed on a Jobin-Yvon T64000 micro-Raman spectrometer equipped with a liquid nitrogen cooled charge coupled device detector**.** All samples were measured after excitation with three different laser wavelengths (488 nm, 514.5 nm and 647nm).

[1] K. C. Mondal, A. Strydom, Z. Tetana, S. D. Mhlanga, M. J. Witcomb, J. Havel, R. Erasmus, N. J. Coville, *Mater. Chem. Phys.*, **2009**, 114, 973.

The presence of boron in the carbon spheres was determined by using laser-ablation inductively coupled plasma optical emission spectrometry (LA-ICP-OES) and Matrix-assisted Laser Desorption Ionization time-of–flight (MALDI-TOF) mass spectrometry. The LA-ICP-MS system consists of a UP-213 Laser Ablation System (New Wave Research) and ICP-MS spectrometer Agilent 7500 series. The laser was operated at the 5th harmonic frequency (213 nm). Experimental calculations used were: repetition rate 20 Hz, laser spot diameter 55 mm, laser irradiance 12.3 $J.cm^{-2}$, raster 1 X 1 mm (3 raster count). The carbon sphere powder and calibration mixtures were directly applied to double-sided tape on a glass slide and ablated into the ICP-MS spectrometer. For calibration, a mixture of activated carbon (ALDRICH, DarcoG60, 100 mesh powder) and boric acid (p.a. Lachema Brno) in the content range of B = 0 – 1.5 % was used (sensitivity < 0.05 %) [14].

4.3 Results and Discussion

4.3.1 Synthesis of carbon spheres

In this study, pyrolysis of acetylene was carried out to make carbon spheres at atmospheric pressure in a flow reactor made of quartz tube that was heated (800 °C) in a furnace. Characterization included HRTEM, TGA and Raman spectroscopy, which were used to determine the sphere morphology and properties.

4.3.1.1 TEM studies

High resolution transmission electron microscopy (HRTEM) was used to examine the morphology of the carbon spheres. In general, the as-prepared products are dark black powders, soft, and light in weight. The HRTEM images indicate that the final products consist of a large quantity of carbon spheres and the carbon spheres have nearly perfect spherical morphology whose surface is very smooth and clean. Multiple conglomerates of the carbon spheres are abundant and chains of bead-like accretions of the carbon spheres are observed in TEM investigations (**Figure 4.2 (a)** and **4.2 (b)**). These carbon spheres

have diameters of 350-700 nm. **Figure 4.2 (a)** shows the HRTEM images of the carbon spheres and **Figure 4.2 (b**) shows the selected area of the electron diffraction pattern (insert). The TEM images show consecutive light and dark concentric contrast areas on an individual sphere, revealing the core/shell geometry of the carbon sphere. An electron diffraction pattern taken from a selected area of the shell, displays rings which indicate that the shell is crystalline in nature. The uniform thickness of the outer shell of these carbon spheres was found to be about 25 nm.

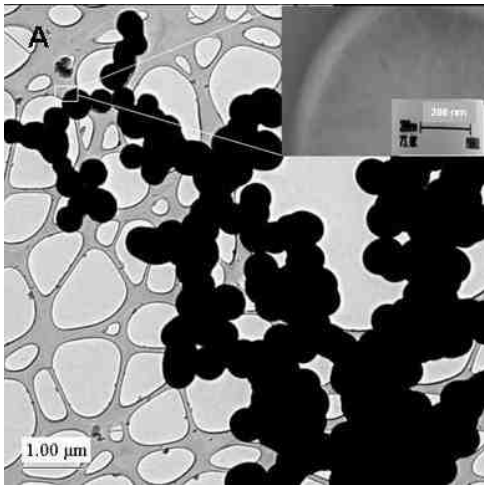

Figure 4.2 (a): TEM images of the CSs. Insert showing the HRTEM image of selected area of the CSs.

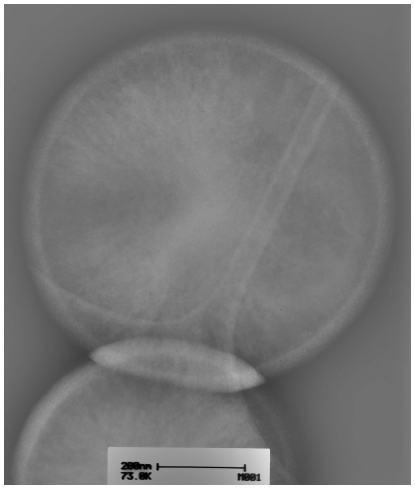

Figure 4.2 (b): HRTEM image of selected area of electron diffraction pattern of the CSs.

4.3.1.2 TGA analysis

The thermal stability of the carbon spheres was assessed by TGA. TGA experiments provide information with regard to the defects when the experiment is done in air, because carbon spheres are very sensitive to oxygen. **Figure 4.3** shows typical curves of carbon spheres, heated to 900 °C in air and N_2 atmosphere. When heated to 900 °C in N_2, about 5 % weight loss of CSs was detected, suggesting that these CSs had a relative high thermal stability in an N_2 atmosphere. When heated in air, the carbon spheres showed stability below 580 °C and the weight loss began at 600 °C. This weight loss below 580 °C may be due to the loss of the amorphous carbon. The steepness of the slope may also

be indicative of lattice defects which enable oxygen to permeate the carbon spheres facilitating rapid oxidation [15].

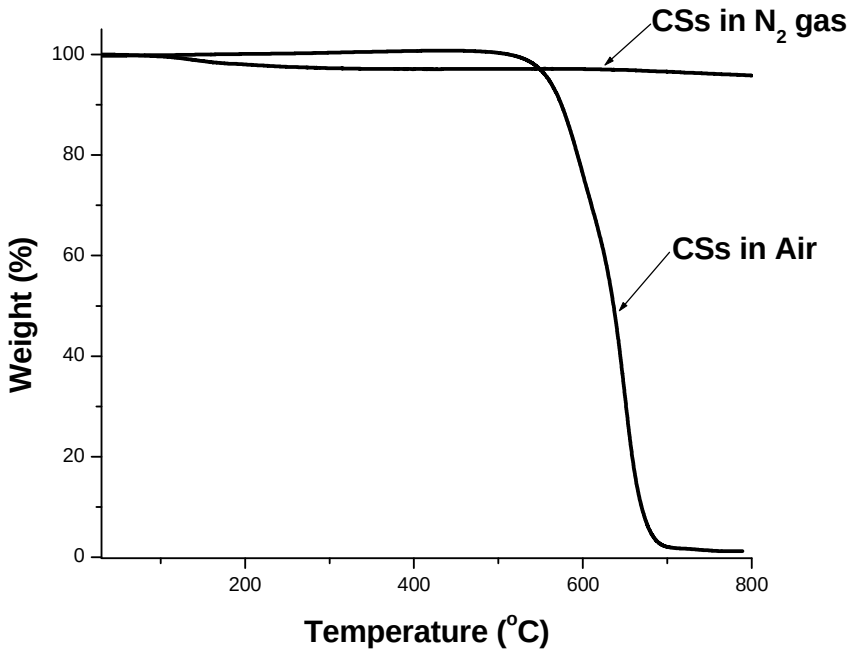

Figure 4.3: TGA curves of carbon spheres in a N_2 atmosphere and in air.

4.3.1.3 Raman spectroscopy

Raman spectroscopy measurements were taken at a 514.5 nm laser excitation wavelength. A typical Raman spectrum of CSs is shown in **Figure 4.4**, where a prominent peak at 1593.0 cm^{-1} and another peak at 1341.3 cm^{-1} can be clearly detected. The peak at 1593.0 cm^{-1} (G-band) corresponds to an E_{2g} mode of graphite and is related to the vibration of sp^2 bonded carbon atoms in a two-dimensional hexagonal lattice, such as in a graphite layer. The peak at 1341.3 cm^{-1} (D-band) is associated with the vibrations of carbon atoms with dangling bonds in disordered graphite planes [16, 17]. Other weak bands at around 1046 cm^{-1} and 1230 cm^{-1} were also observed. The origin of these two weak peaks is not understood currently. Furthermore, the D band has a much wider width in the present observation. The value of I_D/I_G is indicative of the graphitization degree of

the carbon material. Generally, the I_D/I_G ratio would decrease as the content of the amorphous carbon decreases [18]. The intensity ratio of the D to G bands (I_D/I_G) was determined by measuring the area under the curves. The (I_D/I_G) was calculated to be 0.56, and this low I_D/I_G value showed the good crystallinity of the CSs, indicating promising application of CSs in electronics.

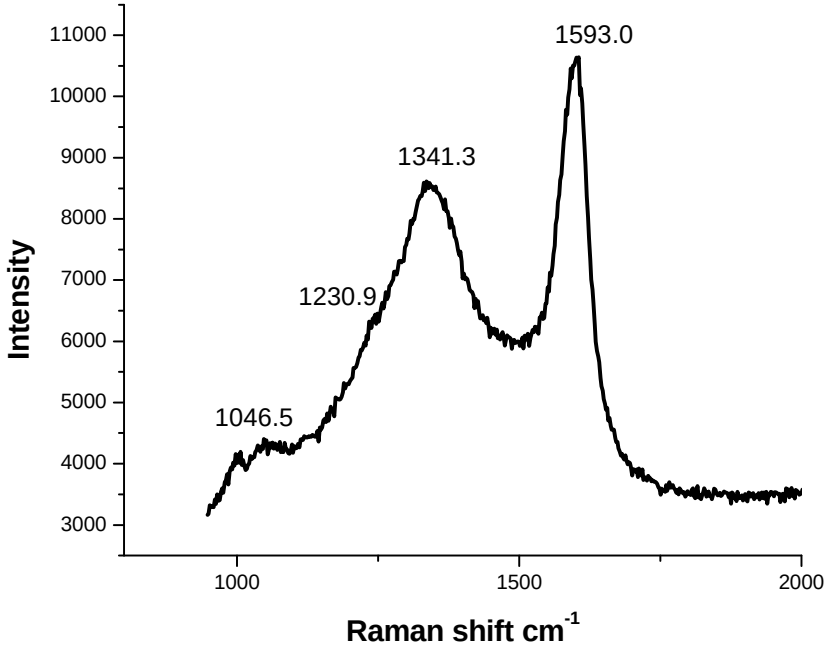

Figure 4.4: Typical Raman spectrum of pristine carbon spheres.

4.3.2 Functionalization of carbon spheres

The carbon spheres were functionalized with cyclopentadiene and cyclohexadiene under an Ar atmosphere. The reactions did not go to completion. The insoluble material which might contain functional groups, but not enough to be soluble, was separated from the soluble material and afforded low yield of functionalized CSs. Unlike the pristine CSs which are known to present poor solubility in common organic solvents, the functionalized CSs were found to be soluble in chloroform, dichloromethane and DMF. These materials were characterized using Raman spectroscopy, TGA and TEM. The

TEM results did not differentiate between the pristine and the functionalized CSs. They both had the same size and morphology.

4.3.2.1 Raman spectroscopy of pristine carbon spheres (CSs) and those functionalized with cyclopentadiene (CS-C_5H_6)

Figure 4.5 shows the Raman spectra (using the 514.5 nm excitation line) of pristine CSs and CSs functionalized with cyclopentadiene. The comparison shows that for functionalized CSs there is a slight shift of the D- and the G-bands. The I_D/I_G ratio for the pristine and the functionalized CSs were found to be 0.78 and 1.23, respectively. This implies that the functionalized CSs were slightly more disordered as compared to the pristine CSs. This was proposed to be due to the incorporation of the functional groups on the CSs.

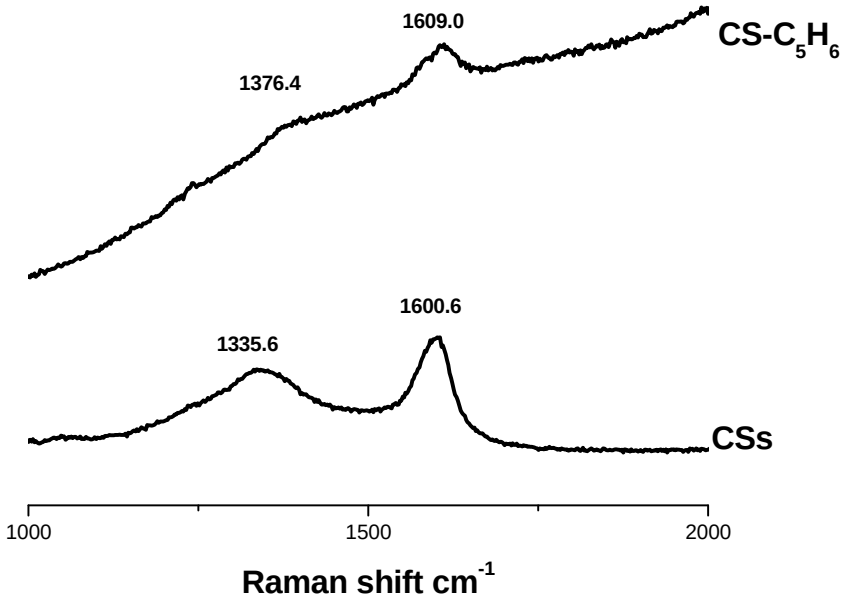

Figure 4.5: Raman spectra of pristine carbon spheres and functionalized carbon spheres (CS-C_5H_6).

4.3.2.2 TGA analysis of CSs functionalized with C_5H_6

The covalent functionalization of the CSs was confirmed by TGA under a N_2 atmosphere. **Figure 4.6** shows that the functionalized CSs could be thermally defunctionalized (i. e. removed from the surface). Compared to the pristine CSs under a N_2 atmosphere, which showed good stability of CSs, the functionalized CSs showed a large weight loss as a function of temperature. This weight loss was due to thermal defunctionalization of the functionalized CSs.

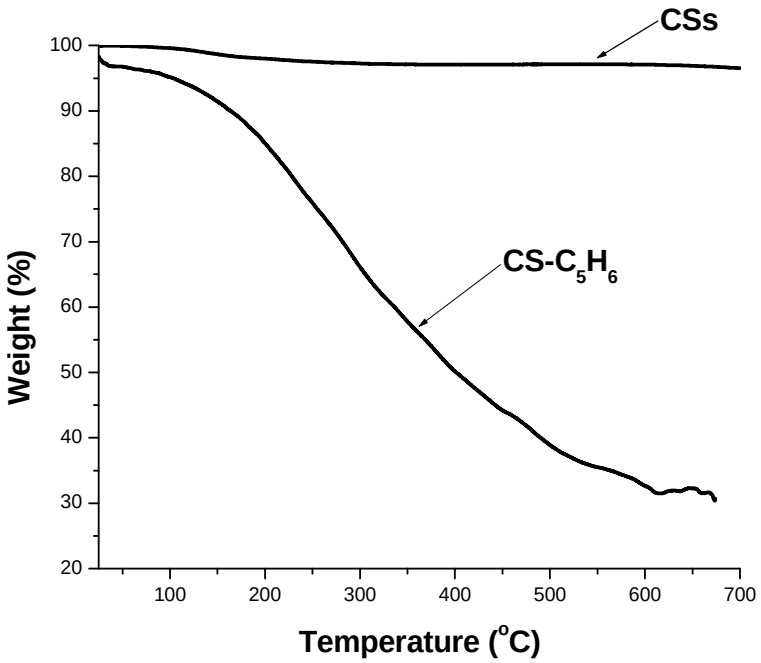

Figure 4.6: TGA curve of the pristine carbon spheres and functionalized carbon spheres (CS-C_5H_6) in a N_2 atmosphere.

4.3.2.3 Raman spectroscopy of carbon spheres functionalized with cyclopentadiene, before and after TGA

The functionalized CSs were analysed by TGA, followed by Raman spectroscopy to confirm the removal of the functional group on the CSs. The Raman spectra (**Figure 4.7**)

show the D- and G-bands of the CSs functionalized with C_5H_6 before and after TGA analysis. From the spectra it can be seen that defunctionalization of the CS-C_5H_6 occurred after the TGA experiment. The spectrum is similar to the one for the pristine CSs, but with I_D/I_G values now equal to 0.79.

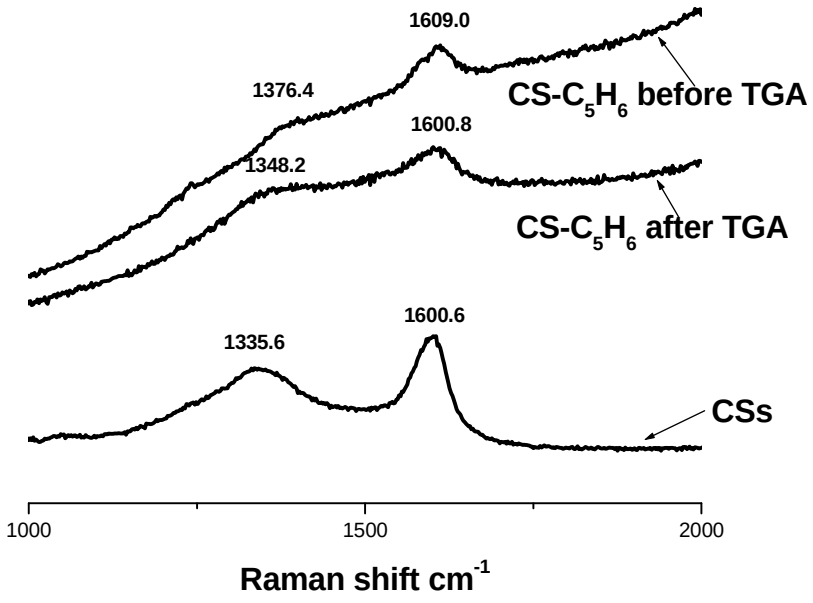

Figure 4.7: Raman spectra of pristine CSs and functionalized carbon spheres (CS-C_5H_6), before and after TGA.

4.3.2.4 Raman spectroscopy of pristine carbon spheres (CS) and those functionalized with cyclohexadiene (CS-C_6H_8)

Carbon spheres were also functionalized using 1,3-cyclohexadiene. The Raman spectra (**Figure 4.8**) of pristine carbon spheres and spheres functionalized with cyclohexadiene show characteristic features with the G-band more intense than the D-band. The spectrum of the pristine CSs shows prominent peaks at about 1330 and 1593 cm^{-1}, indicating the non-graphitic and graphitic nature of the carbon spheres, respectively. The comparison shows that for functionalized CSs there was a slight shift of the D- and the G-bands. The I_D/I_G ratio for the pristine and the CS-C_6H_8 materials were found to be 0.78 and 1.09,

respectively. This implies that the functionalized CSs were more disordered as compared to pristine CSs, due to the introduction of the functional groups on the CSs.

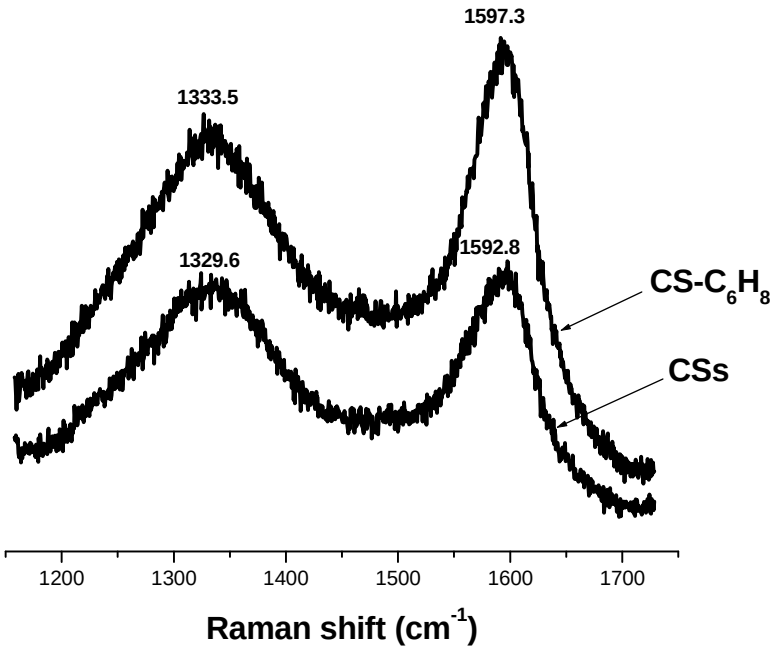

Figure 4.8: Raman spectra of pristine carbon spheres and functionalized carbon spheres (CS-C_6H_8).

4.3.2.5 TGA analysis of CSs functionalized with C_6H_8

Figure 4.9 shows the TGA curves of the pristine CSs and those functionalised with C_6H_8, heated to 800 °C in a N_2 atmosphere. The TGA curves show good stability of pristine CSs while a large weight loss, due to thermal defunctionalization of CS-C_6H_8 is observed. The presented results confirm the functionalization of the CSs.

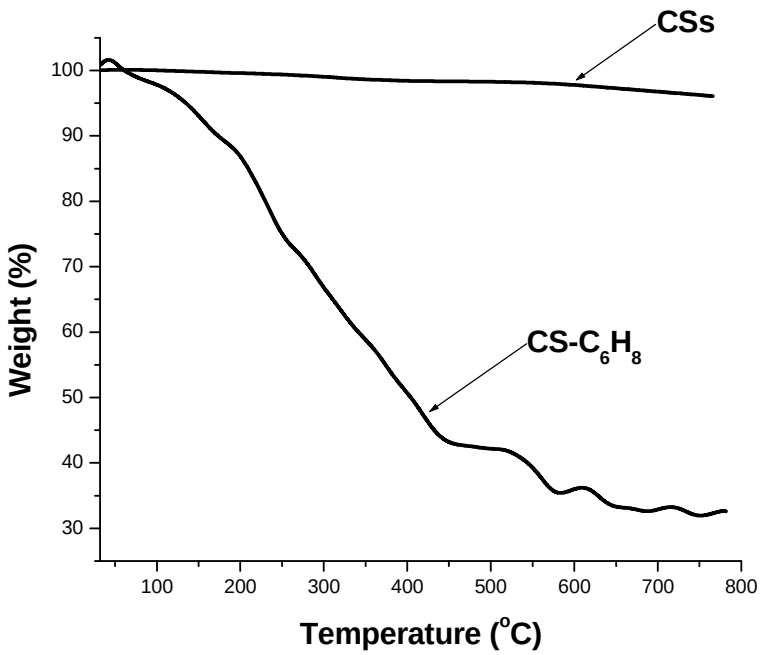

Figure 4.9: TGA curves of pristine CSs and functionalized carbon spheres (CS-C_6H_8) in a N_2 atmosphere.

4.3.2.6 Raman spectroscopy of carbon spheres functionalized with cyclohexadiene, before and after TGA

The CS-C_6H_8 were analysed by TGA followed by Raman spectroscopy to confirm the removal of the functional group on the CSs. The Raman spectra (**Figure 4.10**) show the D- and G-bands of the CS-C_6H_8, before and after TGA analysis. The measured I_D/I_G values for the CSs and the CS-C_6H_8 were found to be 0.78 and 0.77, respectively.

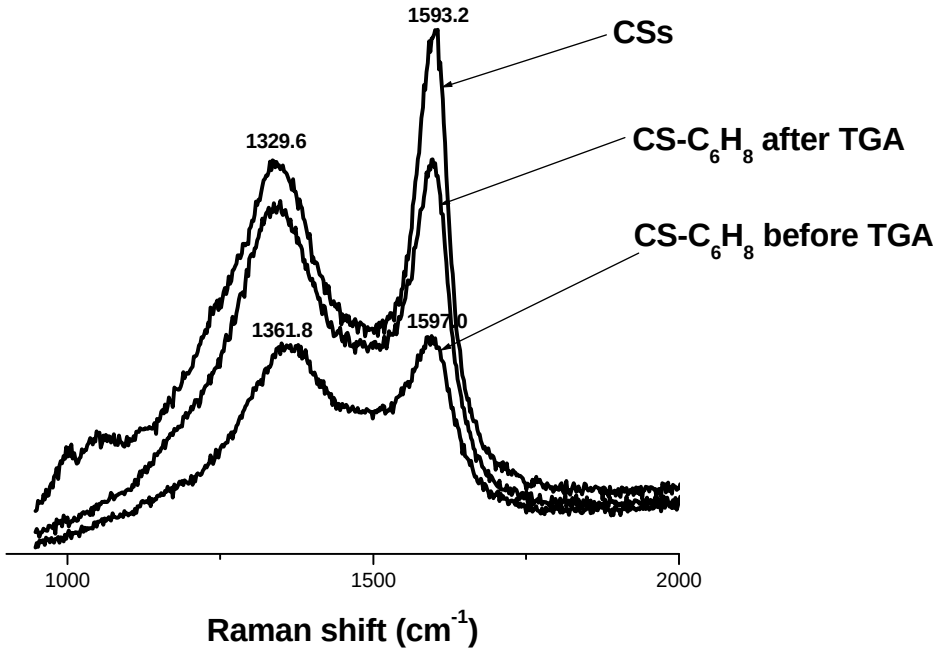

Figure 4.10: Raman spectra of pristine CSs and functionalized carbon spheres (CS-C_6H_8), before and after TGA.

4.3.3 Synthesis of boron-doped carbon spheres[1]

In this study, boron-doped carbon spheres were synthesized by bubbling C_2H_2 through 1.3 M BF_3 in MeOH, in a flow reactor made of quartz tube that was heated (800 °C) in a furnace. As mentioned in the experimental (**Section 4.2.2.2**), a blank run was recorded with C_2H_2 and MeOH and the carbon spheres produced were the same size and gave the same yield as those produced from C_2H_2 in the absence of MeOH. Thus, the CSs synthesized in the presence of boron are compared to the CSs synthesized in the absence of MeOH (reported in **Section 4.2.2.1**). The presence of boron in boron-doped CSs was determined by both MALDI-TOF MS and LA-ICP-OES. The amount of boron present was measured at 0.13 ± 0.03 %. Other characterization techniques used for boron-doped carbon spheres are discussed below. The physical appearance of the boron-doped CSs is similar to that of CSs without boron.

[1] K. C. Mondal, A. Strydom, Z. Tetana, S. D. Mhlanga, M. J. Witcomb, J. Havel, R. Erasmus, N. J. Coville, *Mater. Chem. Phys.*, **2009**, 114, 973.

4.3.3.1 TEM studies

TEM images of carbon spheres with and without boron source are presented in **Figure 4.11**. The CSs without boron source were found to have diameters in the range 350-700 nm. On the other hand, the diameter of the boron-doped CSs were in the range of 650-800 nm, of which about 90 % were found to have the sizes of 650-700 nm. This means that the boron-doped CSs are more uniform in size than undoped CSs. The TEM images of both CSs without boron source (**Figure 4.11A** and an insert) and boron-doped CSs (**Figure 4.11B** and an insert) show a light and dark contrast layers on the carbon sphere, clearly revealing the core/shell geometry of the carbon sphere. The uniform thickness of the outer shell of the undoped carbon spheres was found to be about 25 nm. On the other hand, the uniform thickness of the outer shell of the boron-doped CSs was found to be about 11 nm. This implies that the boron modifies not only the average diameter but also the wall thickness of the carbon spheres, and possibly physical properties of the carbon spheres.

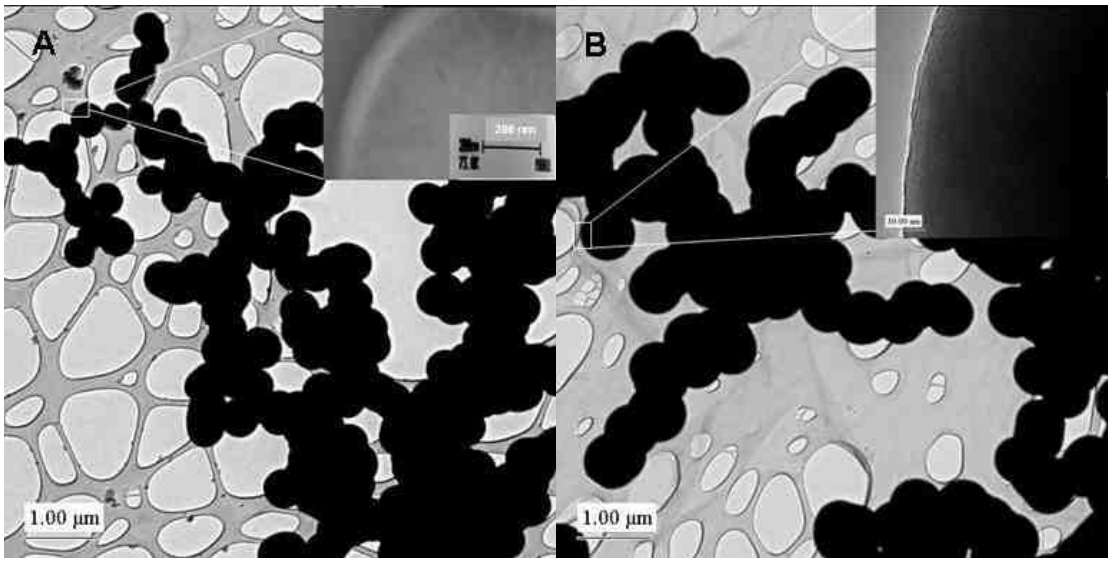

Figure 4.11: TEM image of carbon spheres without boron source (A) and boron-doped carbon spheres (B). Insert showing the HMTEM images of the selected portion of the carbon sphere.

4.3.3.2 Raman spectroscopy

The boron-doped and undoped CSs were studied by Raman spectroscopy. Raman spectra of the boron-doped carbon spheres showing the D and G-bands are presented in **Figure 4.12**. Measurements were taken at 488, 514.5 and 647 nm laser excitation wavelengths. The spectra show prominent peaks at about 1345 cm^{-1} (D band) and 1597 cm^{-1} (G band), indicating the graphitic nature of the carbon spheres. A weak band at around 1046 cm^{-1} was observed for both doped and undoped carbon spheres at 514.5 nm laser excitation. Another weak band was observed at around 1221, 1226 and 1234 cm^{-1} in all laser excitation wavelengths. This kind of band was also observed for the undoped carbon spheres.

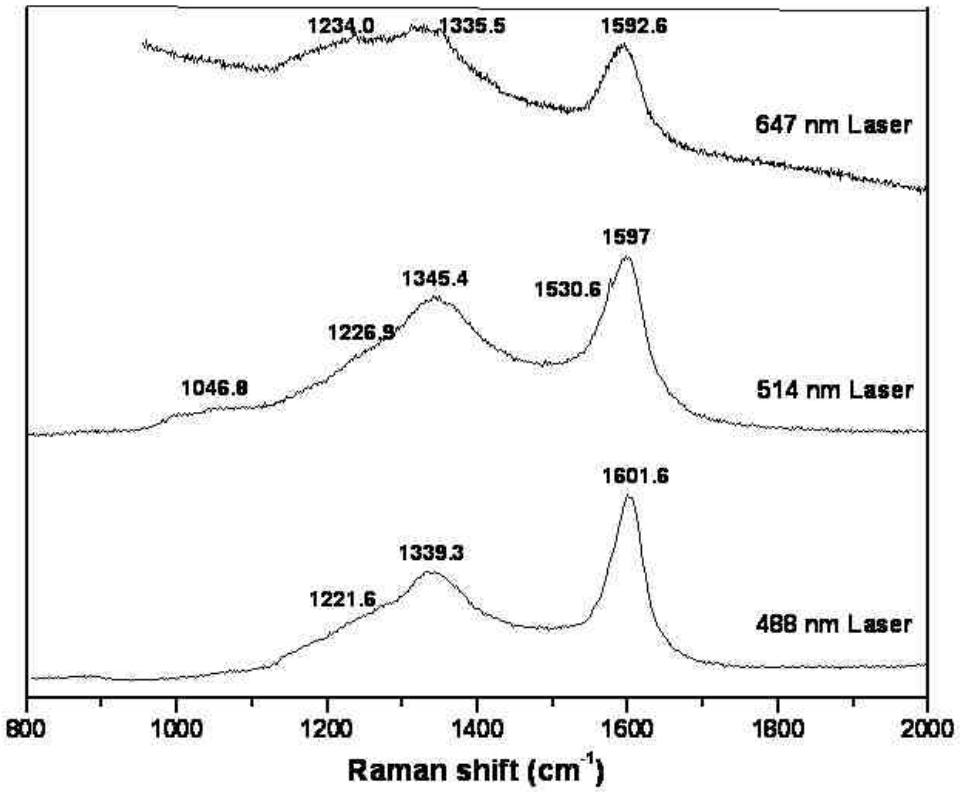

Figure 4.12: Raman spectra of the boron-doped carbon spheres with different laser excitation wavelengths.

It has been observed that the positions of the D- and G-band of carbon spheres shift slightly towards the red side (**Table 4.1**) typically in the 488 and 514.5 nm laser excitation wavelengths for the boron-doped carbon spheres. This is similar to the results proposed by Miao *et al.* [19], who reported that a decrease of the carbon sphere diameter leads to a blue shift of the D- and G-band positions. These results are consistent with the TEM results (**Figure 4.11**) which showed an increase in diameter of the boron-doped carbon spheres. It can be observed from **Table 4.1** that the intensity of the D-band laser excitation line has increased after boron incorporation into the CSs. Usually the I_D/I_G ratio increases on (i) increasing the amount of amorphous carbon in the material and/or (ii) decreasing the graphite crystal size [14]. The G-band width increase of the CSs after the boron incorporation into the graphitic lattice (**Table 4.1**) indicates a decrease in graphitization after boron incorporation. These results were observed at all laser wavelength excitations. The D-band position between 1345.4 and 1335.5 cm^{-1} changed with change of laser excitation from 488 to 647 cm^{-1} after boron incorporation (**Table 4.1**). Kastner and co-workers [20] observed similar effects on their boron-doped carbon nanotubes. Laser excitation results in a resonance enhancement of the contribution from regions near to the observed D-band. These differences are consistent with the presence of boron atoms in the carbon framework, which reduce the ordering of the carbon atoms [21, 22]. Furthermore, a co-worker [14] measured the electrical conductivity of the boron-doped and undoped CSs. The electrical conductivity measurements revealed behaviour in both boron-doped and in undoped CSs that are generally associated with 3-dimensional, semiconducting amorphous materials. The electrical conductivity of the B-doped CSs was found to be lower than that of the undoped CSs by about two orders of magnitude [14]. This effect could be attributed to a higher degree of charge localization which is impeding the charge transport in B-doped CSs compared to the undoped ones.

Table 4.1: Raman spectra data with different laser excitation wavelengths of the boron-doped and undoped carbon spheres

Laser wavelength (nm)	Undoped carbon spheres				Boron-doped carbon spheres			
	I_D/I_G	G-band width (cm^{-1})	D-band position (cm^{-1})	G-band position (cm^{-1})	I_D/I_G	G-band width (cm^{-1})	D-band position (cm^{-1})	G-band position (cm^{-1})
488	**0.62**	**42.2**	**1338.0**	**1597.0**	**0.61**	**49.2**	**1339.3**	**1601.6**
514	**0.56**	**44.5**	**1341.3**	**1593.0**	**0.86**	**56.9**	**1345.4**	**1597.0**
647	**0.47**	**58.7**	**1351.9**	**1595.5**	**0.69**	**56.0**	**1335.5**	**1592.6**

4.4 Conclusion

Carbon spheres with high purity and diameters of 350-700 nm and good features have been synthesized by the CVD method using acetylene as a carbon source. No catalyst was used. Characterization of the CSs by Raman spectroscopy and TGA are indicative of the graphitic nature of the carbon material. In the CSs sp^2 and sp^3 bonding coexist and the CSs exhibit a low degree of graphitization. The CSs were chemically and structurally stable up to 900 °C in an inert atmosphere, or below 600 °C in air. The HRTEM data confirmed the core-shell structure and the crystalline nature of the CSs.

The results on the successful functionalization of CSs with cyclopentadiene and cyclohexadiene under Ar atmosphere were evaluated. It was shown that all the functionalized CSs were more disordered than the pristine CSs. The Raman analysis on CS-C_5H_6 after TGA revealed that defunctionalization at 700 °C under nitrogen atmosphere did occur. The Raman spectrum of the CS-C_5H_6 after TGA analysis was found to be similar to the Raman spectrum of the pristine CSs. Similar TGA and Raman analyses results were noted for the CS-C_6H_8 samples. All the functionalized CSs showed

good solubility in common organic solvents such as chloroform, dichloromethane and DMF.

Finally, a novel method was successfully developed to prepare a high yield of boron-doped CSs (with low B content) and with diameters in the range of 650-700 nm. This was achieved by bubbling C_2H_2 through 1.3 M BF_3 in MeOH at 800 °C without any catalyst. The LA-ICP-OES and MALDI-TOF mass spectrometry observations revealed the incorporation of boron into the carbon spheres. This study demonstrates that the average diameter and the shell thickness of the CSs are influenced by the boron content. The D- and the G-bands positions were shifted towards the red side after B doping. The approach described in this work is a feasible method to fabricate boron-doped carbon spheres [14].

4.5 References

1. M. Aili, W. Xiaomin, L. Tianbao, L. Xuguang, X. Bingshe, *Mater. Sci. Eng. A*, **2007**, 443, 54.
2. J. Chen, A. M. Rao, S. Lyuksyutov, M. E. Itkis, M. A. Hamon, H. Hu, R. W. Cohn, P. C. Eklund, D. T. Colbert, R. E. Smalley, R. C. Haddon, *J. Phys. Chem. B*, **2001**, 105, 2525.
3. J. E. Riggs, Z. Guo, D. L. Carroll, Y.-P. Sun, *J. Am. Chem. Soc.*, **2000**, 122, 5879.
4. J. E. Riggs, D. B. Walker, D. L. Carroll, Y.-P. Sun, *J. Phys. Chem. B*, **2000**, 7071.
5. L. J. Bahr, J. M. Tour, *Chem. Mater.*, **2001**, 13, 3823.
6. S. Pekker, J.-P. Salvetata, E. Jakab, J.-M. Bonard, L. Forro, *J. Phys. Chem. B*, **2001**, 105, 7938
7. P. H. Matter, E. Wang, U. S. Ozkan, *J. Catal.*, **2006**, 243, 395.
8. M. Terrones, P. Redlich, N. Grobert, S. Trasobares, W. K. Hsu, H. Terrone, Y. Q. Zhu, J. P. Hare, C. L. Reeves, A. K. Cheetham, M. Ruhle, H. W. Kroto, D. R. M. Walton, *Adv. Mater.* **1999**, 11, 655.
9. A. B. Fuetes, S. Alvarez, *Carbon*, **2004**, 42, 3049.
10. C. P. Ewels, M. Glerup, *J. Nanosci. Techno.*, **2005**, 5, 1345.
11. S. Saito, *Science*, **1997**, 278, 77.

12. M. Terrones, N. Grobert, H. Terrones, *Carbon*, **2002**, 40, 1665.
13. O. Stephen P. M. Ajayan, C. Colliex, P. Redlich, J. M. Lambert, P. Bernier, P. Lefin, *Science*, **1994**, 266, 1683.
14. K. C. Mondal, A. Strydom, Z. Tetana, S. D. Mhlanga, M. J. Witcomb, J. Havel, R. Erasmus, N. J. Coville, *Mater. Chem. Phys.*, **2009**, 114, 973.
15. Y. Z. Jin, C. Gao, W. K. Hsu, Y. Zhu, A. Huczko, M. Bystrzejewski, M. Roe, C. Y. Lee, S. Acquah, H. Kroto, D. R. M. Walton, *Carbon*, **2005**, 43, 1944.
16. X. G. Yang, C. Li, W. Wang, B. J. Yang, S. Y. Zhang, Y. T. Qian, *Chem. Commun.*, **2004**, 3, 342.
17. T. Jawhari, A. Roid, J. Casado, *Carbon*, **1995**, 33, 1561.
18. J. Y. Miao, D. W. Hwang, K. V. Narasimhulu, P. I. Lin, Y.T. Chen, S. H. Lin, L. P. Hwang, *Carbon*, **2004**, 42, 813.
19. X. Ma, F. Xu, L. Chen, Y. Zhang, Z. Zhang, J. Qian, Y. Qian, *Carbon*, **2006**, 44, 2849.
20. J. Kastner, T. Pichler, H. Kuzmany, S. Curran, W. Blau, D. N. Weldon, M. Delamesiere, S. Draper, H. Zandbergen, *Chem. Phys. Lett.*, **1994**, 221, 53.
21. F. Tuinstra, J. L. Koening, *J. Chem. Phys.*, **1970**, 53, 1126.
22. W. K. Hsu, S. Firth, Ph. Redlich, M. Terrones, H. Terrones, Y. Q. Zhu, N. Grobert, A. Schilder, R. J. H. Clark, H. W. Kroto, D. R. M. Walton, *J. Mater. Chem.*, **2000**, 10, 1425.

CHAPTER 5
CONCLUSIONS AND RECOMMENDATIONS

5.1 Conclusions

5.1.1 On fullerenes

The Diels-Alder reaction, the [4 + 2] cycloaddition reaction, is still one of the most important tools used by organic chemists to construct new molecular systems. Dienophilic properties of the fascinating C_{60} have been widely exploited in such cycloaddition reactions. In particular, this approach has been fruitful in synthesizing a C_{60}-cyclohexadiene monoadduct, though a C_{60}-cyclohexadiene diadduct was also obtained. The cycloaddition product had improved solubility characteristics relative to the unsubstituted fullerene in most organic solvents. The synthesis of the complex 1,4,5,6,7,7-hexachloro-5-norbornene-endo-2,3-heptylimide was successful. The crystal structure of the complex was confirmed by single crystal X-ray diffraction.

In this work, novel C_{60}-containing norbornene copolymers with varying C_{60} contents were prepared via ROMP in the presence of Grubbs' second generation catalyst. The resulting copolymers were characterized using spectroscopic and thermal techniques. The spectroscopic techniques showed successful incorporation of the C_{60} into the copolymers. The thermal techniques showed that the fullerene contents affected the polymer's thermal properties by increasing the glass transition and decomposition temperatures, compared to polynorbornene (**6A-E**) and norbornene derivative polymers (**12A-E**). The amount of fullerene present in the polymer had a major effect on the solubility of the polymer. The solubility behaviour showed the advantage of having a polymer bonded to C_{60}-cyclohexadiene cycloadduct for improved processability. Also, the resulting copolymers revealed that the main fullerene features were retained in the polymers.

5.1.2 On carbon spheres

Carbon spheres (CSs) with high purity, high yield and good features were successfully synthesized by the CVD method using C_2H_2 as a carbon source. The CSs were characterized using Raman spectroscopy, TGA and TEM methods. The consistency of their spheroidal geometry, chemical purity, thermal stability, and the availability of macroscopic quantities makes these CSs promising new materials for application exploration. The low intrinsic mass of these structures suggests that their possible use as components in composite materials for aerospace application may be worthy of investigation. The abundance of defects makes them highly reactive, indicating catalyst support applications and the possibilities of further surface chemical modification uses in a wide range of chemical or biological systems.

Functionalization of the CSs was done using cyclopentadiene and cyclohexadiene using a Diels-Alder strategy as in the first part of the dissertation. The synthesized materials were obtained in low yields. Characterization by Raman spectroscopy and TGA analysis revealed that the functionalized CSs were more disordered after functionalization. Defunctionalization was achieved at high temperature as indicated by TGA results, implying that the CSs were covalently attached to cyclopentadiene and cyclohexadiene. The results showed that the functionalized CSs were more disordered as compared to the pristine CSs. The CSs showed good solubility in organic solvents such as chloroform, dichloromethane and DMF.

Finally, boron-doped CSs with high yield and with diameters in the range of 650-700 nm were successfully prepared using C_2H_2 as a carbon source, and BF_3 in MeOH as a boron source. Characterization by LA-ICP-OES and MALDI-TOF mass spectrometry confirmed the doping of boron into the CSs. TEM analysis implied that the boron modified not only the average diameter, but also the wall thickness of the carbon spheres and possibly the physical properties of the carbon spheres. The approach described in this work is a feasible method to fabricate boron-doped carbon spheres.

5.2 Recommendations for future work

5.2.1 On fullerenes

In this study, it has been not been possible to separate the monoadduct and the diadduct in the C_{60}-cyclohexadiene cycloaddition reaction. While it has been demonstrated that the Diels-alder cycloaddition is an efficient tool for constructing new molecular systems using conventional routes, it is recommended that a microwave approach be used to synthesize the C_{60}-cyclohexadiene cycloadduct. Microwave assisted organic synthesis has numerous advantages over conventional technology: remarkable decreases in the times necessary to carry out reactions (up to three orders of magnitude), improved isolated yields of products (when thermal decomposition is associated with the conventionally heated reactions) and, sometimes, effects of chemo-, regio- and stereoselectivity are also achieved [1].

Fullerene derivatives are known to posses the ability to produce electroactive polymers. Characterization of the C_{60}-based polymers using cyclic voltammetry is necessary to confirm the electroactive property in the polymers. Other physical properties of the C_{60}-containing polymers such as strength, photoconductivity, mechanical properties and optical limiting phenomena can be investigated.

Finally, gel permeation chromatography technique is required to determine the molecular weight distributions of the synthesized polymers.

5.2.2 On carbon spheres

It is evident from this research work that the CVD method is at the moment the best approach for low cost and large scale synthesis of high quality carbon spheres. The functionalization of carbon materials gave soluble derivatives that are easy to analyse and characterize, in low yield. Numerous novel materials such as these organic functionalized CSs derivatives can be synthesized, with a wide variety of properties related to the

attached functional group. It is recommended that thermal Diels-Alder approach be used to drive functionalization reactions to go to completion and to improve the yield of the functionalized CSs.

Studies on the synthesis of boron-dopes CSs using the CVD method were successful. It is recommended that the electrical and thermal transport properties in CSs be further investigated. Indeed the critical parameter will be the amount and type of boron-doping into the CSs. This could be achieved by the use of other volatile boron-containing complexes, including carboranes. Our study has opened up this area of research and many of the experiments used to dope carbon nanotubes can in principle be applied to CSs.

5.3 References

1. P. de la Cruz, A. de la Hoz, F. Langa, B. Illescas, N. Martin, C. Seoane, *Synth. Met.*, **1997**, 86, 2283.

APPENDICES

APPENDIX A

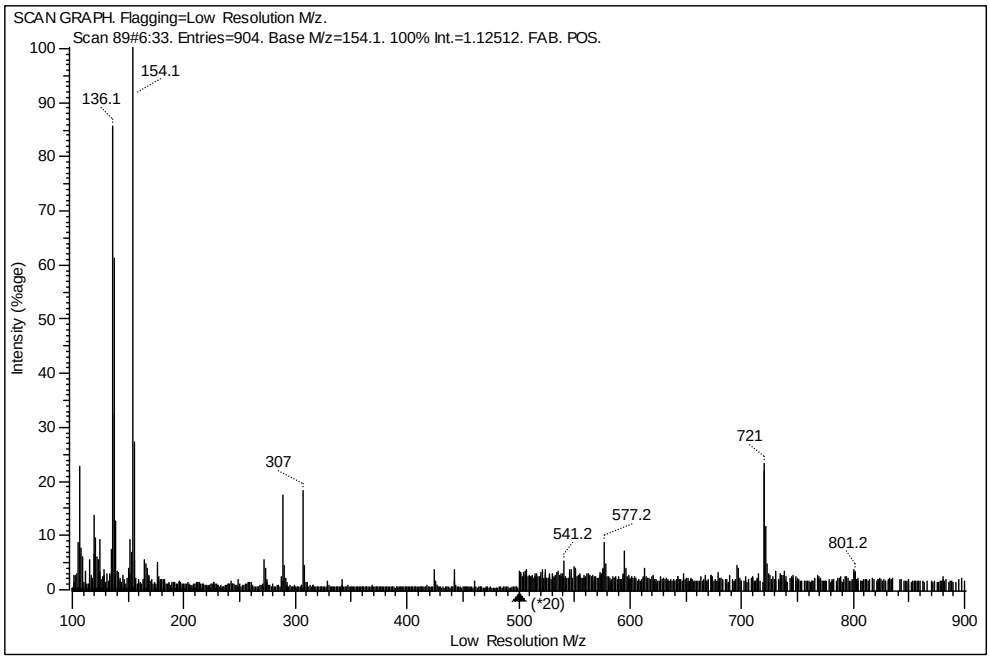

Appendix A1. The mass spectrum of 1:1 C_{60}-cyclohexadiene cycloadduct at 60 °C, for 5 days.

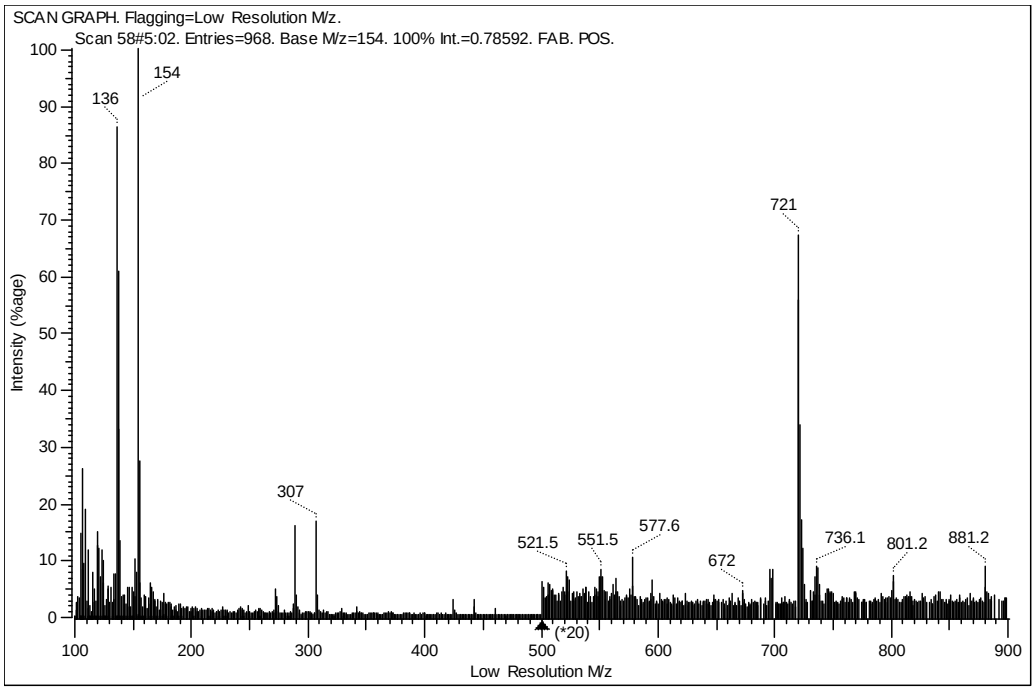

Appendix A2. The mass spectrum of 1:5 C_{60}-cyclohexadiene cycloadduct at 80 °C, for 48 hours.

APPENDIX B

Table 1: Crystal data and structure refinement for 6m_zk1a.

Identification code	6m_zk1a	
Empirical formula	C16 H15 Cl6 N O2	
Formula weight	465.99	
Temperature	173(2) K	
Wavelength	0.71073 Å	
Crystal system	Monoclinic	
Space group	P2(1)	
Unit cell dimensions	a = 11.5554(2) Å	α= 90°.
	b = 13.1210(2) Å	β= 113.3070(10)°.
	c = 13.6705(2) Å	γ = 90°.
Volume	1903.56(5) $Å^3$	
Z	4	
Density (calculated)	1.626 Mg/m^3	
Absorption coefficient	0.913 mm^{-1}	
F(000)	944	
Crystal size	0.20 x 0.19 x 0.08 mm^3	
Theta range for data collection	1.62 to 28.00°.	
Index ranges	-15<=h<=14, -17<=k<=17, -18<=l<=18	
Reflections collected	30508	
Independent reflections	9175 [R(int) = 0.0271]	
Completeness to theta = 28.00°	100.0 %	
Absorption correction	None	
Max. and min. transmission	0.9305 and 0.8384	
Refinement method	Full-matrix least-squares on F^2	
Data / restraints / parameters	9175 / 525 / 580	
Goodness-of-fit on F^2	1.028	
Final R indices [I>2sigma(I)]	R1 = 0.0314, wR2 = 0.0726	
R indices (all data)	R1 = 0.0366, wR2 = 0.0752	
Absolute structure parameter	-0.03(4)	
Largest diff. peak and hole	0.665 and -0.531 $e.Å^{-3}$	

Table 2: Atomic coordinates (x 10^4) and equivalent isotropic displacement parameters ($Å^2$x 10^3) for 6m_zk1a. U(eq) is defined as one third of the trace of the orthogonalized U^{ij} tensor.

	x	y	z	U(eq)
C(1)	7509(3)	1209(3)	9612(3)	26(1)
C(2)	6164(4)	805(3)	9117(3)	28(1)
C(3)	6060(4)	-128(3)	8412(3)	32(1)
C(4)	5781(5)	134(4)	7259(3)	37(1)
C(5)	6529(4)	1001(4)	7085(4)	30(1)
C(6)	7877(4)	1094(5)	7860(3)	33(1)
C(7)	8046(6)	1697(5)	8867(5)	32(1)
C(1A)	7050(12)	1627(8)	9309(9)	28(1)
C(2A)	6701(13)	519(8)	9348(9)	31(1)
C(3A)	5725(13)	140(12)	8282(10)	34(2)
C(4A)	6189(14)	33(13)	7392(12)	33(2)
C(5A)	6912(15)	951(14)	7214(14)	31(2)
C(6A)	8166(15)	1099(16)	8126(13)	31(2)
C(7A)	8168(19)	1829(18)	9015(17)	30(2)
C(1B)	2725(15)	3968(13)	7886(10)	39(1)
C(2B)	2921(7)	3032(5)	8559(6)	46(1)
C(3B)	2273(7)	2925(7)	9340(6)	48(1)
C(4B)	919(6)	2644(5)	8635(6)	55(1)
C(5B)	169(7)	3392(6)	7836(7)	55(1)
C(6B)	432(7)	3457(7)	6843(6)	54(1)
C(7B)	1647(6)	4002(6)	6805(6)	46(1)
C(1C)	2700(17)	3957(15)	7905(11)	40(1)
C(2C)	3083(8)	3271(7)	8891(7)	47(1)
C(3C)	1866(7)	2992(8)	9072(8)	49(1)
C(4C)	619(7)	3405(6)	8535(7)	53(1)
C(5C)	-36(8)	3139(7)	7316(7)	59(2)
C(6C)	340(6)	3881(6)	6660(7)	45(1)
C(7C)	1738(6)	3538(7)	6871(7)	48(1)

C(019)	7209(2)	3254(2)	11491(2)	27(1)
C(021)	9351(2)	3194(2)	12816(2)	27(1)
C(022)	6908(3)	2836(2)	10375(2)	34(1)
C(023)	4166(2)	5755(2)	5960(2)	23(1)
C(024)	4307(2)	4837(2)	5606(2)	22(1)
C(025)	5556(2)	5319(2)	7825(2)	22(1)
C(026)	6334(2)	5541(2)	6454(2)	24(1)
C(027)	5705(2)	4257(2)	7401(2)	22(1)
C(028)	4372(2)	5244(2)	8040(2)	24(1)
C(029)	5646(2)	4495(2)	6261(2)	22(1)
C(030)	5393(2)	6034(2)	6869(2)	22(1)
C(031)	9834(2)	3546(2)	11984(2)	26(1)
C(032)	8993(2)	4184(2)	11334(2)	28(1)
C(034)	8378(2)	1724(2)	11502(2)	31(1)
C(035)	4579(2)	3646(2)	7397(2)	23(1)
C(037)	7933(2)	4284(2)	11719(2)	29(1)
C(040)	8184(2)	2507(2)	12232(2)	24(1)
C(044)	8705(2)	4189(2)	12936(2)	31(1)
O(3)	6211(2)	3223(2)	9564(2)	50(1)
O(4)	9109(2)	1020(2)	11761(2)	49(1)
O(1)	3925(2)	5924(1)	8372(1)	32(1)
O(2)	4327(2)	2786(1)	7113(2)	33(1)
N(1)	3882(2)	4279(2)	7778(2)	24(1)
N(2)	7578(2)	1952(2)	10472(2)	35(1)
Cl(01)	6235(1)	3539(1)	5693(1)	32(1)
Cl(02)	2824(1)	6456(1)	5573(1)	33(1)
Cl(03)	7900(1)	5480(1)	7404(1)	33(1)
Cl(04)	3195(1)	4080(1)	4724(1)	31(1)
Cl(05)	5614(1)	7331(1)	7186(1)	34(1)
Cl(06)	11151(1)	3085(1)	11889(1)	46(1)
Cl(07)	8978(1)	4722(1)	10200(1)	47(1)
Cl(08)	7756(1)	4049(1)	13671(1)	48(1)
Cl(09)	6343(1)	6115(1)	5295(1)	34(1)
Cl(10)	9767(1)	5203(1)	13496(1)	49(1)
Cl(11)	10464(1)	2667(1)	13980(1)	48(1)
Cl(12)	6981(1)	5355(1)	11272(1)	56(1)

Table 3: Bond lengths [Å] and angles [°] for 6m_zk1a.

C(1)-N(2)	1.503(4)
C(1)-C(2)	1.525(5)
C(1)-C(7)	1.527(6)
C(1)-H(1)	1.0000
C(2)-C(3)	1.533(5)
C(2)-H(2A)	0.9900
C(2)-H(2B)	0.9900
C(3)-C(4)	1.518(5)
C(3)-H(3A)	0.9900
C(3)-H(3B)	0.9900
C(4)-C(5)	1.503(5)
C(4)-H(4A)	0.9900
C(4)-H(4B)	0.9900
C(5)-C(6)	1.503(5)
C(5)-H(5A)	0.9900
C(5)-H(5B)	0.9900
C(6)-C(7)	1.532(5)
C(6)-H(6A)	0.9900
C(6)-H(6B)	0.9900
C(7)-H(7A)	0.9900
C(7)-H(7B)	0.9900
C(1A)-C(2A)	1.515(12)
C(1A)-C(7A)	1.521(14)
C(1A)-N(2)	1.521(11)
C(1A)-H(1A)	1.0000
C(2A)-C(3A)	1.530(13)
C(2A)-H(2A1)	0.9900
C(2A)-H(2A2)	0.9900
C(3A)-C(4A)	1.519(14)
C(3A)-H(3A1)	0.9900
C(3A)-H(3A2)	0.9900
C(4A)-C(5A)	1.539(13)
C(4A)-H(4A1)	0.9900
C(4A)-H(4A2)	0.9900

C(5A)-C(6A)	1.505(13)
C(5A)-H(5A1)	0.9900
C(5A)-H(5A2)	0.9900
C(6A)-C(7A)	1.546(14)
C(6A)-H(6A1)	0.9900
C(6A)-H(6A2)	0.9900
C(7A)-H(7A1)	0.9900
C(7A)-H(7A2)	0.9900
C(1B)-N(1)	1.460(18)
C(1B)-C(2B)	1.497(11)
C(1B)-C(7B)	1.510(10)
C(1B)-H(1B)	1.0000
C(2B)-C(3B)	1.534(9)
C(2B)-H(2B1)	0.9900
C(2B)-H(2B2)	0.9900
C(3B)-C(4B)	1.522(9)
C(3B)-H(3B1)	0.9900
C(3B)-H(3B2)	0.9900
C(4B)-C(5B)	1.469(9)
C(4B)-H(4B1)	0.9900
C(4B)-H(4B2)	0.9900
C(5B)-C(6B)	1.507(10)
C(5B)-H(5B1)	0.9900
C(5B)-H(5B2)	0.9900
C(6B)-C(7B)	1.594(9)
C(6B)-H(6B1)	0.9900
C(6B)-H(6B2)	0.9900
C(7B)-H(7B1)	0.9900
C(7B)-H(7B2)	0.9900
C(1C)-N(1)	1.50(2)
C(1C)-C(7C)	1.514(12)
C(1C)-C(2C)	1.533(11)
C(1C)-H(1C)	1.0000
C(2C)-C(3C)	1.564(9)
C(2C)-H(2C1)	0.9900
C(2C)-H(2C2)	0.9900

C(3C)-C(4C)	1.440(10)
C(3C)-H(3C1)	0.9900
C(3C)-H(3C2)	0.9900
C(4C)-C(5C)	1.573(10)
C(4C)-H(4C1)	0.9900
C(4C)-H(4C2)	0.9900
C(5C)-C(6C)	1.499(9)
C(5C)-H(5C1)	0.9900
C(5C)-H(5C2)	0.9900
C(6C)-C(7C)	1.589(9)
C(6C)-H(6C1)	0.9900
C(6C)-H(6C2)	0.9900
C(7C)-H(7C1)	0.9900
C(7C)-H(7C2)	0.9900
C(019)-C(022)	1.527(4)
C(019)-C(040)	1.534(3)
C(019)-C(037)	1.554(3)
C(019)-H(019)	1.0000
C(021)-C(031)	1.524(3)
C(021)-C(044)	1.544(4)
C(021)-C(040)	1.555(3)
C(021)-Cl(11)	1.745(2)
C(022)-O(3)	1.196(3)
C(022)-N(2)	1.372(4)
C(023)-C(024)	1.333(3)
C(023)-C(030)	1.515(3)
C(023)-Cl(02)	1.697(2)
C(024)-C(029)	1.517(3)
C(024)-Cl(04)	1.692(2)
C(025)-C(028)	1.512(3)
C(025)-C(027)	1.544(3)
C(025)-C(030)	1.559(3)
C(025)-H(025)	1.0000
C(026)-C(030)	1.552(3)
C(026)-C(029)	1.555(3)
C(026)-Cl(09)	1.759(2)

C(026)-Cl(03)	1.763(2)
C(027)-C(035)	1.527(3)
C(027)-C(029)	1.564(3)
C(027)-H(027)	1.0000
C(028)-O(1)	1.206(3)
C(028)-N(1)	1.376(3)
C(029)-Cl(01)	1.748(2)
C(030)-Cl(05)	1.750(2)
C(031)-C(032)	1.323(3)
C(031)-Cl(06)	1.689(2)
C(032)-C(037)	1.517(3)
C(032)-Cl(07)	1.697(2)
C(034)-O(4)	1.206(3)
C(034)-N(2)	1.377(4)
C(034)-C(040)	1.509(3)
C(035)-O(2)	1.192(3)
C(035)-N(1)	1.393(3)
C(037)-C(044)	1.551(4)
C(037)-Cl(12)	1.740(2)
C(040)-H(040)	1.0000
C(044)-Cl(10)	1.766(2)
C(044)-Cl(08)	1.766(3)

N(2)-C(1)-C(2)	107.6(3)
N(2)-C(1)-C(7)	109.9(3)
C(2)-C(1)-C(7)	117.5(4)
N(2)-C(1)-H(1)	107.1
C(2)-C(1)-H(1)	107.1
C(7)-C(1)-H(1)	107.1
C(1)-C(2)-C(3)	111.7(3)
C(1)-C(2)-H(2A)	109.3
C(3)-C(2)-H(2A)	109.3
C(1)-C(2)-H(2B)	109.3
C(3)-C(2)-H(2B)	109.3
H(2A)-C(2)-H(2B)	107.9
C(4)-C(3)-C(2)	113.8(4)

C(4)-C(3)-H(3A)	108.8
C(2)-C(3)-H(3A)	108.8
C(4)-C(3)-H(3B)	108.8
C(2)-C(3)-H(3B)	108.8
H(3A)-C(3)-H(3B)	107.7
C(5)-C(4)-C(3)	115.9(3)
C(5)-C(4)-H(4A)	108.3
C(3)-C(4)-H(4A)	108.3
C(5)-C(4)-H(4B)	108.3
C(3)-C(4)-H(4B)	108.3
H(4A)-C(4)-H(4B)	107.4
C(4)-C(5)-C(6)	116.8(4)
C(4)-C(5)-H(5A)	108.1
C(6)-C(5)-H(5A)	108.1
C(4)-C(5)-H(5B)	108.1
C(6)-C(5)-H(5B)	108.1
H(5A)-C(5)-H(5B)	107.3
C(5)-C(6)-C(7)	113.8(4)
C(5)-C(6)-H(6A)	108.8
C(7)-C(6)-H(6A)	108.8
C(5)-C(6)-H(6B)	108.8
C(7)-C(6)-H(6B)	108.8
H(6A)-C(6)-H(6B)	107.7
C(1)-C(7)-C(6)	116.3(4)
C(1)-C(7)-H(7A)	108.2
C(6)-C(7)-H(7A)	108.2
C(1)-C(7)-H(7B)	108.2
C(6)-C(7)-H(7B)	108.2
H(7A)-C(7)-H(7B)	107.4
C(2A)-C(1A)-C(7A)	116.3(12)
C(2A)-C(1A)-N(2)	103.6(8)
C(7A)-C(1A)-N(2)	101.2(10)
C(2A)-C(1A)-H(1A)	111.6
C(7A)-C(1A)-H(1A)	111.7
N(2)-C(1A)-H(1A)	111.6
C(1A)-C(2A)-C(3A)	112.6(11)

C(1A)-C(2A)-H(2A1)	109.1
C(3A)-C(2A)-H(2A1)	109.1
C(1A)-C(2A)-H(2A2)	109.1
C(3A)-C(2A)-H(2A2)	109.1
H(2A1)-C(2A)-H(2A2)	107.8
C(4A)-C(3A)-C(2A)	115.6(12)
C(4A)-C(3A)-H(3A1)	108.4
C(2A)-C(3A)-H(3A1)	108.4
C(4A)-C(3A)-H(3A2)	108.4
C(2A)-C(3A)-H(3A2)	108.3
H(3A1)-C(3A)-H(3A2)	107.4
C(3A)-C(4A)-C(5A)	116.1(12)
C(3A)-C(4A)-H(4A1)	108.3
C(5A)-C(4A)-H(4A1)	108.3
C(3A)-C(4A)-H(4A2)	108.3
C(5A)-C(4A)-H(4A2)	108.3
H(4A1)-C(4A)-H(4A2)	107.4
C(6A)-C(5A)-C(4A)	112.0(13)
C(6A)-C(5A)-H(5A1)	109.2
C(4A)-C(5A)-H(5A1)	109.2
C(6A)-C(5A)-H(5A2)	109.2
C(4A)-C(5A)-H(5A2)	109.2
H(5A1)-C(5A)-H(5A2)	107.9
C(5A)-C(6A)-C(7A)	115.7(14)
C(5A)-C(6A)-H(6A1)	108.4
C(7A)-C(6A)-H(6A1)	108.3
C(5A)-C(6A)-H(6A2)	108.4
C(7A)-C(6A)-H(6A2)	108.3
H(6A1)-C(6A)-H(6A2)	107.4
C(1A)-C(7A)-C(6A)	111.2(11)
C(1A)-C(7A)-H(7A1)	109.4
C(6A)-C(7A)-H(7A1)	109.4
C(1A)-C(7A)-H(7A2)	109.4
C(6A)-C(7A)-H(7A2)	109.3
H(7A1)-C(7A)-H(7A2)	108.0
N(1)-C(1B)-C(2B)	111.7(12)

N(1)-C(1B)-C(7B)	109.1(9)
C(2B)-C(1B)-C(7B)	119.4(9)
N(1)-C(1B)-H(1B)	105.3
C(2B)-C(1B)-H(1B)	105.1
C(7B)-C(1B)-H(1B)	105.0
C(1B)-C(2B)-C(3B)	120.4(11)
C(1B)-C(2B)-H(2B1)	106.7
C(3B)-C(2B)-H(2B1)	107.7
C(1B)-C(2B)-H(2B2)	106.4
C(3B)-C(2B)-H(2B2)	107.8
H(2B1)-C(2B)-H(2B2)	107.1
C(4B)-C(3B)-C(2B)	104.1(6)
C(4B)-C(3B)-H(3B1)	110.9
C(2B)-C(3B)-H(3B1)	110.9
C(4B)-C(3B)-H(3B2)	111.0
C(2B)-C(3B)-H(3B2)	111.0
H(3B1)-C(3B)-H(3B2)	109.0
C(5B)-C(4B)-C(3B)	117.7(6)
C(5B)-C(4B)-H(4B1)	107.9
C(3B)-C(4B)-H(4B1)	107.9
C(5B)-C(4B)-H(4B2)	107.8
C(3B)-C(4B)-H(4B2)	107.9
H(4B1)-C(4B)-H(4B2)	107.2
C(4B)-C(5B)-C(6B)	115.9(6)
C(4B)-C(5B)-H(5B1)	108.3
C(6B)-C(5B)-H(5B1)	108.3
C(4B)-C(5B)-H(5B2)	108.3
C(6B)-C(5B)-H(5B2)	108.4
H(5B1)-C(5B)-H(5B2)	107.4
C(5B)-C(6B)-C(7B)	123.3(7)
C(5B)-C(6B)-H(6B1)	106.5
C(7B)-C(6B)-H(6B1)	106.5
C(5B)-C(6B)-H(6B2)	106.5
C(7B)-C(6B)-H(6B2)	106.5
H(6B1)-C(6B)-H(6B2)	106.5
C(1B)-C(7B)-C(6B)	110.6(8)

C(1B)-C(7B)-H(7B1)	109.6
C(6B)-C(7B)-H(7B1)	109.8
C(1B)-C(7B)-H(7B2)	110.8
C(6B)-C(7B)-H(7B2)	109.7
H(7B1)-C(7B)-H(7B2)	108.2
N(1)-C(1C)-C(7C)	111.0(14)
N(1)-C(1C)-C(2C)	107.9(11)
C(7C)-C(1C)-C(2C)	117.2(11)
N(1)-C(1C)-H(1C)	106.6
C(7C)-C(1C)-H(1C)	106.7
C(2C)-C(1C)-H(1C)	106.9
C(1C)-C(2C)-C(3C)	108.1(10)
C(1C)-C(2C)-H(2C1)	109.0
C(3C)-C(2C)-H(2C1)	109.7
C(1C)-C(2C)-H(2C2)	110.1
C(3C)-C(2C)-H(2C2)	109.7
H(2C1)-C(2C)-H(2C2)	108.2
C(4C)-C(3C)-C(2C)	127.8(7)
C(4C)-C(3C)-H(3C1)	105.4
C(2C)-C(3C)-H(3C1)	105.3
C(4C)-C(3C)-H(3C2)	105.4
C(2C)-C(3C)-H(3C2)	105.4
H(3C1)-C(3C)-H(3C2)	106.0
C(3C)-C(4C)-C(5C)	114.9(7)
C(3C)-C(4C)-H(4C1)	108.6
C(5C)-C(4C)-H(4C1)	108.5
C(3C)-C(4C)-H(4C2)	108.4
C(5C)-C(4C)-H(4C2)	108.5
H(4C1)-C(4C)-H(4C2)	107.5
C(6C)-C(5C)-C(4C)	110.9(7)
C(6C)-C(5C)-H(5C1)	109.4
C(4C)-C(5C)-H(5C1)	109.5
C(6C)-C(5C)-H(5C2)	109.4
C(4C)-C(5C)-H(5C2)	109.5
H(5C1)-C(5C)-H(5C2)	108.1
C(5C)-C(6C)-C(7C)	102.8(7)

C(5C)-C(6C)-H(6C1)	111.1
C(7C)-C(6C)-H(6C1)	111.0
C(5C)-C(6C)-H(6C2)	111.3
C(7C)-C(6C)-H(6C2)	111.4
H(6C1)-C(6C)-H(6C2)	109.1
C(1C)-C(7C)-C(6C)	112.6(11)
C(1C)-C(7C)-H(7C1)	109.9
C(6C)-C(7C)-H(7C1)	108.5
C(1C)-C(7C)-H(7C2)	109.7
C(6C)-C(7C)-H(7C2)	108.5
H(7C1)-C(7C)-H(7C2)	107.6
C(022)-C(019)-C(040)	104.3(2)
C(022)-C(019)-C(037)	113.8(2)
C(040)-C(019)-C(037)	103.11(18)
C(022)-C(019)-H(019)	111.7
C(040)-C(019)-H(019)	111.7
C(037)-C(019)-H(019)	111.7
C(031)-C(021)-C(044)	99.12(19)
C(031)-C(021)-C(040)	106.95(19)
C(044)-C(021)-C(040)	100.80(19)
C(031)-C(021)-Cl(11)	116.46(18)
C(044)-C(021)-Cl(11)	116.80(18)
C(040)-C(021)-Cl(11)	114.51(16)
O(3)-C(022)-N(2)	126.6(3)
O(3)-C(022)-C(019)	125.2(3)
N(2)-C(022)-C(019)	108.2(2)
C(024)-C(023)-C(030)	107.9(2)
C(024)-C(023)-Cl(02)	127.20(19)
C(030)-C(023)-Cl(02)	124.65(17)
C(023)-C(024)-C(029)	107.18(19)
C(023)-C(024)-Cl(04)	128.45(19)
C(029)-C(024)-Cl(04)	123.85(17)
C(028)-C(025)-C(027)	104.93(18)
C(028)-C(025)-C(030)	112.59(18)
C(027)-C(025)-C(030)	102.85(17)
C(028)-C(025)-H(025)	112.0

C(027)-C(025)-H(025)	112.0
C(030)-C(025)-H(025)	112.0
C(030)-C(026)-C(029)	92.57(16)
C(030)-C(026)-Cl(09)	113.89(16)
C(029)-C(026)-Cl(09)	114.22(16)
C(030)-C(026)-Cl(03)	114.38(16)
C(029)-C(026)-Cl(03)	113.09(16)
Cl(09)-C(026)-Cl(03)	108.22(12)
C(035)-C(027)-C(025)	104.73(18)
C(035)-C(027)-C(029)	113.62(19)
C(025)-C(027)-C(029)	103.12(17)
C(035)-C(027)-H(027)	111.6
C(025)-C(027)-H(027)	111.6
C(029)-C(027)-H(027)	111.6
O(1)-C(028)-N(1)	125.8(2)
O(1)-C(028)-C(025)	125.5(2)
N(1)-C(028)-C(025)	108.67(19)
C(024)-C(029)-C(026)	99.96(17)
C(024)-C(029)-C(027)	106.19(18)
C(026)-C(029)-C(027)	100.90(17)
C(024)-C(029)-Cl(01)	115.78(16)
C(026)-C(029)-Cl(01)	116.47(16)
C(027)-C(029)-Cl(01)	115.39(16)
C(023)-C(030)-C(026)	99.45(17)
C(023)-C(030)-C(025)	107.80(18)
C(026)-C(030)-C(025)	100.70(17)
C(023)-C(030)-Cl(05)	115.81(16)
C(026)-C(030)-Cl(05)	116.20(16)
C(025)-C(030)-Cl(05)	114.82(16)
C(032)-C(031)-C(021)	107.7(2)
C(032)-C(031)-Cl(06)	128.3(2)
C(021)-C(031)-Cl(06)	123.77(18)
C(031)-C(032)-C(037)	107.6(2)
C(031)-C(032)-Cl(07)	128.0(2)
C(037)-C(032)-Cl(07)	124.22(19)
O(4)-C(034)-N(2)	125.1(3)

O(4)-C(034)-C(040)	126.6(3)
N(2)-C(034)-C(040)	108.3(2)
O(2)-C(035)-N(1)	125.7(2)
O(2)-C(035)-C(027)	126.6(2)
N(1)-C(035)-C(027)	107.66(19)
C(032)-C(037)-C(044)	99.44(19)
C(032)-C(037)-C(019)	107.5(2)
C(044)-C(037)-C(019)	100.40(19)
C(032)-C(037)-Cl(12)	115.62(18)
C(044)-C(037)-Cl(12)	117.17(18)
C(019)-C(037)-Cl(12)	114.64(17)
C(034)-C(040)-C(019)	105.2(2)
C(034)-C(040)-C(021)	114.2(2)
C(019)-C(040)-C(021)	103.26(18)
C(034)-C(040)-H(040)	111.3
C(019)-C(040)-H(040)	111.3
C(021)-C(040)-H(040)	111.3
C(021)-C(044)-C(037)	92.93(18)
C(021)-C(044)-Cl(10)	113.63(18)
C(037)-C(044)-Cl(10)	114.28(18)
C(021)-C(044)-Cl(08)	114.06(18)
C(037)-C(044)-Cl(08)	113.34(18)
Cl(10)-C(044)-Cl(08)	108.18(13)
C(028)-N(1)-C(035)	114.00(19)
C(028)-N(1)-C(1B)	122.0(8)
C(035)-N(1)-C(1B)	124.0(8)
C(028)-N(1)-C(1C)	121.8(9)
C(035)-N(1)-C(1C)	124.2(9)
C(022)-N(2)-C(034)	114.0(2)
C(022)-N(2)-C(1)	128.3(2)
C(034)-N(2)-C(1)	117.7(3)
C(022)-N(2)-C(1A)	99.1(5)
C(034)-N(2)-C(1A)	146.9(5)

Symmetry transformations used to generate equivalent atoms:

Table 4: Anisotropic displacement parameters ($Å^2 x\ 10^3$)for 6m_zk1a. The anisotropic displacement factor exponent takes the form: $-2\pi^2[\ h^2 a^{*2} U^{11} + ... + 2\ h\ k\ a^*\ b^*\ U^{12}\ ]$

	U^{11}	U^{22}	U^{33}	U^{23}	U^{13}	U^{12}
C(1)	26(2)	25(1)	30(1)	-6(1)	14(1)	-3(1)
C(2)	26(2)	31(2)	29(1)	-6(1)	15(1)	-7(1)
C(3)	36(2)	29(2)	34(2)	-4(1)	16(1)	-10(1)
C(4)	43(2)	38(2)	32(2)	-9(1)	16(2)	-9(2)
C(5)	37(2)	30(1)	26(2)	-5(1)	15(2)	-1(2)
C(6)	36(2)	38(2)	35(2)	-3(2)	23(2)	-3(2)
C(7)	30(2)	31(2)	37(2)	-8(1)	17(2)	-11(1)
C(1A)	27(2)	28(2)	32(2)	-5(2)	14(2)	-6(2)
C(2A)	31(2)	30(2)	32(2)	-4(2)	15(2)	-6(2)
C(3A)	34(3)	34(3)	33(2)	-4(2)	14(2)	-7(2)
C(4A)	35(3)	33(2)	31(2)	-8(2)	15(2)	-4(3)
C(5A)	35(3)	33(3)	30(3)	-2(2)	19(3)	-5(3)
C(6A)	30(3)	34(3)	34(3)	-4(3)	17(3)	-8(3)
C(7A)	28(3)	30(3)	33(3)	-6(3)	16(3)	-8(2)
C(1B)	31(2)	46(2)	46(2)	-1(2)	24(2)	-6(2)
C(2B)	47(2)	45(2)	55(2)	2(2)	31(2)	-8(2)
C(3B)	50(3)	45(2)	61(3)	0(2)	35(2)	-5(2)
C(4B)	51(2)	45(2)	82(3)	8(2)	39(2)	-8(2)
C(5B)	39(2)	56(3)	76(3)	0(3)	30(2)	-5(2)
C(6B)	34(2)	62(3)	65(2)	1(2)	18(2)	-10(2)
C(7B)	31(2)	49(2)	56(2)	2(2)	14(2)	-3(2)
C(1C)	32(2)	48(2)	47(2)	-1(2)	24(2)	-7(2)
C(2C)	48(2)	49(2)	54(2)	4(2)	31(2)	-11(2)
C(3C)	49(2)	50(2)	65(3)	4(2)	40(2)	-12(2)
C(4C)	47(2)	49(2)	79(3)	1(3)	42(2)	-2(2)
C(5C)	41(2)	58(3)	77(3)	1(3)	20(2)	-12(2)
C(6C)	28(2)	51(3)	58(2)	-1(2)	20(2)	-9(2)
C(7C)	32(2)	57(3)	55(2)	-5(2)	19(2)	-7(2)
C(019)	19(1)	30(1)	28(1)	2(1)	5(1)	-2(1)

C(021)	24(1)	26(1)	26(1)	1(1)	3(1)	-4(1)
C(022)	26(1)	48(2)	23(1)	1(1)	4(1)	-17(1)
C(023)	19(1)	28(1)	22(1)	6(1)	9(1)	1(1)
C(024)	19(1)	26(1)	20(1)	0(1)	8(1)	-5(1)
C(025)	18(1)	26(1)	20(1)	1(1)	5(1)	0(1)
C(026)	21(1)	24(1)	26(1)	0(1)	10(1)	-3(1)
C(027)	18(1)	23(1)	25(1)	3(1)	8(1)	2(1)
C(028)	23(1)	31(1)	17(1)	4(1)	7(1)	3(1)
C(029)	21(1)	22(1)	26(1)	-3(1)	13(1)	-1(1)
C(030)	24(1)	18(1)	27(1)	-3(1)	11(1)	-3(1)
C(031)	20(1)	24(1)	34(1)	-2(1)	9(1)	-3(1)
C(032)	26(1)	24(1)	31(1)	3(1)	10(1)	-5(1)
C(034)	30(1)	27(1)	39(1)	-4(1)	18(1)	-11(1)
C(035)	22(1)	28(1)	21(1)	6(1)	8(1)	1(1)
C(037)	22(1)	22(1)	41(1)	4(1)	9(1)	4(1)
C(040)	23(1)	23(1)	25(1)	0(1)	7(1)	-5(1)
C(044)	29(1)	29(1)	35(1)	-10(1)	11(1)	-9(1)
O(3)	38(1)	68(2)	29(1)	11(1)	-4(1)	-12(1)
O(4)	46(1)	27(1)	76(2)	-5(1)	28(1)	-1(1)
O(1)	34(1)	35(1)	32(1)	-2(1)	19(1)	5(1)
O(2)	35(1)	25(1)	41(1)	-1(1)	17(1)	-5(1)
N(1)	21(1)	30(1)	25(1)	5(1)	12(1)	1(1)
N(2)	40(1)	36(1)	32(1)	-11(1)	18(1)	-19(1)
Cl(01)	36(1)	27(1)	42(1)	-6(1)	24(1)	1(1)
Cl(02)	27(1)	38(1)	32(1)	6(1)	10(1)	12(1)
Cl(03)	19(1)	38(1)	41(1)	-3(1)	10(1)	-3(1)
Cl(04)	30(1)	36(1)	24(1)	-5(1)	7(1)	-10(1)
Cl(05)	39(1)	21(1)	45(1)	-5(1)	18(1)	-4(1)
Cl(06)	31(1)	36(1)	78(1)	3(1)	29(1)	4(1)
Cl(07)	47(1)	52(1)	41(1)	17(1)	16(1)	-8(1)
Cl(08)	57(1)	50(1)	49(1)	-20(1)	33(1)	-16(1)
Cl(09)	37(1)	36(1)	36(1)	4(1)	22(1)	-8(1)
Cl(10)	52(1)	38(1)	56(1)	-21(1)	20(1)	-22(1)
Cl(11)	36(1)	51(1)	37(1)	14(1)	-7(1)	-6(1)
Cl(12)	40(1)	31(1)	96(1)	15(1)	24(1)	14(1)

Table 5: Hydrogen coordinates (x 10^4) and isotropic displacement parameters ($Å^2$x 10^3)
for 6m_zk1a.

	x	y	z	U(eq)
H(1)	8067	621	9968	31
H(2A)	5598	1348	8685	33
H(2B)	5885	616	9691	33
H(3A)	6860	-514	8709	38
H(3B)	5383	-578	8435	38
H(4A)	5935	-480	6908	45
H(4B)	4875	303	6900	45
H(5A)	6091	1645	7101	36
H(5B)	6520	932	6360	36
H(6A)	8366	1432	7499	40
H(6B)	8230	402	8069	40
H(7A)	8959	1812	9274	38
H(7B)	7647	2373	8649	38
H(1A)	6301	2045	8869	34
H(2A1)	6360	434	9903	37
H(2A2)	7470	96	9552	37
H(3A1)	5410	-531	8399	40
H(3A2)	5003	618	8045	40
H(4A1)	5453	-101	6720	39
H(4A2)	6744	-573	7542	39
H(5A1)	7047	846	6549	37
H(5A2)	6398	1574	7125	37
H(6A1)	8771	1361	7838	38
H(6A2)	8477	425	8450	38
H(7A1)	8960	1739	9653	35
H(7A2)	8136	2543	8770	35
H(1B)	2545	4525	8306	46

H(2B1)	3839	2965	8978	55
H(2B2)	2661	2441	8070	55
H(3B1)	2676	2382	9869	57
H(3B2)	2306	3573	9720	57
H(4B1)	937	2004	8257	66
H(4B2)	472	2495	9104	66
H(5B1)	314	4073	8175	66
H(5B2)	-734	3226	7624	66
H(6B1)	-308	3794	6296	65
H(6B2)	440	2748	6598	65
H(7B1)	1898	3655	6276	56
H(7B2)	1445	4719	6579	56
H(1C)	2325	4588	8071	48
H(2C1)	3688	3632	9522	56
H(2C2)	3491	2644	8780	56
H(3C1)	1769	2246	8965	59
H(3C2)	2084	3109	9839	59
H(4C1)	667	4156	8612	64
H(4C2)	82	3151	8894	64
H(5C1)	206	2441	7195	71
H(5C2)	-962	3155	7090	71
H(6C1)	320	4590	6900	54
H(6C2)	-218	3825	5896	54
H(7C1)	1783	2784	6890	57
H(7C2)	1950	3774	6274	57
H(019)	6439	3291	11654	33
H(025)	6307	5509	8479	26
H(027)	6522	3931	7860	27
H(040)	7876	2183	12746	29

Table 6: Torsion angles [°] for 6m_zk1a.

N(2)-C(1)-C(2)-C(3)	-167.2(3)
C(7)-C(1)-C(2)-C(3)	68.3(5)
C(1)-C(2)-C(3)-C(4)	-89.5(5)
C(2)-C(3)-C(4)-C(5)	44.5(6)
C(3)-C(4)-C(5)-C(6)	36.5(6)
C(4)-C(5)-C(6)-C(7)	-86.0(5)
N(2)-C(1)-C(7)-C(6)	-171.8(4)
C(2)-C(1)-C(7)-C(6)	-48.4(7)
C(5)-C(6)-C(7)-C(1)	66.7(7)
C(7A)-C(1A)-C(2A)-C(3A)	-91.3(17)
N(2)-C(1A)-C(2A)-C(3A)	158.7(10)
C(1A)-C(2A)-C(3A)-C(4A)	69.7(18)
C(2A)-C(3A)-C(4A)-C(5A)	-48.6(19)
C(3A)-C(4A)-C(5A)-C(6A)	68.0(18)
C(4A)-C(5A)-C(6A)-C(7A)	-92.1(18)
C(2A)-C(1A)-C(7A)-C(6A)	40(2)
N(2)-C(1A)-C(7A)-C(6A)	150.9(15)
C(5A)-C(6A)-C(7A)-C(1A)	44(2)
N(1)-C(1B)-C(2B)-C(3B)	141.6(11)
C(7B)-C(1B)-C(2B)-C(3B)	-89.5(18)
C(1B)-C(2B)-C(3B)-C(4B)	77.4(10)
C(2B)-C(3B)-C(4B)-C(5B)	-63.3(9)
C(3B)-C(4B)-C(5B)-C(6B)	77.7(10)
C(4B)-C(5B)-C(6B)-C(7B)	-75.8(11)
N(1)-C(1B)-C(7B)-C(6B)	168.5(10)
C(2B)-C(1B)-C(7B)-C(6B)	38(2)
C(5B)-C(6B)-C(7B)-C(1B)	27.6(14)
N(1)-C(1C)-C(2C)-C(3C)	176.3(11)
C(7C)-C(1C)-C(2C)-C(3C)	-58(2)
C(1C)-C(2C)-C(3C)-C(4C)	-8.7(16)
C(2C)-C(3C)-C(4C)-C(5C)	66.3(13)
C(3C)-C(4C)-C(5C)-C(6C)	-85.3(9)
C(4C)-C(5C)-C(6C)-C(7C)	74.9(9)
N(1)-C(1C)-C(7C)-C(6C)	-140.6(12)

C(2C)-C(1C)-C(7C)-C(6C)	94.8(18)
C(5C)-C(6C)-C(7C)-C(1C)	-81.8(10)
C(040)-C(019)-C(022)-O(3)	-177.5(3)
C(037)-C(019)-C(022)-O(3)	-65.9(3)
C(040)-C(019)-C(022)-N(2)	2.2(3)
C(037)-C(019)-C(022)-N(2)	113.8(2)
C(030)-C(023)-C(024)-C(029)	-1.1(2)
Cl(02)-C(023)-C(024)-C(029)	-175.20(17)
C(030)-C(023)-C(024)-Cl(04)	170.76(17)
Cl(02)-C(023)-C(024)-Cl(04)	-3.3(3)
C(028)-C(025)-C(027)-C(035)	0.3(2)
C(030)-C(025)-C(027)-C(035)	-117.61(18)
C(028)-C(025)-C(027)-C(029)	119.46(18)
C(030)-C(025)-C(027)-C(029)	1.5(2)
C(027)-C(025)-C(028)-O(1)	-179.3(2)
C(030)-C(025)-C(028)-O(1)	-68.1(3)
C(027)-C(025)-C(028)-N(1)	-0.3(2)
C(030)-C(025)-C(028)-N(1)	110.9(2)
C(023)-C(024)-C(029)-C(026)	-33.7(2)
Cl(04)-C(024)-C(029)-C(026)	153.97(17)
C(023)-C(024)-C(029)-C(027)	70.8(2)
Cl(04)-C(024)-C(029)-C(027)	-101.5(2)
C(023)-C(024)-C(029)-Cl(01)	-159.67(16)
Cl(04)-C(024)-C(029)-Cl(01)	28.0(3)
C(030)-C(026)-C(029)-C(024)	51.42(19)
Cl(09)-C(026)-C(029)-C(024)	-66.3(2)
Cl(03)-C(026)-C(029)-C(024)	169.35(15)
C(030)-C(026)-C(029)-C(027)	-57.38(19)
Cl(09)-C(026)-C(029)-C(027)	-175.07(15)
Cl(03)-C(026)-C(029)-C(027)	60.55(19)
C(030)-C(026)-C(029)-Cl(01)	176.91(16)
Cl(09)-C(026)-C(029)-Cl(01)	59.2(2)
Cl(03)-C(026)-C(029)-Cl(01)	-65.2(2)
C(035)-C(027)-C(029)-C(024)	44.5(2)
C(025)-C(027)-C(029)-C(024)	-68.2(2)
C(035)-C(027)-C(029)-C(026)	148.39(19)

C(025)-C(027)-C(029)-C(026)	35.6(2)
C(035)-C(027)-C(029)-Cl(01)	-85.2(2)
C(025)-C(027)-C(029)-Cl(01)	162.06(15)
C(024)-C(023)-C(030)-C(026)	35.5(2)
Cl(02)-C(023)-C(030)-C(026)	-150.19(17)
C(024)-C(023)-C(030)-C(025)	-69.0(2)
Cl(02)-C(023)-C(030)-C(025)	105.3(2)
C(024)-C(023)-C(030)-Cl(05)	160.82(16)
Cl(02)-C(023)-C(030)-Cl(05)	-24.9(3)
C(029)-C(026)-C(030)-C(023)	-51.80(19)
Cl(09)-C(026)-C(030)-C(023)	66.18(19)
Cl(03)-C(026)-C(030)-C(023)	-168.63(15)
C(029)-C(026)-C(030)-C(025)	58.49(18)
Cl(09)-C(026)-C(030)-C(025)	176.47(15)
Cl(03)-C(026)-C(030)-C(025)	-58.3(2)
C(029)-C(026)-C(030)-Cl(05)	-176.82(16)
Cl(09)-C(026)-C(030)-Cl(05)	-58.8(2)
Cl(03)-C(026)-C(030)-Cl(05)	66.4(2)
C(028)-C(025)-C(030)-C(023)	-47.0(2)
C(027)-C(025)-C(030)-C(023)	65.4(2)
C(028)-C(025)-C(030)-C(026)	-150.67(19)
C(027)-C(025)-C(030)-C(026)	-38.3(2)
C(028)-C(025)-C(030)-Cl(05)	83.7(2)
C(027)-C(025)-C(030)-Cl(05)	-163.89(15)
C(044)-C(021)-C(031)-C(032)	-35.1(2)
C(040)-C(021)-C(031)-C(032)	69.2(2)
Cl(11)-C(021)-C(031)-C(032)	-161.26(18)
C(044)-C(021)-C(031)-Cl(06)	149.96(19)
C(040)-C(021)-C(031)-Cl(06)	-105.7(2)
Cl(11)-C(021)-C(031)-Cl(06)	23.8(3)
C(021)-C(031)-C(032)-C(037)	0.5(3)
Cl(06)-C(031)-C(032)-C(037)	175.09(19)
C(021)-C(031)-C(032)-Cl(07)	-173.85(19)
Cl(06)-C(031)-C(032)-Cl(07)	0.8(4)
C(025)-C(027)-C(035)-O(2)	179.0(2)
C(029)-C(027)-C(035)-O(2)	67.2(3)

C(025)-C(027)-C(035)-N(1)	-0.3(2)
C(029)-C(027)-C(035)-N(1)	-112.1(2)
C(031)-C(032)-C(037)-C(044)	34.2(2)
Cl(07)-C(032)-C(037)-C(044)	-151.22(19)
C(031)-C(032)-C(037)-C(019)	-69.9(3)
Cl(07)-C(032)-C(037)-C(019)	104.6(2)
C(031)-C(032)-C(037)-Cl(12)	160.60(19)
Cl(07)-C(032)-C(037)-Cl(12)	-24.8(3)
C(022)-C(019)-C(037)-C(032)	-46.3(3)
C(040)-C(019)-C(037)-C(032)	66.0(2)
C(022)-C(019)-C(037)-C(044)	-149.8(2)
C(040)-C(019)-C(037)-C(044)	-37.4(2)
C(022)-C(019)-C(037)-Cl(12)	83.7(2)
C(040)-C(019)-C(037)-Cl(12)	-163.95(18)
O(4)-C(034)-C(040)-C(019)	177.0(2)
N(2)-C(034)-C(040)-C(019)	-2.5(3)
O(4)-C(034)-C(040)-C(021)	64.5(3)
N(2)-C(034)-C(040)-C(021)	-115.0(2)
C(022)-C(019)-C(040)-C(034)	0.2(2)
C(037)-C(019)-C(040)-C(034)	-119.0(2)
C(022)-C(019)-C(040)-C(021)	120.1(2)
C(037)-C(019)-C(040)-C(021)	1.0(2)
C(031)-C(021)-C(040)-C(034)	46.5(3)
C(044)-C(021)-C(040)-C(034)	149.6(2)
Cl(11)-C(021)-C(040)-C(034)	-84.1(2)
C(031)-C(021)-C(040)-C(019)	-67.1(2)
C(044)-C(021)-C(040)-C(019)	36.0(2)
Cl(11)-C(021)-C(040)-C(019)	162.29(17)
C(031)-C(021)-C(044)-C(037)	51.9(2)
C(040)-C(021)-C(044)-C(037)	-57.4(2)
Cl(11)-C(021)-C(044)-C(037)	177.84(17)
C(031)-C(021)-C(044)-Cl(10)	-66.2(2)
C(040)-C(021)-C(044)-Cl(10)	-175.58(16)
Cl(11)-C(021)-C(044)-Cl(10)	59.7(2)
C(031)-C(021)-C(044)-Cl(08)	169.13(16)
C(040)-C(021)-C(044)-Cl(08)	59.8(2)

Cl(11)-C(021)-C(044)-Cl(08)	-64.9(2)
C(032)-C(037)-C(044)-C(021)	-51.9(2)
C(019)-C(037)-C(044)-C(021)	58.0(2)
Cl(12)-C(037)-C(044)-C(021)	-177.20(17)
C(032)-C(037)-C(044)-Cl(10)	65.7(2)
C(019)-C(037)-C(044)-Cl(10)	175.61(17)
Cl(12)-C(037)-C(044)-Cl(10)	-59.6(2)
C(032)-C(037)-C(044)-Cl(08)	-169.71(17)
C(019)-C(037)-C(044)-Cl(08)	-59.8(2)
Cl(12)-C(037)-C(044)-Cl(08)	65.0(2)
O(1)-C(028)-N(1)-C(035)	179.1(2)
C(025)-C(028)-N(1)-C(035)	0.1(3)
O(1)-C(028)-N(1)-C(1B)	-0.4(5)
C(025)-C(028)-N(1)-C(1B)	-179.4(5)
O(1)-C(028)-N(1)-C(1C)	-1.3(6)
C(025)-C(028)-N(1)-C(1C)	179.7(5)
O(2)-C(035)-N(1)-C(028)	-179.2(2)
C(027)-C(035)-N(1)-C(028)	0.2(3)
O(2)-C(035)-N(1)-C(1B)	0.3(6)
C(027)-C(035)-N(1)-C(1B)	179.6(5)
O(2)-C(035)-N(1)-C(1C)	1.2(6)
C(027)-C(035)-N(1)-C(1C)	-179.5(5)
C(2B)-C(1B)-N(1)-C(028)	-125.0(11)
C(7B)-C(1B)-N(1)-C(028)	100.8(12)
C(2B)-C(1B)-N(1)-C(035)	55.6(12)
C(7B)-C(1B)-N(1)-C(035)	-78.5(12)
C(2B)-C(1B)-N(1)-C(1C)	-47(100)
C(7B)-C(1B)-N(1)-C(1C)	179(100)
C(7C)-C(1C)-N(1)-C(028)	125.7(11)
C(2C)-C(1C)-N(1)-C(028)	-104.6(13)
C(7C)-C(1C)-N(1)-C(035)	-54.6(13)
C(2C)-C(1C)-N(1)-C(035)	75.0(14)
C(7C)-C(1C)-N(1)-C(1B)	23(100)
C(2C)-C(1C)-N(1)-C(1B)	153(100)
O(3)-C(022)-N(2)-C(034)	175.6(3)
C(019)-C(022)-N(2)-C(034)	-4.1(3)

O(3)-C(022)-N(2)-C(1)	-6.6(4)
C(019)-C(022)-N(2)-C(1)	173.7(2)
O(3)-C(022)-N(2)-C(1A)	-5.5(5)
C(019)-C(022)-N(2)-C(1A)	174.8(4)
O(4)-C(034)-N(2)-C(022)	-175.2(2)
C(040)-C(034)-N(2)-C(022)	4.3(3)
O(4)-C(034)-N(2)-C(1)	6.7(4)
C(040)-C(034)-N(2)-C(1)	-173.8(2)
O(4)-C(034)-N(2)-C(1A)	6.7(8)
C(040)-C(034)-N(2)-C(1A)	-173.8(7)
C(2)-C(1)-N(2)-C(022)	-60.1(4)
C(7)-C(1)-N(2)-C(022)	68.9(5)
C(2)-C(1)-N(2)-C(034)	117.6(3)
C(7)-C(1)-N(2)-C(034)	-113.3(4)
C(2)-C(1)-N(2)-C(1A)	-62.4(8)
C(7)-C(1)-N(2)-C(1A)	66.7(9)
C(2A)-C(1A)-N(2)-C(022)	-131.0(8)
C(7A)-C(1A)-N(2)-C(022)	108.2(12)
C(2A)-C(1A)-N(2)-C(034)	47.2(13)
C(7A)-C(1A)-N(2)-C(034)	-73.6(13)
C(2A)-C(1A)-N(2)-C(1)	47.2(8)
C(7A)-C(1A)-N(2)-C(1)	-73.6(13)

Symmetry transformations used to generate equivalent atoms:

Table 7: Hydrogen bonds for 6m_zk1a [Å and °].

D-H...A	d(D-H)	d(H...A)	d(D...A)	<(DHA)